DISTINCT MITOTIC ARRESTS BY PRAIRIE ASTERACEAE PLANT EXTRACTS AND EXPLORATION OF THE TRANSCRIPTOMIC RESPONSE OF HT-29 CANCER CELLS TO ANTI-MITOTIC CHEMICALS

Haley Allard
Bachelor of Science, Agricultural Biotechnology, University of Lethbridge, 2019

A thesis submitted
in partial fulfilment of the requirements for the degree of

MASTER OF SCIENCE

in

BIOLOGICAL SCIENCES

Department of Biological Sciences
University of Lethbridge
LETHBRIDGE, ALBERTA, CANADA

DISTINCT MITOTIC ARRESTS BY PRAIRIE ASTERACEAE PLANT EXTRACTS AND EXPLORATION OF THE TRANSCRIPTOMIC RESPONSE OF HT-29 CELLS TO ANTI-MITOTIC CHEMICALS

HALEY ALLARD

Date of defense: December 13, 2021

Dr. R. Golsteyn Thesis Supervisor	Associate professor	Ph.D.
Dr. J. McCune Thesis Examination Committee Member	Assistant professor	Ph.D.
Dr. D. Yevtushenko Thesis Examination Committee Member	Associate professor	Ph.D.
Dr. R. Laird Chair, Thesis Examination Committee	Professor	Ph.D.

ABSTRACT

We investigate the mitotic activities of Canadian Asteraceae plant extracts and use two experimental approaches to study mitotic arrests. We used taxonomy and phylogeny as a basis for investigating extracts from the species *Ratibida columnifera, Arnica fulgens,* and *Hymenopappus filifolius* for anti-mitotic activity. The extracts were tested for anti-mitotic activity against cancer cells measured by rounded cell morphology and phosphorylated histone H3 assays. The extracts demonstrated distinct effects on the mitotic spindle, with different microtubule distortions and centrosome morphologies. In a second approach, we used transcriptomic analysis to compare mitotic arrests induced by sesquiterpene lactones or the cancer drug Taxol®. Transcriptomic analysis revealed differences in overall gene expression related to specific biological processes including transcripts related to microtubule regulation. Isolation of the plant extract chemicals as well as identification of protein targets may provide new chemicals suitable for studying mitosis and possible use in future precision medicines.

PREFACE

A version of Chapter 2 has been published. Layla Molina, Haley K. Allard, Sophie M. Kernéis, and Roy M. Golsteyn. Connecting plant species and natural products from the Canadian prairie ecological zone to biomedical knowledge. *Botany*. **e- First.** doi.org/10.1139/cjb-2021-0067. I assisted in the writing and editing of this review article.

Contribution of Authors (Chapter 2):

Layla Molina: Investigation, Writing

Haley K. Allard: Investigation, Writing

Sophie M. Kernéis: Conceptualization, Investigation, Writing

Roy M. Golsteyn: Conceptualization, Supervision, Funding acquisition, Writing.

ACKNOWLEDGEMENTS

I would like to express my sincere gratitude to my supervisor Dr. Roy Golsteyn for providing this opportunity. My project would not have been possible without his positivity, direction, and advice. Thank you to my supervisory committee members Dr. Jenny McCune and Dr. Dymtro Yevtushenko. I would also like to thank Dr. Robert Laird for contributing to my thesis defence as the thesis examination chair.

I am grateful to members of the Biological Sciences Department Dr. Andy Hudson and Jennifer Burke for their intellectual and technical assistance provided. Thank you to Dr. Athan Zovoilis from the Chemistry and Biochemistry Department for sharing his bioinformatics knowledge, and to his laboratory members Riya Roy, Liam Mitchell, and Travis Haight, for their collaboration. I am extremely grateful to Athan's student Luke Saville for his transcriptomics instruction, advice, and encouragement.

Thank you to my laboratory members Araba Sagoe-Wagner, Shannon Healy-Knibb, Genevieve May, Tanner Lockwood, and Rebecca Runions, for their discussions and technical support. Thank you to past laboratory members Layla Molina for her mentorship.

This achievement would not have been possible without my family and friends. Thank you to my husband Christopher Allard for continually loving and encouraging me. To my parents, Carl and Marilyn, my brothers Ryan, Caslo, Logan and his wife Alexandra Vanderploeg, and my in-laws Tami Buroker, John Derksen, and Katie Allard, I express my gratitude for their love and moral support. Thank you to my friends Haley Shade, Rachael Heise, Sarah Hirtle, Kristian Smits, Jed Lloren, and Max Erickson for making my M. Sc. a memorable and enjoyable experience.

TABLE OF CONTENTS

LIST OF TABLES

LIST OF FIGURES

LIST OF ABBREVIATIONS

6-OAP	6-O-Angeloylplenolin
APC/C	Anaphase promoting complex/cyclosome
ATCC	American Type Culture Collection
ATP	Adenosine triphosphate
ATPase	Adenosine triphosphatase
BSA	Bovine serum albumin
Bub	Budding uninhibited by benzimidazole proteins
Cdc20	Cell-division cycle protein 20
CDK	Cyclin-dependent kinase
cDNA	Complementary deoxyribonucleic acid
CuAAC	Copper (I)-catalyzed azide-alkyne cycloaddition
Cul3	Cullin-3
DAPI	4′, 6-diamidino-2-phenylindole
DAVID	Database for Annotation, Visualization and Integrated Discovery
DCM	Dichloromethane
DET	Differentailly expressed transcripts
DGE	Differential gene expression
DMSO	Dimethyl sulfoxide
DNA	Deoxyribonucleic acid
EGTA	Ethylene glycol tetraacetic acid
EtOH	Ethanol
GPS	Global positioning system
HT-29	Human colorectal adenocarcinoma cell line
KEAP1	Kelch-like ECH associated protein 1
Mad	Mitotic-arrest-deficient proteins
mRNA	Messenger ribonucleic acid
NEB	New England Biolabs
NF-κB	Nuclear factor kappa-light-chain-enhancer of activated B cells
NMR	Nuclear magnetic resonance
NT	Not-treated
PBS	Phosphate buffered saline
PH3	Phospho-histone H3

Plk-1	Polo-like kinase-1
Parth	Parthenolide
PulA	Pulchelloid A
RNA	Ribonucleic acid
RPMI	Roswell Park Memorial Institute medium
SAC	Spindle assembly checkpoint
SCF	Skp, Cullin, F-box containing complex
Skp1	S-phase kinase-associated protein 1
UPS	Ubiquitin-proteasome system
VASCAN	Database of vascular plants of Canada

CHAPTER 1

Introduction

This thesis is about using different experimental approaches to investigate Canadian plant species for anti-mitotic chemicals. A knowledge gap exists between the process of mitosis and the entirety of the proteins involved. Novel anti-mitotic chemicals can be used to develop our understanding of the complex protein interactions that facilitate mitosis. Recently our laboratory found anti-mitotic chemicals within the plants *Gaillardia aristata* Pursh. and *Hymenoxys richardsonii* Hook. The discovery of these sesquiterpene lactones, puchelloid A and hymenoratin, led us to ask if other Asteraceae species in the prairie ecological zone contain related anti-mitotic chemicals. We hypothesize that Canadian Asteraceae species are sources of different but related anti-mitotic chemicals that will induce distinct mitotic arrests. In one experimental approach (phylogeny), we investigated extracts from Asteraceae species of different tribes for anti-mitotic activity. We compared the effects of extracts prepared from the species *Ratibida columnifera, Arnica fulgens,* and *Hymenopappus filifolius* on components of the mitotic spindle: microtubules and centrosomes. The different microtubule distortions and centrosome morphologies induced by these extracts suggest that they have different chemicals and corresponding cellular targets. This project was the first in our laboratory to use taxonomic and phylogenetic information as a guide toward a species, *H. filifolius,* and test it for anti-mitotic activity.

In a second approach, we tested whether different types of mitotic arrests could be distinguished by transcriptomic analysis. To understand the possible reasons for differences in mitotic arrest, we introduce sesquiterpene lactones and their possible interaction with E3 ligases. We also provide a rationale for using transcriptomic analysis

to investigate the gene expression of cells arrested in mitosis by different natural products. This was the first time that transcriptomics were used to investigate plant extract chemicals in our laboratory. The second chapter is a pre-print of an accepted review article which I coauthored with other members of our laboratory, which describes the connections between Canadian prairie Asteraceae species, natural products, and biomedicine. This article describes information that supports the investigation of Asteraceae species from Canadian ecological zones as sources of natural products of scientific importance.

1.1 Anti-mitotic chemicals from the Asteraceae plant family and their activities

The Asteraceae plant family produces special metabolites called sesquiterpene lactones. These chemicals are 15 carbon molecules synthesized from three isoprene rings fused to a fused α-methylene-γ-lactone ring. There are over 5000 sesquiterpene lactones (Chadwick et al., 2013), and within the chemical class numerous biological activities including anti-cancer and anti-inflammatory have been reported (Moujir et al., 2020). In our laboratory, we have identified anti-mitotic sesquiterpene lactones pulchelloid A (pulA), from Asteraceae species *Galliardia aristata* (Bosco, 2017; Bosco et al., 2021) and hymenoratin, from *Hymenoxys richardsonii* (Molina et al., 2021b). The plant extracts containing these sesquiterpene lactones share mitotic arrest characteristics such as inducing ~30% cell rounding and distorting mitotic spindles. As reviewed by Bosco and Golsteyn (2017) the sesquiterpene lactones 6-O-angeloylplenolin, 9β-acetoxycostunolide, coronpilin, costunolide, dehydroleucodine, NP136, NP176, NP339, parthenolide, psilostachyin A, psilostachyin C, santamarine, and xanthatin have anti-mitotic activities. Monopolar, multipolar, hyperpolymerized, and disorganized mitotic spindles were observed in cells

treated with these chemicals (Bosco & Golsteyn, 2017). Since that review the sesquiterpene lactones 2α-hydroxyalantolactone (Hegazy et al., 2021), ivalin (Liu et al., 2019), pulA, and hymenoratin have been added to the list, bringing the total of anti-mitotic sesquiterpene lactones up to 17 out of the 5000. The biological activity of sesquiterpene lactones has been primarily attributed to the α-methylene-γ-lactone moiety (Zhang et al., 2005) (**Figure 1B**) which reacts by Michael-type addition to cysteine residues. This was determined by Kupchan et al. (1970) who investigated the reaction of sesquiterpene lactones with nucleophilic l-cysteine. The products of the cysteine addition were isolated, separated with chromatography, and examined by NMR, which showed spectra signals indicating the reaction between sesquiterpene lactones with cysteine occurred at the α-methylene-γ-lactone. Other chemicals that contain a Michael acceptor similar to the α-methylene-γ-lactone, but are not sesquiterpene lactones, demonstrate anti-mitotic activity (Rundle et al., 2006). There are sesquiterpenes such as artesunate, and zerumbone which do not have the α-methylene-γ-lactone moiety but still demonstrate anti-mitotic activity (Sithara et al., 2018; Wen et al., 2018). These studies, combined with the diversity of anti-mitotic morphologies lead us to suspect that the non-lactone component of these chemicals modulates their protein interactions, including anti-mitotic activities. The mechanisms of action behind anti-mitotic sesquiterpene lactones remains unknown.

The range of phenotypes observed within anti-mitotic sesquiterpene lactones may be due to a potential interaction with members of the ubiquitin-proteasome system (UPS). Targeted degradation of proteins by ubiquitin-ligase enzymes regulates many cell processes including mitosis. The addition of ubiquitin to proteins is mediated by enzymes called E1 (ubiquitin-activating), E2 (ubiquitin-conjugating) and E3 ligases (substrate-specificity) (Cardozo & Pagano, 2004). Polyubiquitin-labeled proteins are then recognized by the 26S proteasome and degraded (Dang et al., 2021). Three ubiquitin ligases, APC/C, Cul3, and SCF, have been found to have activity during mitosis (Sumara et al., 2008). The anaphase promoting complex/cyclosome (APC/C) is an E3 ligase that mediates the ubiquitin-proteolytic degradation of securin to allow sister chromatid separation. The APC/C only promotes anaphase progression after it is activated by binding to Cdc20, which is part of the SAC protein complex. This checkpoint is modulated by its key components Mad2 and Bub3 proteins that localize to unattached kinetochores to prevent un-equal sister chromatid separation (Lara-Gonzalez et al., 2012). Mad2 binds to Cdc20 in the presence of unattached kinetochores, sequestering it from activating the APC/C. When the APC/C is inactive, it cannot target proteins for degradation, thereby arresting cells in mitosis until the checkpoint is satisfied. Once activated, the APC/C can target proteins such as cyclins A and B for degradation, downregulating mitotic CDK activity, thus allowing cells to progress into G1 (McLean et al., 2011).

Proteasome inhibitors can have a variety of cellular effects depending on which part of the proteasome they inhibit. The drug Bortezomib inhibits the proteasome by binding to the β5 catalytic subunit of the 20S catalytic core complex and is used to treat multiple myeloma (Gandolfi et al., 2017). Because NF-κB is activated by proteasomal degradation of its

regulatory Iκ-βα subunit, Bortezomib is effective in treating this cancer by inhibiting the proteasome and therefore the activation of NF-κB, which is upregulated in multiple myeloma. Inhibiting overall proteasome function affects a broad selection of cellular proteins, and therefore it is important to find chemicals that have greater specificity, such as by inhibiting specific E3 ligases (Jia & Sun, 2011). Small molecules such as MLN492 that can inhibit specific E3 ligases have fewer under-desired effects compared to broad proteasome inhibitors (Chen et al., 2011). Sesquiterpene lactones may be able to serve as E3 ligase inhibitors by binding to cysteine residues in their substrate recognition sites. The sesquiterpene lactone britanin binds selectively to cystein-151 of Kelch-like ECH associated protein 1 (KEAP1), demonstrated by crystal structures reported by Wu et al. (2017). KEAP1 is the substrate recognition component of the Cullin3-based Cullin-RING E3 ubiquitin ligase (Dinkova-Kostova et al., 2017). Activity based profiling has shown that cysteines are available on 211 of the 600 available E3 ligases (Kiely-Collins et al., 2021). Because the chemistry of sesquiterpene lactones enables adduct formation with cysteine residues, it is possible that some of these E3 ligases may be targets of sesquiterpene lactones.

We suspect more anti-mitotic sesquiterpene lactones exist within Canadian members of the Asteraceae family, which are understudied for their biological activity (Chapter 2). One approach for finding new chemicals is to use taxonomy and phylogeny to guide natural product investigation. There are examples in the natural product literature that describe how related plant species have distinct but related special metabolites. The chemicals, paclitaxel and docetaxel, are both cancer drugs present in different species within the *Taxus* genus (Molina et al., 2021a). Derivatives of the sesquiterpene lactone artemisinin, isolated

from *Artemisia annua*, are used in the treatment of malaria (Ho et al., 2014). Other members of this genus have been investigated and are found to contain many phytochemicals including sesquiterpene lactones and demonstrate anti-cancer activity (Ho et al., 2014). Previous investigation by our laboratory has shown that extracts of *G. aristata* (tribe Helenieae) and *A. cordifolia* (tribe Madieae), caused different mitotic arrests in cancer cells as shown by different microtubule distortions and protein interactions (Molina, 2018). In this thesis we investigated other members of the Asteraceae family of the Helianthieae, Madieae, and Bahieae tribes as sources of anti-mitotic chemicals. We had collected the species *R. columnifera* (tribe Heliantheae) and *A. fulgens* (tribe Madieae) without the guidance of phylogeny. Baldwin et al. (2002) proposed phylogenetic relationships that place the Heliantheae tribe closer to Helenieae than Madieae (**Figure 2**). We used these proposed relationships to direct our investigation of Canadian Asteraceae tribes that were also outside of Helenieae. For this project, species of tribes that were located in the Southern Alberta region and outside of the Helenieae tribe were selected for study. These criteria led us to investigate *H. filifolius*, as well as *R. columnifera,* and *A. fulgens.* We expected to observe different anti-mitotic arrests in these selected species because distantly related species *G. aristata* and *A. cordifolia* demonstrated different anti-mitotic activities (L. Molina, 2018). Photos taken by our laboratory of the species we investigated are found in **Figure 2**.

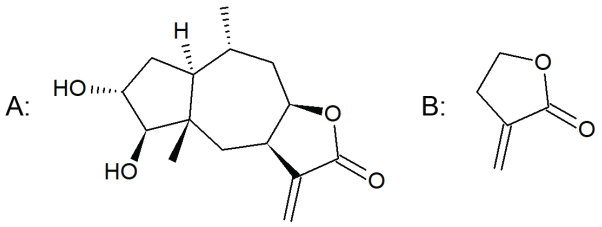

Figure 1. Hymenoratin, a sesquiterpene lactone isolated from *H. richardsonii* (**A**) and α-methylene-γ-lactone (**B**) the moiety primarily responsible for sesquiterpene lactone activity.

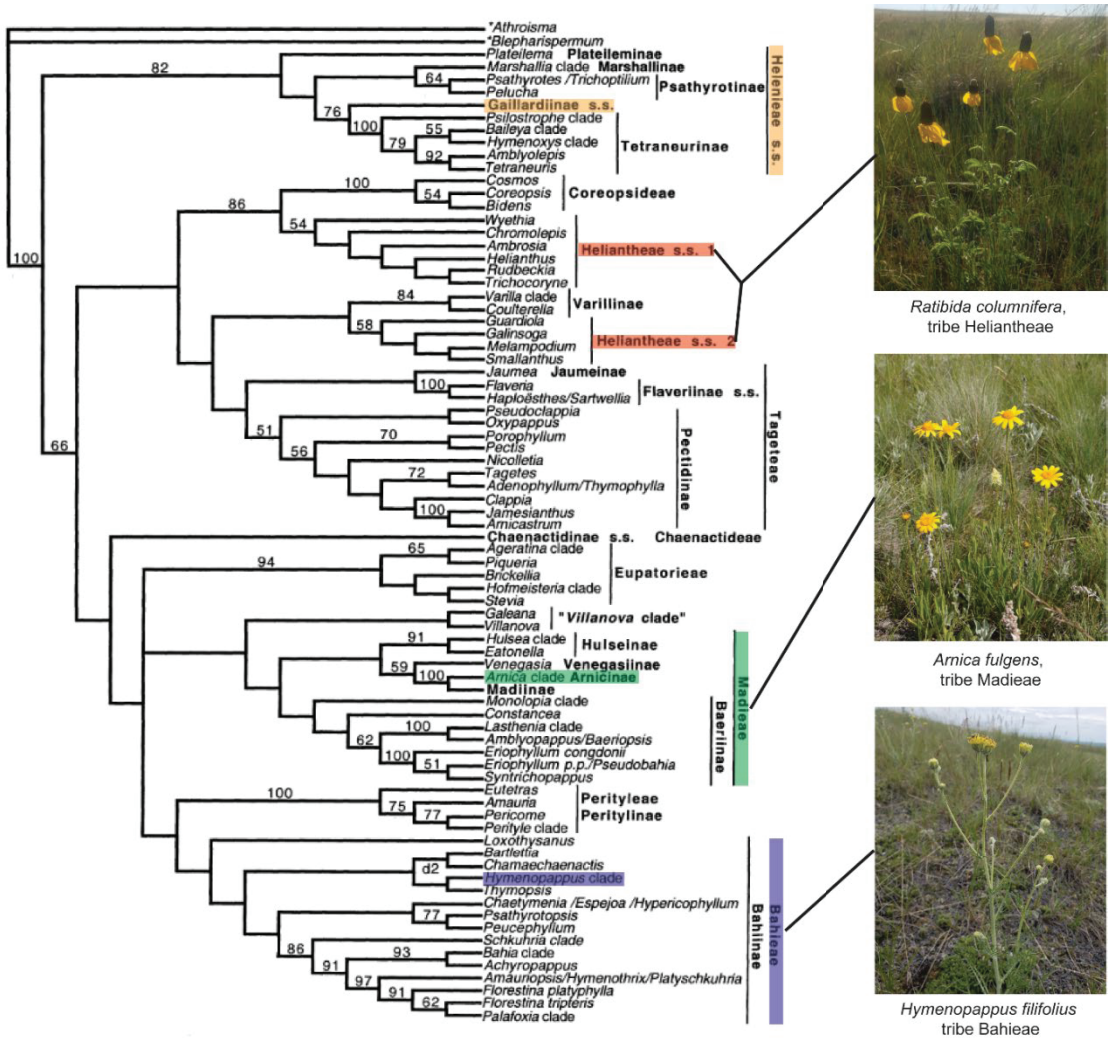

Figure 2. Phylogenetic tree of Asteraceae tribes, determined by minimum-length parsimony analysis of 18S-26S nuclear rDNA ITS regions (adapted from (Baldwin et al., 2002). Tribes and genera of interest are highlighted yellow, red, green, and blue.

1.2 Asteraceae species investigated in this thesis

1.2.1 Ratibida columnifera (Nutt.) Wooton and Standley

Commonly named Upright prairie coneflower and Redspike Mexican-hat, *R. columnifera* is a member of the *Heliantheae* tribe and a native species distributed in Canada from British Columbia to Manitoba (Wolf, 2006). *R. columnifera* varieties have been cultivated since the 1830's for garden use (Hind, 2006) since the species is tolerant of many soil types and produces showy blooms. This perennial herb stands 30 to 50 cm tall, with stiff, coarsely hairy stems; pinnately parted alternate leaves; several long-pedunculate terminal heads containing yellow to brownish purple drooping rays, dark disc flowers; short achenes that are compressed and broad, and a chaffy pappus (Wooton & Standley, 1915).

Various *Ratibida* species including *R. columnifera* have been investigated for their chemical constituents. *R. latipalearis* is a Mexican species traditionally used by the Tarahumara indigenous peoples to treat skin conditions and inflammation (Rojas et al., 1991). The sesquiterpene lactone ratibinolide II was isolated from this species, although no biological activity was reported. Two sesquiterpene lactones, isoalloalantolactone and elema-l,3,11-trien-8,12-olide, were isolated from *R. mexicana* (Calera et al., 1995). These two sesquiterpene lactones were tested against breast, lung, and colon cancer cell lines and found to be cytotoxic with ED_{50} values ranging from 1.0 - 4.5 μg/mL. The mechanism of action of the chemicals was not described. The chemical content of *R. columnifera* has been investigated. In 1985 several unique sesquiterpene lactones called ratibidanolides were isolated, in addition to isolantolactone, and other xanthanolides (Herz et al., 1985). Later, it was found that one of the xanthanolide sesquiterpene lactones, 9-oxo-seco-ratiferolide-5α-O-(2-methylbutyrate) was cytotoxic and arrested cells in the G2/M phase

(Cui et al., 1999). The authors tested this chemical for its ability to inhibit or promote tubulin polymerization/depolymerization and found that it was not arresting cells through this mechanism.

1.2.2 Arnica fulgens Pursh.

A. fulgens is a member of the *Madieae* tribe and is native in Canada (Brouillet et al., 2010). The plant is 20 – 60 cm tall with solitary stout stems. It's leaves appear in 2 – 4 pairs, and are entire, pubescent, and glandular. The basal leaves are petiolate, and oblanceolate to oblong with axillary tufts of brown hair, whereas the cauline leaves sessile or short-stalked, lanceolate or linear. The heads can be present in 1-3, with yellow to orange ray flowers, and yellow discs, with involucres 10-15 mm high, achenes hairy, pappus white to somewhat brownish and barbellate (Moss & Packer, 1983).

Members of the *Arnica* genus have been investigated for their chemical contents. The arnica genus is well known in the natural product field. *Arnica montana* preparations are widely used as homeopathic medicines for many conditions, and are a source of sesquiterpene lactone helenalin (Drogosz & Janecka, 2019). Helenalin and other sesquiterpene lactones inhibit NF-κB transcription factor to inhibit inflammatory pathways that may have a role in cancer progression (Moujir et al., 2020). The pseudoguaianolides carabrone, 2,3-dihydroaromaticin, and the cis-isomer of 2,3-dihydroaromaticin were isolated from *A. cordifolia* (Merfort & Wendisch, 1993). The sesquiterpene lactones chamissonolide, 6-deoxychamissonolide, 2-deacetyl-4-tigloylchamissonolide, and 11α,13-dihydroarnifolin were isolated from *A. angustifolia* spp. *attenuate* (Schmidt & Willuhn, 2000). Ivalin, an anti-mitotic sesquiterpene lactone (Liu et al., 2019) was found also within *A. angustifolia* spp. *angustifolia* by Schmidt and Willuhn (2000). Extracts from *A. fulgens*

were examined by one group who investigated twelve *Arnica* extracts for their ability to inhibit human neutrophil elastase release and NF-κB. Their findings indicated that the *A. fulgens* extract contained the sesquiterpene lactones florlenalin, arnifolin, dihdryohelenalin, xanthalongin, and chamissonolid, and had of 30 - 50% inhibitory activity against HNE and NF-κB activity (Ekenaes et al., 2008).

1.2.3 *Hymenopappus filifolius* Hooker.

As part of our investigation of the phylogeny relationship species and anti-mitotic activities, we collected *H. filifolius* because it was reported to be in Alberta and was a member of tribe Bahieae, distant from the Helenieae tribe (**Figure 2**). *H. filifolius,* commonly known as Fine-leaved Woolly-white, is described as a perennial 5 – 10 cm tall, with basal leaves that are 2-pinnate with 2-50 lobes, and 0-12 cauline leaves; up to 60 solitary heads, consisting of only disc florets with yellow corollas 2.2-7 mm and white to yellowish phyllaries (Moss & Packer, 1983). Its distribution extends from Texas and New Mexico and North to Alberta and Saskatchewan (Wolf, 2006).

We consulted the National Center for Biotechnology Information (PubMed, PubChem), CAS Scifinder and found no studies investigating the chemical profile or bioactivity of *H. filifolius*. We found one ecological study looking at soil respiration in Southwestern US that included *H. filifolius* in its vegetation list (Breecker et al., 2012). The chemical contents of two related *Hymenopappus* species have been investigated. Three sesquiterpene lactones, one germacrene lactone and two guaianolides have been isolated from *H. newberryi* (Bohlmann, 1984). Later, three germacranolides and 4 guaiainolides were isolated from *H. scabiosaeus*, and 3 guaianolides from *H. tenuifolius* (Eid et al., 1988). The biological activity of special metabolites from this genus has not been investigated.

1.3 Why transcriptomics

There are numerous studies that demonstrate the activity of plant extracts and natural products in tissue culture models, but the mechanism of action can be difficult to determine. Morphological assays can provide direction toward affected organelles and pathways like mitosis and membrane trafficking, but there may be many genetic and protein interactions responsible for these outcomes. Analysis of RNA molecules (transcriptomics) provides unbiased insight into specific gene expression such as quantitative expression analysis, transcript isoforms, and alternative splicing patterns (Manzoni et al., 2018). Expression profiles can be used to find new chemicals that inhibit pathways that are targeted by other drugs (Stockwell et al., 2012). Kim and Kim (2020) investigated the xanthophyll carotenoid astaxanthin which previously demonstrated anti-proliferative effects against breast cancer cells. They performed transcriptomic analysis between gastric cancer cells treated with the small molecule, and untreated cells. Through this analysis they showed that astaxanthin suppresses upregulation of PI3KC2 and PLCγ1 and therefore their downstream targets. One study investigating the effects of an anti-mitotic sesquiterpene lactone 2α-hydroxyalantolactone has been conducted. The authors found genes pointing to G2/M arrest and DNA damage as responsible mechanisms of action for (Hegazy et al., 2021). We seek to test transcriptomics as an additional approach to explore of the effects of anti-mitotic natural products in human cancer cells within our laboratory.

Transcriptomic analysis should be able to differentiate mitotic arrests for several reasons. Although chromatin condenses during mitosis, slowing a majority of gene expression, transcription levels remain high for Cyclin B1 during mitosis suggesting that certain areas of chromatin remain open (Sciortino et al., 2001). Additionally, mitotic cells have specific

expression profiles due to accumulation of transcripts produced in G1/S (Liu et al., 2017). Response to anti-mitotic chemicals can be detected at the transcriptional level. One anti-mitotic chemical of interest for our study is Taxol® (paclitaxel), a natural product first isolated from the bark of the Pacific Yew tree (*Taxus brevifolia* Nutt.) and a widely-used cancer drug (Kearns, 1997). It acts as microtubule stabilizing agent by binding to a hydrophobic pocket within β-tubulin, promoting the formation of microtubules and preventing disassembly, inducing mitotic arrest because of spindle assembly checkpoint activation (Yang & Horwitz, 2017). Differences are observed between transcriptomic profiles of cells treated with microtubule stabilizing versus destabilizing agents. Tubulin genes TUBB, TUBA, and TUBG were differentially expressed between retinal pigment epithelial 1 cells treated with paclitaxel and those treated with a microtubule destabilizing agent, combretastatin A-4 (Gasic et al., 2019). To date, no study has been performed using transcriptomic analysis to differentiate types mitotic arrests. In this thesis we test transcriptomic analysis as a technique to detect differences in mitotic arrests induced by anti-mitotic chemicals.

1.4 Hypothesis and objectives

These data and research in the laboratory led us to hypothesize that extracts prepared from different Canadian Asteraceae species induce different mitotic arrests, which may be due to different chemicals. Testing this hypothesis is important because it may lead to the discovery of sources of new anti-mitotic chemicals, which may be useful as future precision medicines and as tools for better understanding mitosis. To test this hypothesis, we propose the following objectives.

1. Investigate Asteraceae species *A. fulgens*, *R. columnifera*, and *H. filifolius* from the tribes Madieae, Heliantheae, and Bahieae for anti-mitotic activities by testing extracts for anti-mitotic activities.

2. Explore mitotic arrests induced by Canadian Prairie Asteraceae plant extracts and anti-mitotic natural products with cell biology and transcriptomic analysis.

We report for the first time, that indeed different extracts from plants within different tribes, and chemicals isolated from prairie plants can induce measurable and different mitotic arrests.

CHAPTER 2

Connecting plant species and natural products from the Canadian prairie ecological zone to biomedical knowledge

Layla Molina, Haley K. Allard, Sophie M. Kernéis, and Roy M. Golsteyn

This chapter has been accepted for publication by the journal "Botany."

2.1 Abstract

Natural products from plants in Canadian ecological zones are understudied. There are, however, sound scientific arguments to justify investigation of natural products from plant species found within these zones. We review a broad range of scientific and local literature describing the features of the Canadian prairie ecological zone and the Asteraceae taxonomical family. Species from Asteraceae are well represented in the prairie ecological system, although very few have been investigated for natural products with bio-medical properties. Data from a range of sources that address ecological interactions, abiotic features, and Traditional Knowledge provide a foundation for future scientific studies of plant natural products found within Canadian borders. We draw from discoveries of the Asteraceae family and one of its major classes of secondary metabolites, sesquiterpenes, to stimulate research of Asteraceae species in Canada.

2.2 Asteraceae natural products as sources of bioactive molecules

Plants from the taxonomical family, Asteraceae, are historically and scientifically recognized as sources of beneficial natural products (metabolites), such as treatments for malaria (*Artemisia annua* L.) (Septembre-Malaterre et al., 2020), respiratory diseases (*Echinacia spp.*) (Barrett, 2003), use as sweetners (*Stevia spp.*) (Soejarto et al., 2019), or wellness (*Achillea millefolium* L.) (Benedek & Kopp, 2007). Primary metabolites are essential for growth and include well known chemical families such as proteins, carbohydrates, lipids, chlorins (chlorophylls), and nucleic acids. Secondary metabolites, such as flavonoids, alkaloids, or terpenoids, including sesquiterpenes, are not thought to have vital roles; instead they act as supportive metabolites that evolved from ecological pressures (Hartmann, 1996). Secondary metabolites may be critical for defensive strategies against herbivores or pathogens, plant-plant competitions, or beneficial interactions for plants such as the attraction of pollinators or symbionts. They may also have protective roles against abiotic stressors such as changes in temperature, light intensity, UV exposure, among others (Pavarini et al., 2012). It is noteworthy that the precise boundaries of primary and secondary metabolites are becoming blurred (Erb & Kliebenstein, 2020).

The Asteraceae, also known as Compositae family, is the largest family of flowering plants containing 32,913 species in 1,911 genera distributed around the world except for Antarctica (Royal Botanic Gardens Kew and Missouri Botanic Garden, 2013). It was taxonomically divided into 11 subfamilies and 35 tribes by Panero and Funk (2002) after analysis of DNA sequence data of chloroplasts genes. It is a monophyletic family characterized by a special type of inflorescence called pseudanthium, flower head, or capitulum, where disc and ray florets are arranged on a receptacle centripetally and are

surrounded by bracts that form the involucre. This family presents anthers fused in a ring with the pollen pushed out by the style, and achenes (cypselas) usually with a pappus (**Figure 3**). There is a large morphological variation among its members, existing annual and perennial herbs, shrubs, vines, or trees, and although they are more common in open areas, they can be found in almost every type of habitat from forests to high elevation grasslands (Panero & Funk, 2002).

Several Asteraceae species are well known because they contribute to our diets, such as lettuce (*Lactuca sativa* L.), chicory (*Cichorium intybus* L.), and artichoke (*Cynara cardunculus var. scolymus* L.). Within the category of medicinal plants, *Artemisia annua* from Asteraceae, is the source of artemisinin and its derivatives artesunate and dihydroartemisinin are major antimalarial drugs. The discovery that *A. annua* was able to inhibit malarial parasite growth and the subsequent isolation of the sesquiterpene lactone artemisinin is attributed to Dr. Tu Youyou (Miller, 2011). For this discovery, Dr. Youyou was awarded the Nobel Prize in 2015 (Youyou, 2016). The best-known species of this family in the prairie ecological zone is the sunflower (*Helianthus annuus* L.).

We consulted natural product related databases (Sorokina & Steinbeck, 2020), including National Center for Biotechnology Information (PubMed, PubChem), Google Scholar, VASCAN, as well as numerous limited print publications that are cited herein. Scientific information about the biological and medical potential of prairie plant species, including those from Asteraceae is limited. We review information from a diverse set of sources that support continued investigation of Asteraceae species from the prairie ecological zone for natural products, especially secondary metabolites such as sesquiterpene lactones.

Members of the Asteraceae family produce a wide range of other secondary metabolites including: monoterpenes, diterpenes, triterpenes, sesquiterpenes, polyacetylenes, flavonoids, phenolic acids, benzofurans, and coumarins (Zdero & Bohlmann, 1990). They do not produce major classes of alkaloids, only pyrrolizidine alkaloids are found in Senecioneae and Eupatorieae tribes. The accumulation of lactonized sesquiterpenes and polyacetylenes, as well as the presence of many highly oxidized compounds, have been recognized as unique chemical signatures for most of the members of this family (Zdero & Bohlmann, 1990). Therefore, these compounds may be responsible for the unique medicinal uses that have been attributed to this family.

Vascular plants in Canada have been enumerated using provincial boundaries. The province of Alberta, which overlaps with much of the prairie ecological zone, has 1636 native vascular plant species belonging to 123 families (Kershaw & Allen, 2020). A widely used taxonomical key developed by Moss and Packer (1983) reported 1475 native plant species in Alberta. It is reported that 55% of the species present in Alberta (661,848 km2) can be found in Waterton Lakes National Park (505 km2), which is nestled in the south west corner of the province but only covers 0.08% of the provincial surface area (Kuijt, 1982).

Documents of the Flora of North America have recorded 2413 Asteraceae species and 418 genera for the United States and Canada (Committee, 1993). The Database of Vascular Plants of Canada (VASCAN) currently reports 691 species of the Asteraceae family from 163 genera and 19 tribes of the 4 subfamilies Asteroideae, Cichorioideae, Carduoideae, and Mutisioideae distributed across the ecological zones (Brouillet et al., 2010). It includes plants having one or more of five statuses. The status of native is given when a taxon is

present in a region as a result of natural processes and not human intervention. Taxa are considered introduced if they were established after European colonization for accidental or deliberate human activity. The status of ephemeral refers to taxa that recur in the wild in a near-annual basis, usually from cultivation, but is not permanent. The VASCAN database catalogues a taxon as excluded when it has been reported from a region but it is not established, or it was erroneously determined, and as extirpated if it was native to the region but it is now considered eradicated (Brouillet et al., 2010). From these 691 species, 332 are present in the prairie region (provinces of Alberta, Saskatchewan, and Manitoba) from 106 genera and 18 tribes. 245 species are native to this region, 58 introduced, 27 excluded, and 2 ephemerals. In Alberta, which includes the prairie ecological zone, there are 270 species from 91 genera and 16 tribes from the Asteraceae family: 207 natives, 51 introduced, 11 excluded, and 1 ephemeral. **Table 1** lists the Asteraceae species present in the prairies and their status in this region. Presence can refer to either Alberta, Saskatchewan, Manitoba, or combinations thereof. It is striking that only 9 of these species are described in Health Canada's NHPD monographs, and of those, only 3 are native plants (**Table 2**). The biotic and abiotic conditions of the prairies as well as association with Traditional Knowledge provide support for investigation of the biomedical properties of this family.

Figure 3. Botanical description of Asteraceae flower heads.The key morphological features that characterize the flower heads of members of the Asteraceae taxonomical family are shown as a side view (**A**). A side view of the flower from *Gaillardia aristata* Pursh (Blanket flower), which is a striking flower present in the prairie ecological zone that contains bioactive sesquiterpene lactones. Scale bar is shown (**B**). A top view of the flower from *G. aristata*. Scale bar is shown (**C**).

Table 1. Asteraceae family members in Canada according to the database of vascular plants (VASCAN). The status within the Prairie region is indicated in parenthesis as follows: native (N), introduced (I), ephemeral (EP), or excluded (EX).

Subfamily	Tribe	Genus	Species
Asteroideae	Anthemideae	*Achillea*	*A. alpina* L. (N), *A. borealis* L. (N).
		Anthemis	*A. arvensis* L. (1753) (I), *A. cotula* L. (I).
		Arctanthemum	*A. arcticum* (L.) Tzvelev (N).
		Artemisia	*A. abronatum* L. (I), *A. absinthium* L. (I), *A. biennis* Willd (I), *A. borealis* Pall (N), *A. campestris* L. (N), *A. cana* Pursh (N), *A. dracunculus* L. (N), *A. frigida* Willd. (N), *A. hyperborea* Rydberg (N), *A. longifolia* Nutt. (N), *A. ludoviciana* Nutt. (N), *A. michauxiana* Bess. (N), *A. norvegica* Fr. (N), *A. pontica* L. (N), *A. tilesii* Led. (N), *A. tridentata* Nutt. (N), *A. vulgaris* L. (I).
		Cota	*C. tinctoria* L. (I).
		Leucanthemum	*L. vulgare* Lam. (I).
		Matricaria	*M. chamomilla* L. (I), *M. discoidea* DC.(I).
		Tanacetum	*T. balsamita* L. (I), *T. bipinnatum* L. Sch. Bip. (N), *T. parthenium* L. Sch. Bip. *(I), T. vulgare* L. (I).
		Tripleurospermum	*T. inodorum* L. Sch. Bip. (I).
	Astereae	*Almutaster*	*A. pauciflorus* (Nutt.) Á. Löve & D. Löve (N).
		Aster	*A. alpinus* L. (N).
		Boltonia	*B. asteroides* (L.) L'Hér. (N).
		Canadanthus	*C. modestus* (Lindl.) G.L. Nesom (N).
		Dieteria	*D. canescens* Nutt. (N).
		Doellingeria	*D. engelmannii* (D.C. Eaton) Semple, Brouillet & G.A. Allen (N), *D. umbellate* Nees (N).
		Ericameria	*E. nauseosa* Pall. ex Pursh G.L. Nesom (N).

		Erigeron	*E. acris* L. (N), *E. annuus* L. (N)), *E. aureus* Greene (N), *E. caespitosus* Nutt. (N), *E. canadensis* L. *(I), E. compositus* Pursh (N), *E. divergens* Torr. A. Gray (N), *E. elatus* Greene (N), *E. evermannii* Rydb. (EX), *E. flagellaris* A. Gray (N), *E. formosissimus* Greene (EX), *E. glabellus* Nutt. (N), *E. glacialis* (Nutt.) A. Nelson (N), *E. grandiflorus* Hook. (N), *E. humilis* Graham (N), *E. hyssopifolius* Michx. (N), *E. lackschewitzii* G.L. Nesom W.A. Weber (N), *E. lanatus* Hook. (N), *E. lonchophyllus* Hook. (N), *E. nivalis* Nutt. (N), *E. ochroleucus* Nutt. (N), *E. pallens* Cronquist (N), *E. peregrinus* Greene (N), *E. philadelphicus* L. (N), *E. pumilus* Nutt. (N), *E. radicatus* Hook. (N), *E. speciosus* (Lindl.) DC. (N), *E. strigosus* Muhl. ex Willd (N), *E. trifidus* Hook. (N), *E. arthurii* B. Boivin (N).
		Eucephalus	*E. engelmannii* (D.C. Eaton) Greene (N).
		Eurybia	*E. conspicua* (Lindl.) G.L. Nesom. (N), *E. sibirica* (L.) G.L. Nesom. (N).
		Euthamia	*E. graminifolia* L. Nutt. (N).
		Grindelia	*G. hirsutula* Hook. Arn. (N), *G. paysonorum* H. St. John (EX Quebec), *G. squarrosa* (Pursh) Dunal (N).
		Gutierrezia	*G. sarothrae* Pursh Britt. Rusby (N).
		Heterotheca	*H. villosa* (Pursh) Shinners (N).
		Machaeranthera	*M. tanacetifolia* (Kunth) Nees (N).
		Pyrrocoma	*P. lanceolata* (Hook.) Greene (N), *P. uniflora* (Hook.) Greene (N).
		Solidago	*S. altissima* L. (N), *S. bellidifolia* Greene (EX), *S. bernardii* B. Boivin (N), *S. bicolor* L. (EX), *S. canadensis* L. (N), *S. gigantea* Aiton (N), *S. glutinosa* Nutt. (N), *S. hispida* Muhl. ex Willd (N), *S. jejunifolia* E. S. Steele (N), *S. juncea* Aiton (N), *S. lepida* DC. (N), *S. lutescens* Lindley ex DC (N), *S. missouriensis* Nutt. (N), *S. mollis* Bartl. (N), *S. multiradiata* Aiton (N), *S. nemorallis* Aiton (N), *S. ptarmicoides* (Torr. & A. Gray) B. Boivin (N), *S. riddellii* Frank ex Riddell (N), *S. rigida* L. (N), *S. simplex* Kunth (EX), *S. uliginosa* Nutt. (N).
		Stenotus	*S. armerioides* Nutt. (N).
		Symphyotrichum	*S. ascendens* (Lindl.) G.L. Nesom (N), *S. boreale* (Torr. & A. Gray) Á. & D. Löve (N), *S. campestre* (Nutt.) G.L. Nesom (N), *S. chilense* (Nees) G.L. Nesom (EX), *S. ciliatum* (N), *S. ciliolatum* (Lindl.) Á. & D. Löve (N), *S. cordifolium* (L.) G.L. Nesom (N), *S. cusickii* (A.Gray) G.L. Nesom (N), *S. eatonii* (A .Gray) G.L. Nesom (N), *S. ericoides* (L.) G.L. Nesom (N), *S. falcatum* (Lindl.) G.L. Nesom (N), *S. firmum* (Nees) G.L. Nesom (N), *S.*

			foliaceum (Lindl. ex DC.) G.L. Nesom (N), *S. laeve* (L.) Á. & D. Löve (N), *S. lanceolatum* (Willd.) G.L. Nesom (N), *S. lateriflorum* (L.) Á. & D. Löve (N), *S. novae-angliae* (L.) G.L. Nesom (N), *S. novi-belgii* (L.) G.L. Nesom (EX), *S. praealtum* (Poir.) G.L. Nesom (EX), *S. puniceum* (L.) Á. & D. Löve (N), *S. robynsianum* (J. Rousseau) Brouillet & Labrecque (N), *S. sericeum* (Vent.) G.L. Nesom (N), *S. spathulatum* (Lindl.) G.L. Nesom (N), *S. subspicatum* (Nees) G.L. Nesom (N).
		Tonestus	*T. lyallii* (A. Gray) A. Nelson (N).
		Townsendia	*T. condensata* Parry ex A. Gray (N), *T. exscapa* (Richardson) Porter (N), *T. hookeri* Beaman (N), *T. parryi* DC. Eaton (N).
	Bahieae	*Hymenopappus*	*H. filifolius* Hook. (N).
		Picradeniopsis	*P. oppositifolia* (Nutt.) Rydb. *(I).*
	Calendulae	*Calendula*	*C. arvensis (*Vaill.) L. (EX).
	Chaenactideae	*Chaenactis*	*C. douglasii* (Hook.) Hook. & Arn. (N).
	Coreopsideae	*Bidens*	*B. amplissima* Greene (I), *B. beckii* Torr. ex Spreng. (N), *B. cernua* L. (N), *B. frondosa* L. (N), *B. tripartita* L. (N), *B. vulgata* Greene (N)
		Coreopsis	*C. tinctoria* Nutt. (N).
		Thelesperma	*T. subnudum* A. Gray (N).
	Eupatorieae	*Ageratina*	*A. altissima* (L.) R.M. King & H. Rob. (EX).
		Brickellia	*B. grandiflora* (Hook.) Nutt. (N).
		Conoclinium	*C. coelestinum* (L.) DC. (EP).
		Eupatorium	*E. perfoliatum* L. (N).
		Eutrochium	*E. maculatum* (L.) E.E. Lamont (N), *E. purpureum* (L.) E.E. Lamont (EX).
		Liatris	*L. aspera* Michx. (EX), *L. ligulistylis* (A. Nelson) K. Schum. (N), *L. punctata* Hook. (N).
	Gnaphalieae	*Anaphalis*	*A. margaritaceae* L. (N).
		Antennaria	*A. alpina* (L.) Gaertn. (N), *A. anaphaloides* Rydb. (N), *A. aromatica* Evert (N), *A. corymbosa* E. Nels. (N), *A. dimorpha* Nutt. (N), *A. friesiana* (Trautv.) Ekman (EX), *A. howellii* Greene (N), *A. lanata* (Hook.) Greene (N), *A. luzuloides* Torr. & Gray (N), *A.*

			media Greene (N), *A. microphylla* Rydb. (N), *A. monocephala* DC. (N), *A. neglecta* Greene (N), *A. parlinii* Fern. (N), *A. parvifolia* Nutt. (N), *A. plantaginifolia* (L.) Richards (EX), *A. pulchella* Greene (EX), *A. pulcherrima* (Hook.) Greene (N), *A. racemosa* Hook. (N), *A. rosea* Greene (N), *A. umbrinella* Rydb. (N).
		Gamochaeta	*G. purpurea* (L.) Cabrera (N).
		Gnaphalium	*G. palustre* Nutt. (N), *G. uliginosum* L. (I).
		Logfia	*L. arvensis* L. (I).
		Pseudognaphalium	*P. macounii* (Greene) Kartesz (N), *P. thermale* (E. E. Nelson) G. L. Nesom (N).
		Psilocarphus	*P. brevissimus* Nutt. (N), *P. elatior* Gray (EX).
	Helenieae	*Gaillardia*	*G. aristata* Pursh (N), *G. pulchella* Foug. (I).
		Helenium	*H. autumnale* L. (N).
		Hymenoxys	*H. richardsonii* (Hook.) Cockerell (N).
		Tetraneuris	*T. acaulis* (Pursh) Greene (N).
	Heliantheae	*Ambrosia*	*A. acanthicarpa* Hook. (N), *A. artemisifolia* Meyen & Walp. (N), *A. psilostachya* DC. (I), *A. trifida* L. (N).
		Balsamorhiza	*B. sagittata* (Pursch) Nutt. (N).
		Cyclachaena	*C. xanthiifolia* Nutt. (N).
		Echinacea	*E. angustifolia* DC. (N).
		Galinsoga	*G. parviflora* Cav. (I), *G. quadriradiata* Ruiz & Pav. (I).
		Helianthus	*H. annuus* L. (N), *H. giganteus* L. (EX), *H. laetiflorus* Pers. (EX), *H. maximiliani* Schrad. (N), *H. nuttallii* Torr & A. Gray (N), *H. pauciflorus* Nutt. (N), *H. petiolaris* Nutt. (N), *H. tuberosus* L. (N).
		Heliopsis	*H. helianthoides* L. Sweet (N).
		Iva	*I. axillaris* Pursh (N).

		Ratibida	*R. columnifera* (Nutt.) Wooton & Standl. (N).
		Rudbeckia	*R. laciniata* L. (N), *R. hirta* L. (N).
		Xanthium	*X. spinosum* L. (EP), *X. strumarium* L. (N).
	Inuleae	*Inula*	*I. helenium* L. (N).
	Madieae	*Arnica*	*A. angustifolia* Vahl (N), *A. chamissonis* Less. (N), *A. cordifolia* Hook. (N), *A. fulgens* Pursch (N), *A. gracilis* Rydb. (N), *A. lanceolata* Nutt. (N), *A. latifolia* Bong. (N), *A. lonchophylla* Greene (N), *A. longifolia* D.C. Eaton (N), *A. louiseana* L. 1753 not Boehm. 1760 (N), *A. mollis* Hook. (N), *A. ovata* Greene (N), *A. parryi* Gray (N), *A. rydbergii* Greene (N), *A. sororia* Greene (N).
		Madia	*M. glomerata* Hook. (I).
	Senecioneae	*Erechtites*	*E. hieraciifolius* (L.) Raf. ex DC. (EX).
		Jacobaea	*J. vulgaris* Gaert (I).
		Packera	*P. aurea* (L.) A. & D. Löve (N), *P. cana* (Hook.) W.A. Weber & A. Löve (N), *P. contermina* (Greenm.) Bain (N), *P. heterophylla* (Fishc.) Wieb. (N), *P. hyperborealis* (Greenm.) A. & D. Löve (EX), *P. indecora* (Greene) A. & D. Löve (N), *P. pauciflora* (Pursch) A. & D. Löve (N), *P. paupercula* (Michx.) A. & D. Löve (N), *P. plattensis* (Nutt.) W.A. Weber & A. Löve (N), *P. pseudaurea* (Rydb.) W.A. Weber & A. Löve (N), *P. streptanthifolia* (Greene) A. & D. Löve (N), *P. subnuda* (DC.) D.K. Trock & T.M. Barkely (N), *P. tridenticulata* (Rydb.) W.A. Weber & A. Löve (EX).
		Petasites	*P. frigidus* (L.) Fries (N).
		Senecio	*S. eremophilus* Rich. (N), *S. fremontii* Torr. & A. Gray (N), *S. hydrophiloides* Rydb. (N), *S. integerrimus* Nutt. (N), *S. lugens* Rich. (N), *S. megacephalus* Nutt. (N), *S. triangularis* Hook. (N), *S. viscosus* L. (I), *S. vulgaris* L. (I).
		Tephroseris	*T. palustris* (R.Br.) DC. (N).
	Tageteae	*Dyssodia*	*D. papposa* Cav. (I).
Carduoideae	Cardueae	*Arctium*	*A. lappa* L. (I), *A. minus* (Hill) Bernh. 1800 not Schkuhr 1803 (I), *A. tomentosum* Mill. (I).
		Carduus	*C. nutans* L. (I).

		Carthamus	*C. tinctorius* L. (I).
		Centaurea	*C. cyanus* L. (I), *C. diffusa* Lam. (I), *C. solstitialis* L. (I), *C. stoebe* L. (I).
		Cirsium	*C. arvense* (L) Scop. (I), *C. discolor* (Muhl. ex Willd.) (N), *C. drummondii* Torr. & A. Gray (N), *C. flodmanii* (Groesser et al.) Arthur (N), *C. foliosum* (Hook.) DC. (N), *C. hookerianum* Nutt. (N), *C. muticum* Michx. (N), *C. scariosum* Nutt. (N), *C. undulatum* (Nutt.) Spreng. (N), *C. vulgare* (Cheng et al.) Ten. (I).
		Echinops	*E. sphaerocephalus* L. (EP).
		Onopordum	*O. acanthium* L. (EX).
		Rhaponticum	*R. repens* L. Hidalgo. (I).
		Saussurea	*S. amara* L. (EX), *S. americana* D.C. Eaton. (N), *S. angustifolia,* Willd. DC (N). *S. nuda* Ledebour. Icon. (N).
		Silybum	*S. marianum* L. Gaertn. (I).
Cichorioideae	Cichorieae	*Agoseris*	*A. glauca* (Pursh) Raf. var. agrestis (Osterh.) (EX), *A. aurantiaca* (Hook.) Greene (N), *A. glauca* (Pursh) Raf. (N), *A. parviflora* (Nutt.) D. Dietr. (EX).
		Askellia	*A. elegans* (Hook.) W.A. Weber, 1984 (N), *A. pygmaea* W.A. Weber (N).
		Cichorium	*C. endivia* L. (EX), *C. intybus* L. (I).
		Crepis	*C. atribarba* A. Heller (N), *C. capillaris* (L.) Wallr. (I), *C. intermedia* A. Gray (N), *C. modocensis* E. Greene (EX), *C. occidentalis* Nutt. (N), *C. runcinata* (James) Torr. & A. Gray (N), *C. tectorum* L. (I).
		Helminthotheca	*H. echioides* (L.) Holub (I).
		Hieracium	*H. albiflorum* (Hook.) F.W. Schultz & Sch. Bip. (N), *H. scouleri* F.W .Schultz & Sch. Bip. (N), *H. umbellatum* L. (N).
		Krigia	*K. biflora* (Walter) S.F.Blake 1915 (N).
		Lactuca	*L. canadensis* L. (EX), *L. floridana* (L.) Gaertn. 1791 (N), *L. ludoviciana* (Nutt.) Riddell 1835 (N), *L. sativa* L. (EX), *L. serriola* L. (I), *L. virosa* L. 1753 not Thunb. 1800 nor Luce nor Hablitz (EX).
		Lapsana	*L. communis* L. (I).

		Lygodesmia	*L. juncea* (Pursh) D. Don ex Hooker (N).
		Microseris	*M. nutans* (Hook.) Sch. Bip. (N).
		Mulgedium	*M. pulchellum (Pursh)* G. Don (N).
		Nabalus	*N. alatus* Hook. (1833) (N), *N. albus* (L.) Hook. (N), *N. racemosus* (Michx.) Hook (1833) (N), *N. sagittatus* (A. Gray) Rydb. (1900) (N).
		Nothocalais	*N. cuspidata* (Pursh) Greene (N).
		Pilosella	*P. aurantiaca* (L.) F.W. Schultz & Sch. Bip. (I), *P. caespitosa* (Dumort) P.D. Sell & C. West (I), *P. tristis* (Willd. ex Spreng.) F.W. Schultz & Sch. Bip. (N).
		Shinnersoseris	*S. rostrata* (A. Gray) Tomb (N).
		Sonchus	*S. arvensis* L. (I), *S. asper* (L.) Hill 1769 (I), *S. oleraceus* L. 1753 not Wall. 1831 (I).
		Stephanomeria	*S. runcinata* Nutt. (N), *S. tenuifolia* (Torrey) H.M. Hall (N).
		Taraxacum	*T. ceratophorum* (Ledeb.) Schinz ex Thellung (N), *T. erythrospermum* Andrz. ex Besser (I), *T. lapponicum* Kihlman ex Handel-Mazzetti (EX), *T. officinale* (L.) Weber ex F.H.Wigg. (I), *T. scopulorum* (A. Gray) Rydb. (N).
		Tragopogon	*T. dubius* Scopoli (I), *T. porrifolius* L. (I), *T. pratensis* L. (I).
	Vernonieae	*Vernonia*	*V. fasciculata* Michx. (N).
Mutisioideae	Mutisieae	*Adenocaulon*	*A. bicolor* Hook (N).

Table 2. Asteraceae species present in the prairie region which appear in Health Canada's NHPD monographs.

Species	Status	Traditional Uses	Active phytochemical(s)	Phytochemical Reference
Arctium lappa L.	Introduced	Diuretic and pain relief	Arctigenin and onopordopicrin	(de Almeida et al., 2012; Hyam et al., 2013)
Artemisia vulgaris L.	Introduced	Stimulates bile secretion and appetite, aids digestion	Apigenin	(Omar et al., 2019)
Cichorium intybus L.	Introduced	Prebiotic and digestive health aid	Chicoric acid	(Street et al., 2013)
Echinacea angustifolia DC.	Native	Relief of upper respiratory tract infections and sore throat	Echinacoside and cynarine	(Linde et al.)
Helianthus annuus L.	Native	Cholesterol management	Oleic and linoleic acids, phytosterols	(Adeleke & Babalola, 2020)
Helianthus tuberosus L.	Native	Relieves digestive irregularity	Inulin	(Srinameb et al., 2015)
Matricaria chamomilla L.	Introduced	Relief of mouth/throat irritation and inflammation	Apigenin-7-glucoside and luteolin-7-O-B-D-glucoside	(Haghi et al., 2014)
Silybum marianum L. Gaertn.	Introduced	Hepatoprotectant and relief of indigestion	Silymarin	(Bijak, 2017)
Tanacetum parthenium L. Sch.-Bip	Introduced	Digestive aid and migraine relief	Parthenolide and other sesquiterpene lactones	(Pareek et al., 2011)

2.3 The prairie ecological zone

The prairie ecological zone is one of the fifteen zones of Canada. It extends from the western edge of Alberta to the eastern edge of Manitoba and has its base in the Canada-United States border, comprising the northern extension of the Great Plains of North America (Marshall et al., 1999). It is characterized by relatively little topographic relief, grasslands, limited forests, and a sub-humid to semiarid climate (**Figure 4**). Despite a strong presence of agricultural activity, little research has been done regarding the potential biological activities of its native flora. Similar to other ecological zones in the biosphere, Asteraceae is one of the major botanical families in the prairies.

Figure 4. The prairie ecosystem in Alberta, Canada. This is an image of the prairie ecosystem in Alberta taken at 49°05 N and 112°28 W (approximately 100 km East of the Rocky Mountains and 15 km North of the Canadian-American border). The worn path around the boulder was made by grazing mammals and is a testimony to the herbivory that occurs in this region. The boulder is an erratic, deposited during the last ice age. It measures approximately 1.5 metres across. Although not visible, there are at least ten forb species that are present and blooming at time the photo was taken. Very few of these species have been investigated for the biomedical properties of their secondary metabolites.

2.4 Secondary metabolites and the prairie ecological herbivory

Secondary metabolism in plants may have evolved to interact with molecular targets that affect physiological functions in competing organisms (e.g. microorganisms, non-host plants, animals) (Wink, 2003). These organisms, in turn, can develop adaptive responses constituting plant-animal interactions. This coevolutionary adaptation process has contributed to the multitude of bioactive compounds found in plants (Wöll et al., 2013). We focus on the prairie ecological zone because it is a region in which vascular plants and grazing herbivores have co-existed since the Eocene Epoch (45,000,000 years ago) (Stebbins, 1981). In modern times, the prairies were occupied by vast herds of *Bison bison*

(American bison, also known as buffalo), which are herbivores that weigh between 400-1,000 kg as adults. The bison were extirpated from Alberta by 1879 (Adams et al., 2004) and replaced immediately by domestic cattle. In 1880-1882 the number of cattle imported in Alberta increased from 1,352 to 16,282 with nearly 104,000 cattle registered by 1886 (Evans, 1978). There has been a nearly continuous grazing by herbivores on prairie grasslands (Mijaljica et al., 2012).

The bison had major effects upon prairie flora and contributed to patch dynamics, in which they reduce plant height, decrease grass numbers, and increase forb numbers (Myster, 2011). Grazing by large mammalian herbivores does reduce reproductive success and abundance yet increases diversity of prairie plant species (Bakker et al., 2006; Spotswood et al., 2002). Although much less studied, it was reported that below-surface organisms such as nematodes and mammals (*Cynomys ludovicianus*; prairie dogs) may be the largest contributor to herbivory in the United States grasslands (Ingham & Detling, 1984; Myster, 2011). It is not reported if the major below-surface mammal in Canadian prairies, the ground squirrel, *Urocitellus richardsonii,* impacts below-surface herbivory.

Detailed examples of plant toxins affecting animal grazing are not common; the possum (*Trichosurus vulpecula*, a marsupial) alters its foraging behaviour relative to the concentration of plant toxin, eucalyptus oil, a terpene (Nersesian et al., 2011). The concept of adaptive plant-herbivore behaviour in the prairie ecological zone is largely based on empirical data with little supportive experiment data to this day (Briske, 1996; Laycock, 1978). It would stand to reason that plants in grassland communities have developed significant secondary metabolites that affect animal physiology leading to avoidance (Briske, 1996). Some secondary metabolites produced by plants have a toxic effect in

grazing animals. Grazing domestic animals are known to be at risk to intoxication by secondary metabolites from plant species within the prairie ecological zone, such as *Thermopsis rhombifolia* Nutt. ex Pursch (Fabaceae; buffalo bean) (Keeler & Baker, 1990; Keeler et al., 1986) or *Delphinium nuttallianum* Pritz. ex Walp. (Ranunculaceae; Larkspur) (Pfister et al., 1996). To support the agricultural development of the prairies, native plant species on the prairies have been investigated for toxicity at the whole animal level. In the province of Alberta, 42 native plant species from forbs to trees have been identified as toxic to livestock (Majak et al., 2008). A document circulated by the Government of Alberta lists 133 introduced and native plant species or genera that are toxic to humans and livestock of which the greatest number were members of Asteraceae (Government of Alberta, 1995). Although the type of secondary metabolite and its toxic dose have been frequently identified, the mechanism of action (host target receptor) is usually not known.

More recently, in European grasslands (not North American prairie), it has been proposed that at low concentrations certain secondary metabolites may benefit grazing herbivores by providing antioxidant or anti-parasite properties (Poutaraud et al., 2017). Some grazing animals in North American ecological zones display a preference for a plant species over another. In studies of deer (*Odocoileus*) and their consumption of prairie Fabaceae species, *Dalea purpurea* Vent. was consumed in preference relative to *Amorpha canescens* Pursh. (Nisi et al., 2015). Changes in plant defenses over a period of 39 years were observed in the investigation of aphids and *Arabidopsis thaliana* L. (Brassicaceae) interactions in Europe (Züst et al., 2012). Albeit a study of insect herbivore, it provides biological evidence of an interaction that is consistent with the notion of similar outcomes with mammalian herbivores. The possibility of relationships between animals and plants likely

harbouring secondary metabolites is supported by an investigation of foraging habits of pygmy rabbits (*Brachylagus idahoensis*) and plants of *Artemisia* spp (Sagebrush) (Ulappa et al., 2014). The presence of secondary metabolites negatively influenced the selection of foraging by this small herbivore.

There are several examples of co-evolution between diverse organisms in the prairie ecological zone that are astonishing in their specificity and reside under a theme of connectivity in biology. The monarch butterfly (*Danaus plexippus*) feeds on the toxic prairie plant, milkweed (*Asclepias incarnata* L. (Apocynaceae)) which protects the butterfly against parasites, such as *Ophryocystis elektroscirrha* (Smilanich & Nuss, 2019). An example of a vertebrate (avian) and Asteraceae species relationship in the prairie setting is shown with the sage grouse (*Centrocersus urophasianus*) and the silver sagebrush (*Artemisia cana* Pursh.) (Adams et al., 2004). The sage grouse is a silver sagebrush obligate, with 100% of its food requirement in winter provided by this plant. The plant also provides nesting sites and cover from mammalian predators. The *Artemisia spp.* are poisonous to livestock and humans (Alberta-Agriculture, 1995) but the phytochemical relationship between sage-grouse and *Artemisia spp*. has not been identified. Secondary metabolites from the sesquiterpene lactone class that are assigned to defense mechanisms may also have roles in tissue specific development in seedlings, moving them to a primary metabolite role (Padilla-Gonzalez et al., 2016; Spring et al., 2020).

2.5 Secondary metabolites and prairie abiotic features

The abiotic features of an ecological zone impact the secondary metabolites that can be isolated from plants within that zone. The prairie ecological zone of Canada has a dramatic range of abiotic features. Over a 30-year period at a central site (Lethbridge, AB) in the

prairies, the maximum daily average temperature was calculated to be 26.1°C, with the extreme of 39.4°C. In the same period, the minimum daily average was -12.1°C with the extreme -42.8°C, a temperature range of 81°C (Government of Canada, 2021a). The temperature range varies per year, as does the number of days per year with temperatures above -5°C during the past 50 years; ranging between 141 to 213 days. Similar wide variations are observed with season precipitation in the form of snow and rain. Over a 50-year period, the amount of precipitation ranged between 111 to 554 mm. The mean daily insolation is 3.7-5.1 Wh/m^2, the highest of the fifteen Canadian ecozones, with the greatest intensity occurring in June (Government of Canada, 2021b). The 20-year average of direct normal irradiation is 1,900 Wh/m^2 in the prairie zone, in contrast to 1,300 Wh/m^2 for most other ecological zones at the similar latitude. Abiotic conditions are known to affect secondary metabolite concentrations (Rodziewicz et al., 2014). It is likely that plants in the prairie ecological system vary their secondary metabolite concentrations and have co-evolved means to stabilize metabolite concentrations in response to abiotic variation. There are reports, however, of how abiotic features such light intensity affects the concentration of sesquiterpene lactones in the prototype prairie Asteraceae, (*Helianthus annuus* L.) (Spring et al., 1986) and that flavonoid synthesis correlates with latitude of the host plant (Jaakola & Hohtola, 2010).

2.6 Prairie plants with medical and wellness properties

As a result of connections to ecological systems plants may synthesize metabolites that are structurally similar to animal metabolites, such as hormones, signal transduction ligands, or neurotransmitters, and may affect human physiology due to the resemblance in potential target sites (Briskin, 2000). Natural products can potentially modulate cellular responses that are of interest in biological research or drug development. Furthermore, because some

natural products have evolved to modify animal physiology, they have inherent medicinal properties, which contributes to their success as medicines (Newman & Cragg, 2020).

2.7 Indigenous Knowledge and prairie plants

The prairie ecological zone in Canada and the United States has been home since time immemorial to members of North American First Nation communities. One of these, known as the Niitsitapi People (Blackfoot Confederacy), uses prairie plant species for medicinal purposes. The Niitsitapi hold an oral tradition and exchanges with scientific communities are not frequent, but some information has been made available publicly for all communities. A regional publication from 1987 lists 185 species of plants that are recognized from Traditional Knowledge as having medicinal properties (Johnston, 1987). A publication from 1974 lists 100 plant species with medicinal properties used by two of the Niitsitapi tribes, the Kainai and the Pikanii, who are located in southern Alberta (Hellson, 1974). Some information about medicinal plants from the Kainai tribe has been shared in a website (Galileo-Educational-Network, 2016) which provides recorded audio and written information about 61 plants.

Several plant species that are found in the prairies are also distributed in other ecological zones and are recognized as medicinal plants by First Nations from those regions. The Asteraceae family was well represented amongst the medicinal plants known to First Nation communities across North America (Shemluck, 1982). This listing included 474 species, of which it is noteworthy that scientifically well known *Achillea* and *Artemisia* species (Asteraceae) were widely used by different tribes for a large number of ailments; whereas other listed species, some which are found in the prairies such as *Hymenopappus filifolius* Hook (Asteraceae) are not described in biomedical literature. Medicinal plants

from the boreal plain ecological zone in central and northern Alberta that are known to Cree peoples were reviewed in 1982 by an Elder, Dr. Anne Anderson (Anderson, 1982). The information collected by Dr. Anderson was further studied and described in a MSc thesis (Wood, 1996). Kindscher (1992) reported an ethnobotanical study of 203 prairie plant species present in the prairie ecological system of the United States (Kindscher, 1992). Other regions outside of the prairie ecological zone, but which harbour plant species that are established in the prairies are part of Traditional Knowledge from the Thompson First Nations (Central British Columbia) (Turner et al., 1990) and Wood Cree First Nations (Central Saskatchewan) (Leighton, 1985), and the First Nation communities of boreal forests in western Canada (Marles et al., 2012). An encyclopedic reference of 3000 plant species known in Traditional Knowledge to First Nation communities of North America, which includes the prairie zone and the Blackfoot Confederacy is described by Moerman (2009). A survey of the information about prairie plants reveals several themes about western scientific and Traditional Knowledge:

1. The majority of plant species are not described as Traditional medicine in printed sources. It is noteworthy that the information about medicinal plants in different public sources are only partially overlapping, suggesting that much knowledge remains to be shared or exchanged between western scientific and First Nation communities.
2. There are relatively few references to cancer treatments, consistent with the difficulty of detecting internal tumours (Moerman, 2009). For example, there are 523 references to treatment for eye afflictions compared to 55 for cancer.
3. Specifically to Traditional Knowledge of Niitsitapi communities, very few plant species with medicinal properties have been investigated by Western scientific methods.

4. Asteraceae species that are globally distributed such as *Achillea millefolium* (Yarrow) or *Helianthus annuus* (Sunflower) have also been identified by distant cultures in Europe and Asia and by Niitsitapi communities for their medicinal properties (Johnston, 1987; Laws, 2015; Moerman, 2009).

The relationship between Traditional Knowledge and Western biomedical information has been recognized in the investigation of natural products globally. It has been reported that inclusion of Traditional Knowledge in western scientific studies increases the success of finding pharmacologically important compounds (Balick, 1990). Incorporating Traditional Knowledge has not been widely used in investigation of plant species in the Prairie ecological zone (Kindscher, 1992), although there are a small number of studies performed in other zones. Uprety et al. (2012) analyzed 49 publications related with the medicinal uses of North American Aboriginal people, including Canada's First Nations, Metis, and Inuit, and reported 546 medicinal plant taxa used by Aboriginal people of the Canadian boreal forest. The anti-diabetic properties of plants known to the Cree First Nations led to the isolation of several compounds including those with specific enzyme targets in glucose metabolism (Downing et al., 2019; Muhammad et al., 2012; Nistor Baldea et al., 2011; Shang et al., 2015). A study comparing anti-fungal activity of plants in Eastern Canada revealed a greater activity in extracts prepared from species identified by Traditional Knowledge when compared to those selected without ethnobotanical information (Jones et al., 2000). Examples of considering North American ethnobotanical knowledge to find anticancer activity screening include testing 29 plants used by the Gwich'in First Nation (Northwest Territories and Yukon) (Deeg et al., 2012), and testing of two plants used by Indigenous Peoples in New Mexico USA (Daniels et al., 2006). The exchange of

Aboriginal Traditional Knowledge to western scientific knowledge remains incomplete in Canada. Currently, there are no studies published in which Canadian Niitsitapi Traditional Knowledge of prairie plants was incorporated into a western scientific study.

In countries other than Canada, Indigenous Traditional Knowledge has contributed to the discovery of anti-cancer compounds from a variety of chemical scaffolds (Khadem & Marles, 2011). Comparison of the success of drug screening programs using either unbiased selection of plant materials to ethnobotanical biased selection favours the inclusion of ethnobotanical knowledge. Kindscher and colleagues tested published medicinal plants and were able to detect anti-cancer activity in tests *in vitro*. Similar trends were observed in studies of bioactive plants from rainforests (Balick, 1990), midwestern regions of United States (Lewis & Elvin-Lewis, 1995), and British Columbia (McCutcheon et al., 1992; McCutcheon et al., 1995). The increase in successful discovery of active compounds might be due to Traditional Knowledge about the best harvest conditions which would include time of year, which part of the plant, and which plant within a population. Traditional Knowledge from other cultures, such as from Chinese Traditional medicine, was used to guide the investigation of 15 plant species that are distributed in both Canadian and Chinese ecological zones (Ramirez-Erosa et al., 2007). In this study, the plants collected in Canada were found to have similar properties to those reported for plants collected in China.

The best methods to exchange western scientific and Traditional Knowledge have yet to be established, although notable progress has been made. Guidelines to promote equitable knowledge exchange are proposed by Canadian Tri-Council research agencies and by public Canadian universities, including the University of Lethbridge, which is situated in

the prairies and Treaty 7 ancestral lands. In addition to these guidelines, our laboratory has chosen to only investigate a Traditional Knowledge perspective of a plant if a member of a First Nations community performs experiments in the laboratory.

2.8 The majority of cancer drugs are derived from plant natural products

A study of drugs from 1981 to 2019 revealed the leading contribution of natural products for drug development (Newman et al., 2000). If biologics and vaccines are removed from the 247 agents approved for anticancer therapy, 75% of the agents are natural small molecules, derivatives of them, or synthetic products that were developed to mimic natural products. Even if the synthetic mimics of natural products are not counted, 41% of the approved anticancer small molecules are natural products or their derivatives. Examples from this list include the anticancer agents and their derivatives: camptothecin, isolated from the tree *Camptotheca acuminata* Decne (Nyssaceae) (Wall & Wani, 1996); the *Vinca* spp. alkaloids, vinblastine and vincristine, from the periwinkle *Catharanthus roseus* L. (Apocynaceae); paclitaxel, isolated from the bark of the Pacific Yew tree *Taxus brevifolia* Nutt. (Taxaceae) (Cragg, 1998). Plant natural products have had an enormous impact in the discovery of anti-cancer drugs, as paclitaxel and its derivatives, and by inspiring cell cycle targets for new anticancer drugs (Newman et al., 2000).

2.9 The majority of plants species have not been investigated for biomedical properties

Only a small percentage of plants have been investigated for their bioactive properties. It is estimated that there are 383,671 vascular plant species identified in the biosphere (Lughadha et al., 2016), of which 10,636 vascular plant species are restricted geographically to North America (USA and Canada) (Ulloa Ulloa et al., 2017). Miller (2011) estimates that between 540 to 23,490 new drugs remain to be found from all plants

in the biosphere (Miller, 2011). This estimate considers that discovery of 135 natural drugs resulted from the only 2,000 plant species that were chemically described are from about 60,000 species that had been screened. An uncertainty on these estimates is whether all species have additive potential to synthesize new compounds or whether they are somewhat chemically redundant. However, most plant screenings are conducted for one bioactivity and other uses are not investigated (Miller, 2011). Moreover, this estimation is only taking into account natural products approved for medicinal purposes.

There are arguments that suggest a sufficient number of plant species have been characterized to identify phytochemicals and further investigation is unlikely to discover new chemicals. There is a compelling example to suggest otherwise: the discovery of docetaxel, a natural product isolated from the English yew, *Taxus baccata* L. (Taxaceae) (Potier et al., 1994). Docetaxel is a member of the taxane class of natural products that has become one of most widely used anti-cancer treatments. Its discovery was inspired by the isolation of paclitaxel from the Pacific yew, *T. brevifolia*, whose distribution is limited to western Canada and the Northwestern United States (Goodman, 2001 2001). *T. baccata*, whose toxic properties have been known since antiquity, is restricted to the European continent and the perimeter of the Mediterranean Sea (Iszkuło et al., 2016). The two species are closely related yet distinct. Each produces taxanes that are also closely related but distinct and individually have improved the lives of millions of cancer patents (**Figure 5**). The two natural products bind to the same protein (tubulin) and inhibit cell proliferation (Ringel & Horwitz, 1991; Schiff et al., 1979) but they affect cancer cell lines differently (Verweij et al., 1994), have different pharmacokinetic profiles in patients (Kearns, 1997), and have different drug costs (Clegg et al., 2002). It is difficult to comprehend the

magnitude of possibilities of natural products from plants, but as exemplified by paclitaxel and docetaxel, all natural products may need to be studied for their potential to affect human physiology or provide a benefit.

The biomedical properties of many of the vascular plants geographically restricted to North America and Alberta are not well studied. By contrasting examples, the species *Achillea millefolium*, which is present in Alberta prairies and globally distributed, was the topic of 679 publications referenced in the National Center for Biotechnology Information (NCBI/PubMed) as of January 2021. Whereas the species, *Arnica fulgens* Pursh (Asteraceae, Foothills arnica), a member of the well known *Arnica* genus and is abundant but geographically restricted to prairies, is not described in any biomedical publications.

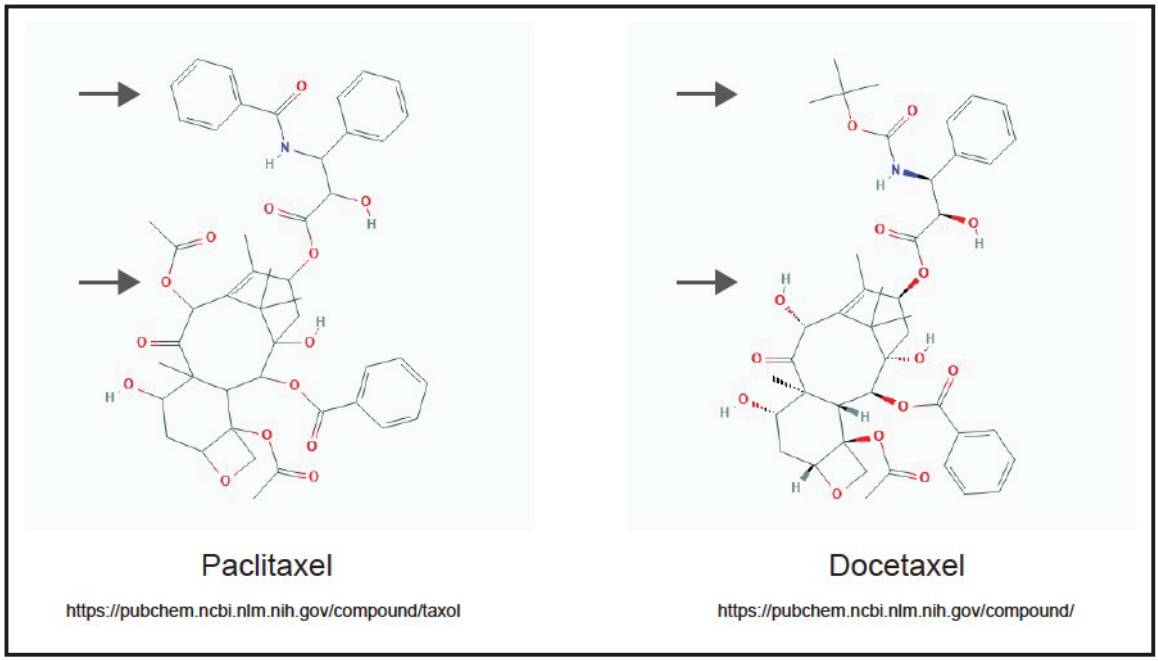

Figure 5. The two best anti-cancer drugs are from two closely related plant species. The chemical structures of paclitaxel (Taxol®, left) and docetaxel (Taxotere®, right) are shown. The arrows point to functional groups that differ between the two natural products. Paclitaxel was first isolated from the plant species *Taxus brevifolia* (Pacific yew), which is distributed throughout British Columbia and present in Waterton National Park, Alberta. Docetaxol was first isolated from *Taxus baccata* (English yew) in France.

The chemical structures are found in the National Center for Biotechnology Information website: https://pubchem.ncbi.nlm.nih.gov/compound/taxol and https://pubchem.ncbi.nlm.nih.gov/compound/Docetaxel.

2.10 Sesquiterpene lactones

The Asteraceae family is known for the production of a class of secondary metabolites called sesquiterpene lactones (Seaman, 1982). Sesquiterpene lactones (SLs) are compounds with a 15-carbon backbone that includes a lactone group. Its biosynthesis starts from the union of three isoprene units, which are 5-carbon derivatives of the mevalonic acid, creating an acyclic farnesyl pyrophosphate (FPP), the simplest sesquiterpene structure.

Sesquiterpene lactones have been isolated from many plant families such as Apiaceae, Magnoliaceae, Acanthaceae, Solanaceae, Araceae, Euphorbiaceae, amongst others (Chadwick et al., 2013), but they can be found almost ubiquitously in the Asteraceae family. SLs are found predominantly in tissues attractive to herbivores, such as leaves, phyllaries, and achenes, and stored in glandular trichomes or laticifers to be secreted in the surface of these organs (Chadwick et al., 2013). A range of biological activities has been attributed to them, from allelopathy, insect feeding deterrent, antibiotic, antifungal, and antiparasitic, to allergenic, toxic, and antiproliferative effects in animal and human cells.

Sesquiterpene lactones have been shown to have cytotoxic effects in cancer cells (Ghantous et al., 2010; Picman, 1986); however, little research has been done regarding their mechanism of action leading to cell death. Our laboratory collected the information about previous research made with SLs reporting a cell cycle arrest and a compilation can be found in the review from (Bosco & Golsteyn, 2017). Strikingly, all sesquiterpene lactones with described anti-mitotic activity to date were isolated from species from the Asteraceae family. We have identified and characterized seven species from the Asteraceae family

that are predominant in the prairie ecosystem and have anti-mitotic activity (Bosco, 2017; Bosco et al., 2021; Molina, 2018; Molina et al., 2021b). We believe that the anti-mitotic activity of SLs present in Asteraceae species is understudied and that more chemicals and plants need to be investigated. **Table 1** provides a list of Asteraceae species for launching these studies. It is likely that this argument can be applied to other plant families and Canadian ecological zones for other biomedical activities, hinting at the vast potential of natural products that remain to be discovered.

CHAPTER 3

Materials and Methods

3.1 Plant collection

The aerial plant parts of the species represented in **Table 3**. were collected from the locations indicated in **Table 4**. Plants were harvested and stored at room temperature in paper bags until processed for extract preparation. Plant taxonomy was confirmed to species by consulting the Flora of Alberta (Moss & Packer, 1983). Information including site description, location, associated species and collection date and were stored and a voucher was deposited in the University of Lethbridge Herbarium.

Table 3. Canadian prairie Asteraceae species under investigation.

Scientific Name	Common Name	Asteraceae Tribe	Extract Library Code
Arnica fulgens Pursh	Foothill Arnica, Shining Arnica	Madieae	PP-1050
Ratibida columnifera (Nutt.) Wooton and Standl.	Prairie Cone-flower	Heliantheae	PP-1140
Hymenoappus filifolius Hooker	Fineleaved Wooly-white	Bahieae	PP-1400

Table 4. Collection information for plants under investigation.

Plant Code	Harvesting Date	Location (GPS coordinates)		Amount (g)	
		Latitude	Longitude	Wet	Dry
PP-1050	17 June 2019	49°05.802	-112°28.619	356.5	98.5
PP-1140	15 July 2019	49°40.06	-112°49.13	187.0	70.5
PP-1400	26 June 2020	49.09968	-112.47302	43.0	15.0

3.2 Extract preparation

Post-harvest, plants were placed to dry in a dehydrator at 40°C for 48-72 hours. Entire dried plants were stored in paper bags at room temperature in a dark and dry environment until extraction. To prepare plant extracts, the dried material was ground at room temperature with a blender followed by mortar and pestle until a fine powder was obtained. The solvents 100% dichloromethane (DCM) or 75% ethanol (EtOH/water) were added to the powder to make 10% w/v suspensions. Extract suspensions gently shaken in darkness on an orbital shaker at room temperature for 24 h. The suspensions were vacuum filtered to collect soluble fractions and dried at room temperature in a chemical fume hood for 2 – 4 days. The dried soluble fractions were collected, weighed, and labelled with a given code number and letter. Extracts made with EtOH were denoted with a letter "A" whereas DCM extracts were denoted with the letter "B". Extracts were stored in darkness at room temperature until samples were taken for experimental use. Samples were dissolved in dimethylsulfoxide (DMSO) (Sigma-Aldrich; D2438) to 50 mg/mL concentrations, centrifuged at 10,000 x g for 10 min and supernatants were stored at -20°C. Small aliquots were made to avoid freeze/thaw cycles.

3.3 Cell culture

For all biological assays the human colorectal adenocarcinoma HT-29 cell line was used, a cell line provided by the American Type Culture Collection (ATCC). The cells were cultured in RPMI 1640 medium (ThermoFisher; 21870-092) supplemented with 2 mM GlutaMAX (ThermoFisher; 35050-061) and 10% (v/v) heat inactivated fetal bovine serum (ThermoFisher; 1248028). HT-29 cells were seeded at densities of either 3.0×10^5 per 25 cm^2 or 1.0×10^6 per 75 cm^2 flasks. Cells were cultured at 37°C in 5% CO_2 for 48-72 h and the media were changed prior to treatment. The compounds nocodazole (Sigma-Aldrich;

M1404) and paclitaxel (Sigma; T7402) were dissolved in dimethyl sulfoxide (DMSO) (Sigma-Aldrich; D2438) to 200 ng/mL and 100 μM concentrations. The sesquiterpene lactones parthenolide (Sigma-Aldrich; P0667-5MG) and pulchelloid A were dissolved in DMSO to concentrations 10 mM. Pulchelloid A was obtained by biology guided fractionation from *G. aristata* leaves by the laboratory of Dr. Raymond Anderson (Bosco et al., 2021). All compounds were stored at -20°C. As a negative solvent vehicle control, DMSO was added to not-treated (NT) cell groups at equal volume to the highest volume of plant extract or compound treatment added. The total volume of DMSO added never exceeded more than 1% (v/v).

3.4 Cell rounding activity assay

HT-29 cells were seeded at 2.0 x 10^5/well in a 6 well culture plate and incubated for 48 or 72 h prior to treatment to reach a cell confluency of 50-70%. NT cells were used as a negative control, and nocodazole (200 ng/mL) was included as a positive control for cell rounding. Images were captured after 16 or 24 h of treatment with an Infinity 1 camera powered by Infinity Capture imaging software (Lumenera Corporation) on an Olympus CKX41 inverted microscope. Images were processed using Adobe Photoshop (CC 2015 16.0). Adherent (interphase) cells and rounded (mitotic) cells were manually counted using Image J (1.47v) software and the percentage of rounded cells in the total sample was determined. Each experiment was performed at least three times and the mean and standard error of the mean of the percentage of rounded cells were calculated.

3.5 Immunofluorescence microscopy

3.5.1 Alpha tubulin and PH3 immunofluorescence assays

HT-29 cells were seeded at a density of 2.0 x 10^5/well in 6 well culture plates and incubated at 37°C for 48 or 72 h prior to treatment. After 16 hours of treatment, cells were fixed. Fixation for α-tubulin or PH3 immunofluorescence was performed with 3% (v/v) paraformaldehyde (Fisher Scientific; 30525-89-4) diluted in PBS at room temperature for 20 min. Fixation was quenched with 50 mM NH_4Cl in PBS. Cells were permeabilized for 5 min using 0.2% (v/v) Triton X-100 in PBS and blocked for 30 min with 3% (w/v) BSA in PBS-T (0.1% (v/v) Tween-20 diluted in PBS). Cells were then incubated at 4°C overnight with the primary antibodies anti-phospho-Ser10 histone H3 (Millipore; 06-570(CH) in a 1:1000 dilution, anti-α-tubulin (Santa Cruz Biotechnology; sc-53030) in a 1:200 dilution. After washing with PBS-T, cells were incubated with secondary antibodies for 45 min at room temperature as follows: Alexa Fluor 488 rabbit anti-rat IgG (ThermoFisher; A11006; 1:200) for anti-α-tubulin, Alexa Fluor 594 AffiniPure goat anti-rabbit IgG (Jackson ImmunoResearch; 111-585-003; 1:300) for anti-phospho-Ser10 histone H3. Nuclei were stained with 300 nM DAPI (4′, 6-diamidino-2-phenylindole) (Fisher; LSD1306) in PBS for 15 min. Cells were observed and recorded with a CytationTM 5 Cell Imaging Multi-Mode Reader using Gen5 software (BioTek Instruments, USA).

Cells positive for phospho-Ser10 histone H3 and total number of cells (DAPI stained) were counted with Gen5 software using exposure settings from not-treated cells as the threshold for fluorescent signal. A minimum of 200 cells were counted for each treatment and the mean and standard error of the mean percentage of PH3-positive cells of at least three independent experiments were calculated. For the analysis of the mitotic spindles, at least three independent experiments were performed and a minimum of 50 mitotic cells per

treatment were observed in total to evaluate mitotic spindle morphology. DMSO-treated mitotic cells were used as a reference for normal, non-distorted mitotic spindles. The mean percentage and standard error of the mean of distorted spindles was calculated for each treatment.

3.5.2 Gamma tubulin immunofluorescence assay

We modified the immunofluorescence protocol for γ-tubulin analysis as follows. HT-29 cells were seeded at a density of 2.0 x 10^5/well on glass coverslips in 6 well culture plates. After 16 h of treatment, cells were treated for 90 sec with 0.05% (v/v) Triton X-100 in a PBS buffer containing 0.5 mM $MgCl_2$ and 1 mM EGTA as per Pepper and Brinkley (1979) prior to fixation with ice cold 100% methanol. This buffer was used as the base instead of PBS or PBS-T for all steps of the protocol to reduce background staining appearance in images. We used anti-γ-tubulin antibodies (Sigma-Aldrich; T6557) in a 1:1000 dilution as the primary antibody, and Alexa Fluor 488 rabbit anti-mouse (ThermoFisher: 11059, 1:400) as secondary antibody for anti-γ-tubulin. Nuclei were stained with DAPI as previously described.

Coverslips were mounted onto microscope slides using ProLong Gold Antifade reagent (ThermoFisher; P36934) and viewed with an Olympus BX41 microscope using an Infinity 3 camera operated by Infinity Capture imaging software (Lumenera Corporation). Images were prepared for analysis using Adobe Photoshop (CC 2015 16.0) software.

For γ-tubulin image analysis, images were rotated till at least two of the centrosomes in individual cells were aligned along the x axis of the image. Areas 375 x 375 pixels containing individual cells were analyzed using ImageJ software. The plot profile of the selected area was analyzed to obtain the gray value intensities of each pixel inside of the

area. These values were listed and recorded for 15 cells in each treatment group. GraphPad Prism 9 software was then used to calculate the mean and SEM of plot profiles from 15 cells in each treatment group, for three independent experiments.

3.6 Statistical analysis

Data were analyzed using Microsoft Excel 2016 and GraphPad Prism 9 software. Data were plotted as means from three independent experiments ± standard error of the mean. One-way analysis of variance (ANOVA) with Tukey's post hoc test were used to analyze results from light microscopy and immunofluorescence microscopy assays. Differences were considered significant when $p < 0.05$.

3.7 Analysis of transcriptome of cells treated with anti-mitotic chemicals

3.7.1 Collection of RNA from mitotic cells

HT-29 cells were seeded at 0.3 x 10^6 cells into T25 flasks and incubated for 48 or 72 h prior to treatment to reach a cell confluency of 50-70%. HT-29 cells were treated with pulchelloid A (pulA) at 10 µM and parthenolide (Sigma-Aldrich; P0667-5MG) at 20 µM. Cells treated with paclitaxel at 100 nM as a positive control for mitotic arrest, and cells treated with 0.05% DMSO as a not treated control group. After 16 h treatment images were captured with an Infinity 1 camera powered by Infinity Capture imaging software (Lumenera Corporation) on an Olympus CKX41 inverted microscope. The not treated control group cells were lifted with trypsin, while cells treated with paclitaxel, parth, and pulA were collected via mechanical shake-off (Lewis et al., 2013). A minimum of 1 x 10^6 cells were collected for each sample.

The cell suspensions were centrifuged for 5 min at 1000 × *g* and re-suspended in 1 mL TRIzol reagent (Fisher; 15596026) for 2 min. The mixture was phase separated by the

addition of 500 µL amene stabilized chloroform (Sigma-Aldrich; C2432). The TRIzol/chloroform suspension was incubated for 2.5 min with mixing by inversion, and then centrifuged at 12,000 × *g* at 4°C for 15 min. The aqueous layer containing the RNA was transferred to a new tube which was then mixed with 500 µL of isopropanol (Fisher Scientific; BP26181) and incubated for 1 h at -20°C. After incubation, the mixture was centrifuged for 10 min at 12,000 × *g* at 4°C. After discarding the supernatant, the pellet was re-suspended in 1 mL of 75% ethanol/water and centrifuged for 5 min at 7600 × *g* at 4°C. The supernatant was discarded, and the pellet was allowed to dry for 10 min. The air-dried pellet was resuspended in 50 µL of nuclease free water and heated at 55°C for 15 min. RNA samples were given a code that corresponded to the date of extraction (DDMMYY) and the treatment group. The RNA was further processed using RNA Clean and Concentrator (Zymo Research; R1017) kit to remove residual DNA. Total RNA was analyzed for the nucleic acid to protein ratio (A260:A280) and concentration in ng/µL using a BioDrop µLITE+ (Biochrom) and stored at -80 °C.

3.7.2 Long RNA Library Construction

To create cDNA libraries a minimum of 300 ng up to 1000 ng total RNA was depleted for ribosomal RNA using NEBNext® rRNA Depletion Kit (NEB, E6310). The ribosomal depleted RNA was then 2.2× bead cleaned using Omega NGS Total Pure Mag Beads (Omega). NEBNext® Ultra™ II DNA Library Prep Kit for Illumina® (NEB; E7660) was used to prepare libraries with 1:5 adaptor dilutions. PCR reaction conditions were 15 cycles following kit temperatures and times. Index primers were optimized according to (NEB; E7420) using NEBNext® Multiplex Oligos for Illumina® (NEB; E7335) for 2.5 µL of index and universal primer per library. Samples were 0.9× bead cleaned prior and then

visualized using Agilent Bioanalyzer 2100 High Sensitivity DNA kit to confirm presence of cDNA library in sample and analyze library length in base pairs.

3.7.3 qPCR Analysis

Quantitative PCR was performed using the NEB Library Quant Kit (NEB; E7630) to determine the concentration of amplifiable DNA within cDNA libraries. Reactions were arranged so that cDNA was diluted to 1:10,000 in nuclease free water. Total reaction volume was 10 µl. Analysis of kit DNA standards and cDNA libraries was performed on two biological replicates and three technical replicates. The Bio-Rad CFX384 Real-time detection system was used for qPCR with measurements taken during extension steps. Thermocycler conditions were as follows: 1 min at 95°C (15 s at 95°C and 45 s at 63°C) × 40 cycles. The following equation was used to calculate the concentration of cDNA libraries:

$$calculated\ library\ [pM] = \frac{library\ Ct - b}{a}$$

Where $b =$ the intersect, and $a =$ the slope of the line of the kit DNA standards standard curve, and $ct =$ qPCR cycle threshold. The final adjusted library concentration was calculated using the manufacturer's protocol. The cDNA libraries were sequenced using Illumina® HiSeq 3000/4000 System following manufacturer's instructions. The resulting sample reads were obtained in fastq file format. Each library was Illumina® sequenced once with a depth of > 20 M reads.

3.8 Bioinformatics analysis

Gene expression analysis was performed for HT-29 cells treated with paclitaxel, parth, and pulA. Illumina® sample reads were first trimmed to remove adaptors using cutadapt 1.18

(Martin, 2011). The reads were then aligned against a human genome reference acquired from ensemble (GRCh38/November 2018, primary assembly) using hisat2-2.1.0 in paired end mode. We used samtools-1.6 to convert the generated SAM format files to BAM format files. The BEDtools 2.26.0 bamToBed function was then used to convert the BAM files to BED format. We then used StringTie-1.3.4d to assemble the alignments and estimate the expression levels using the ensembl GRCh38 release 104 .gff3 file as a reference annotation. We used the R (version 3.4.3) package DESeq2 (Love et al., 2014) to perform differential gene expression analysis on the files produced from StringTie. A separate DESeq2 analysis was performed for each treatment group to compare the transcript counts between each treatment and the not treated control group. From these analyses we obtained the $\log_2$(fold change), p-values, and Benjamini-Hochberg adjusted p-value (padj) for each transcript that was differentially expressed. We performed principal component analyses with the resulting datasets to measure variability between replicates and treatments using R. The transcript IDs were converted to stable gene IDs using ensemble Biomart and gene lists were uploaded to the Database for Annotation, Visualization and Integrated Discovery (DAVID) v6.8. The DAVID Functional Annotation Tool was used to identify the biological processes represented by the genes in the dataset. We used R to generate diagrams representing microtubule genes and their expression in each dataset.

CHAPTER 4

Results

4.1 Investigation of mitotic arrests induced by Asteraceae extracts using cell biology techniques

The search for chemicals with anti-mitotic activities is important because they can be used as scientific tools with which to study cell division, and sometimes they may become anti-cancer medicines. We have observed that extracts prepared from different Asteraceae species can arrest cancer cells in mitosis. Previous work in our laboratory has led to isolation of different sesquiterpene lactones that are the source of the anti-mitotic activity - pulchelloid A from *Gaillardia aristata* and hymenoratin from *Hymenoxys richardsonii* (Molina et al., 2021b). These results have led us to ask whether other Asteraceae species in the prairie ecological zone contain anti-mitotic sesquiterpenes, and if so will there be a diversity in the biological activity of these chemicals that reflects taxonomical diversity? We chose to investigate *Ratibida columnifera* Nutt., a member of the Heliantheae tribe, which is closely related to tribe Helenieae and the Gaillardiineae subtribe (**Figure 2**). The Bahieae tribe was also of interest because it is distantly related to Helenieae and closely related to tribe Madieae, which contains *Arnica* species. Therefore, we selected *Hymenoppapus filifolius* Hook. of tribe Bahieae and *Arnica fulgens* Pursh. (Madieae) for investigation. We tested the capacity of extracts from above-ground material to induce anti-mitotic effects in cancer cells by measuring cell rounding activity, phosphorylation of histone H3, and morphology of the mitotic spindles and centrosomes.

4.1.1 Asteraceae species extracts induce rounded cell accumulation in HT-29 cells

We used a phenotypic assay for cell rounding to test Asteraceae species from different tribes for mitotic arrest activity. During mitosis, cells acquire a rounded shape to ensure

equal segregation of genetic material and cytoplasm (Cadart et al., 2014). After treatment. The number of rounded cells are counted and divided by the total number of cells to obtain the percentage of rounded cells. The mean percentage of rounded cells and the standard deviation was calculated for each concentration from three independent experiments and compared to every other treatment mean for statistical significance.

We added the extract solvent DMSO as our negative control (NT, not-treated), and the tubulin toxin nocodazole, which causes mitotic arrest, as our positive control. Extracts prepared with 75% (v/v) ethanol identified by the letter A in their extract code, and 100% dichloromethane extracts identified with the letter B were applied to HT-29 cancer cells. Six extracts in total were prepared from three Asteraceae species. The extracts were tested on HT-29 cancer cells at a range of concentrations to observe cell rounding activity. Photos representing NT and nocodazole treated HT-29 cells for each extract experiment are included in each figure.

The first species we investigated was *R. columnifera* a member of the Heliantheae tribe. This tribe is closely related to the Helenieae tribe that contains *G. aristata* and *H. richardsonii* (Baldwin et al., 2002). To test *R. columnifera* extracts for cell rounding activity, PP-1140A and PP-1140B were applied to HT-29 cells at concentrations of 1.5 – 50 µg/mL for 16 h. The percentage of rounded cells from three experiments were compared to NT cells (**Figure 6B**). The percentage of rounded HT-29 cells was 4.8 ± 1% for NT cells, as expected. After 16 h nocodazole-treated cells had a mean percentage of 58.2 ± 9 % and after 24 h were nearly completely rounded (99.1 ± 0.7%).

Extract PP-1140A at concentrations of 1.5 and 5 µg/mL demonstrated cell rounding percentages of 4.5 ± 1%, and 5.0 ± 0.9%, respectively. At 15 µg/mL PP-1140A had 16.8 ±

0.8% rounded cells. Cells lost flat morphology and were not rounded or adhered to the substrate (**Figure 6A**) at 50 µg/mL, therefore that concentration was determined to be toxic. Cells treated with PP-1140B had 4.3 ± 1% rounded cells at 1.5 µg/mL and 21.0 ± 0.9% at 5 µg/mL. PP-1140B was toxic to cells at concentrations of 15 and 50 µg/mL. When compared to the percentage of rounded cells in NT cells, PP-1140A at 15 µg/mL and PP-1140B at 5 µg/mL were significantly different (**Figure 6B**).

Our laboratory had identified mitotic activity within extracts of the species *Arnica cordifolia* Hook. (Molina, 2018) of the Madieae tribe. We therefore selected a species from this tribe, *Arnica fulgens* Pursh. for cell rounding activity. In testing *A. fulgens,* we explored if this observation that Asteraceae species from the same tribe contain similar anti-mitotic activities would be supported in the *Arnica* genus. We therefore treated HT-29 cells with two *A. fulgens* extracts. An ethanolic extract, PP-1050A, was used at concentrations of 0.5 to 15 µg/mL, and a dichloromethane extract, PP-1050B, was used at concentrations of 0.15 – 5 µg/mL. After 24 h, photographs were taken, and the images were used to determine the percentage of rounded cells for each treatment. As observed in **Figure 7B**, the ethanolic extract PP-1050A induced 6.0 ± 1% at 0.5 µg/mL, 5.6 ± 2% at 1.5 µg/mL, 17.3 ± 6% at 5 µg/mL, and 52.7 ± 12% at 15 µg/mL. Following a similar trend, the dichloromethane extract PP-1050B also increased the percentage of rounded cells. PP-1050B-treated cells had 5.6 ± 2% at 0.15 µg/mL, 7.7 ± 2% at 0.5 µg/mL, 15.1 ± 5% at 1.5 µg/mL, and 53.9 ± 22% at 5 µg/mL. When we compared the rounded cell percentages of each treatment to NT cells, significant differences were found between NT and PP-1050A at 15 µg/mL, and PP-1050B at 5 µg/mL.

We then tested the species *Hymenopappus filifolius* for cell rounding activity. This species is a member of the Bahieae tribe, which is more closely related to the Madieae rather than Heliantheae or Helenieae tribes. HT-29 cells were treated with PP-1400A or PP-1400B at concentrations of 15-50 µg/mL. In addition to our controls of DMSO and nocodazole, a *G. aristata* extract (PP-190D) was used as a third extract control. This extract was prepared alongside PP-1400A and PP-1400B and was used as a control for extract preparation. After treatment with PP-190-D at 50 µg/mL the percentage of rounded cells was 49.3 ± 8%. PP-1400A treated cells had a moderate increase in rounded cells with increasing concentrations of extract (**Figure 8**). The percentage of rounded cells were 5.5 ± 0.4% at 1.5 µg/mL, 6.1 ± 0.8% at 5 µg/mL, and 15.9 ± 0.4% at 15 µg/mL. Cells lost flat morphology and were not rounded nor adhered to the substrate at 50 µg/mL and therefore that concentration was determined to be toxic to cells. Although the primary activity of PP-1400A at 50 µg/mL appeared to be cytotoxic, we were still able to observe rounded cells (**Figure 8A**). Cells treated with extract PP-1400B had rounded cell percentages of 5.4 ± 0.6% at 1.5 µg/mL and 22.2 ± 5.6 at 5 µg/mL. Concentrations above 5 µg/mL were toxic to HT-29 cells, demonstrated by loss of flattened interphase cells (**Figure 8**). Although we could observe some rounded cells, the cell rounding percentages of PP-1400A or PP-1400B were not significantly different from those of NT cells (**Figure 8A**).

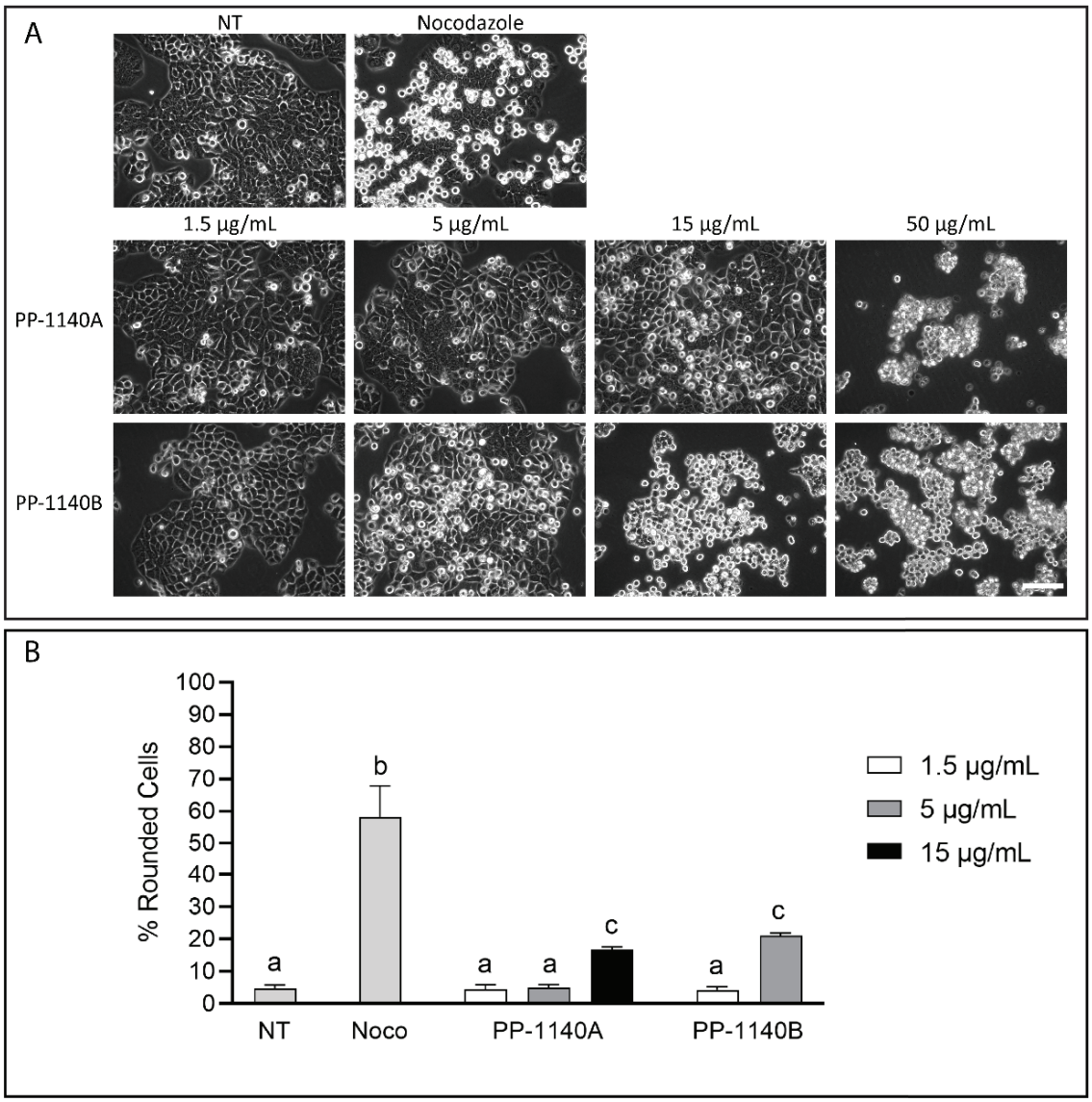

Figure 6. Accumulation of HT-29 cells with rounded morphology when treated with *Ratibida columnifera* extracts (PP-1140A: EtOH extract, PP-1140B: DCM).. NT and nocodazole at 200 ng/mL were used as negative and positive controls for cell rounding. Scale bar: 100 µm (**A**). Rounded cells were counted from light microscopy photos taken 16 h post treatment. Treatments that are significantly different from other treatments are represented with a different letter (a, b, c). Statistical significance determined via one-way ANOVA followed by Tukey's post hoc tests ($p < 0.05$). Data values represent means ± SEM, n = 3 (**B**).

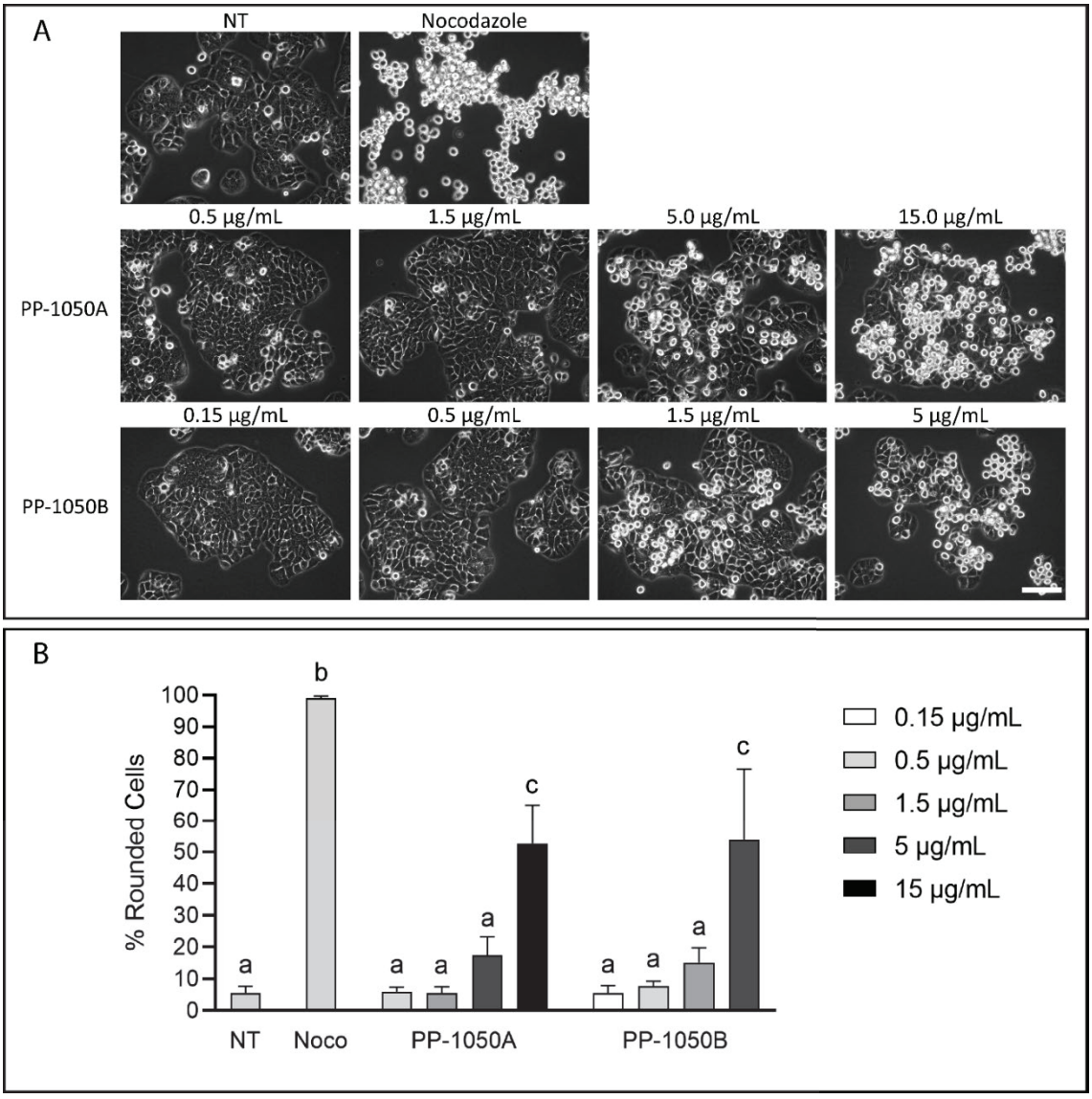

Figure 7. Percentage of HT-29 cells that acquire rounded morphology when treated with *Arnica fulgens* extracts (PP-1050A: EtOH extract, PP-1050B: DCM).NT and nocodazole at 200 ng/mL were used as negative and positive controls for cell rounding. Scale bar: 100 µm (**A**). Rounded cells were counted from light microscopy photos taken 24 h post treatment. Treatments that are significantly different from other treatments are represented with a different letter (a, b, c). Statistical significance determined via one-way ANOVA followed by Tukey's post hoc tests ($p < 0.05$). Data values represent means ± SEM, n = 3 (**B**).

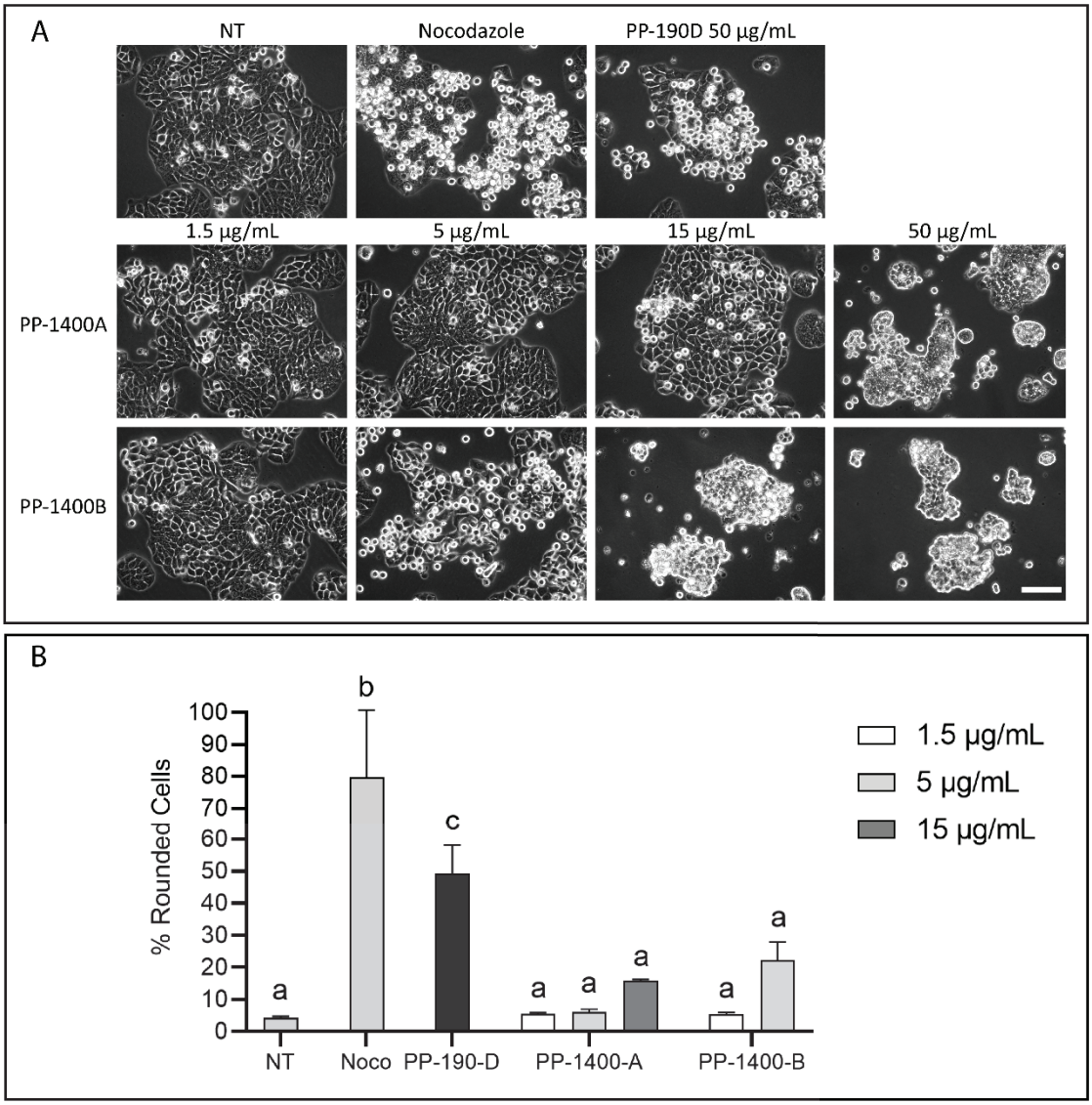

Figure 8. Percentage of HT-29 cells that acquire rounded morphology when treated with *Hymenopappus filifolius* extracts (PP-1400A: EtOH extract, PP-1400B: DCM). NT and nocodazole at 200 ng/mL were used as negative and positive controls for cell rounding. *G. aristata* extract PP-190D was used as positive cell rounding extract control. Rounded cells were counted from light microscopy photos taken 16 h post treatment. Scale bar: 100 µm (**A**). Treatments that are significantly different from other treatments are represented with a different letter (a, b, c). Statistical significance determined via one-way ANOVA followed by Tukey's post hoc tests ($p < 0.05$). Data values represent means ± SEM, n = 3 (**B**).

4.1.2 Asteraceae species extracts induce mitotic arrest demonstrated by PH3 immunofluorescence assay

Although cell rounding is a characteristic of mitotic cells, it is possible for human cells to be rounded without being in mitosis. We tested whether cells that were rounded after extract treatment contained other features of mitosis, such as changes in chromosome and histone organization. We performed immunofluorescence assays using anti-phosphohistone H3 (PH3) antibodies and DAPI to stain DNA. As with the cell rounding assay, NT cells and nocodazole were used as negative and positive controls. The highest concentration of each extract that induced an increase in rounded cells was used in these experiments. HT-29 cells were treated for 16 h after which photos were taken for analysis. For each experiment, a mitotic index was calculated by counting the number of PH3 positive cells amongst DAPI stained cells. Experiments were performed in triplicate and the mitotic index values were compared between treatments to determine significant differences.

HT-29 cells with either not treated, or treated with nocodazole, or with *R. columnifera* extracts PP-1140A and PP-1140B at 5 µg/mL for 16 h and then subjected to the PH3 immunofluorescence assay. The mean percentage of PH3 positive NT HT-29 cells was 4.9 ± 0.8%, and nocodazole-treated cells had 60.8 ± 13 %, values that were similar to the cell rounding percentages, as expected. As shown in **Figure 9** and **Figure 12**, the percentage of PH3 positive cells for PP-1140A at 5 µg/mL was comparable to that of NT cells at 6.0 ± 2%. Extract PP-1140B at 5 µg/mL accumulated more mitotic cells than NT cells at 12.8 ± 6%. The mitotic indices of these extracts were not statistically significantly different from those of NT cells.

We tested *A. fulgens* extracts PP-1050A at 15 µg/mL, and PP-1050B at 5 µg/mL for 16 h. Consistent with the observations of the cell rounding assay, cells treated with PP-1050 extracts had more cells in mitosis than NT cells, but fewer mitotic cells than nocodazole (**Figure 10**). We found that PP-1050A induced 33.2 ± 16% mitotic cells, and PP-1050B induced 27.1 ± 4% mitotic cells (**Figure 12**). Both mitotic indices were significantly different from those of NT cells.

Although the rounded cell percentages were not significantly different between NT cells and *H. filifolius* extracts, we performed an immunofluorescence microscopy experiment to determine whether the rounded cells we had observed were in mitosis. We found that PP-1400 extracts slightly increased the percentage of mitotic cells (**Figure 11**). After treatment with PP-1400A the mitotic index was 8.6 ± 2%, and after treatment with PP-1400B the percentage was 10.5 ± 2% (**Figure 12**). The results of this immunofluorescence assay supported the cell rounding results, *H. filifolius* extracts increased the number of mitotic cells but they were not significantly different from those of NT cells.

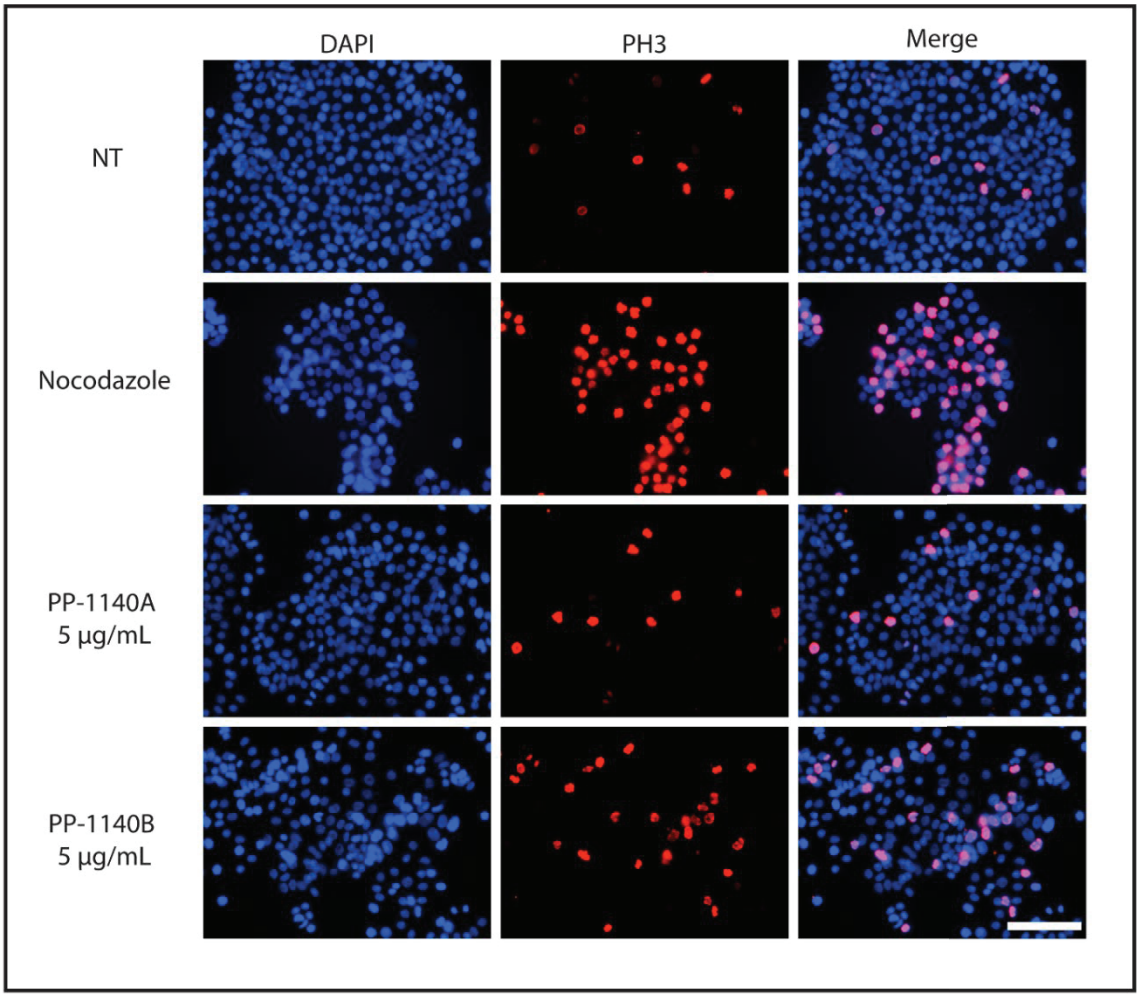

Figure 9. Mitotic cells accumulated after treatment with *R. columnifera* extracts PP-1140A and PP-1140B (A: EtOH, B: DCM) at 5 µg/mL for 16 h. Negative control: NT. Positive control: nocodazole 200 ng/mL. Analysis by immunofluorescence microscopy. Red: 61hosphor-histone H3 (mitotic cells). Blue: DAPI (DNA). Scale bar: 100 µm.

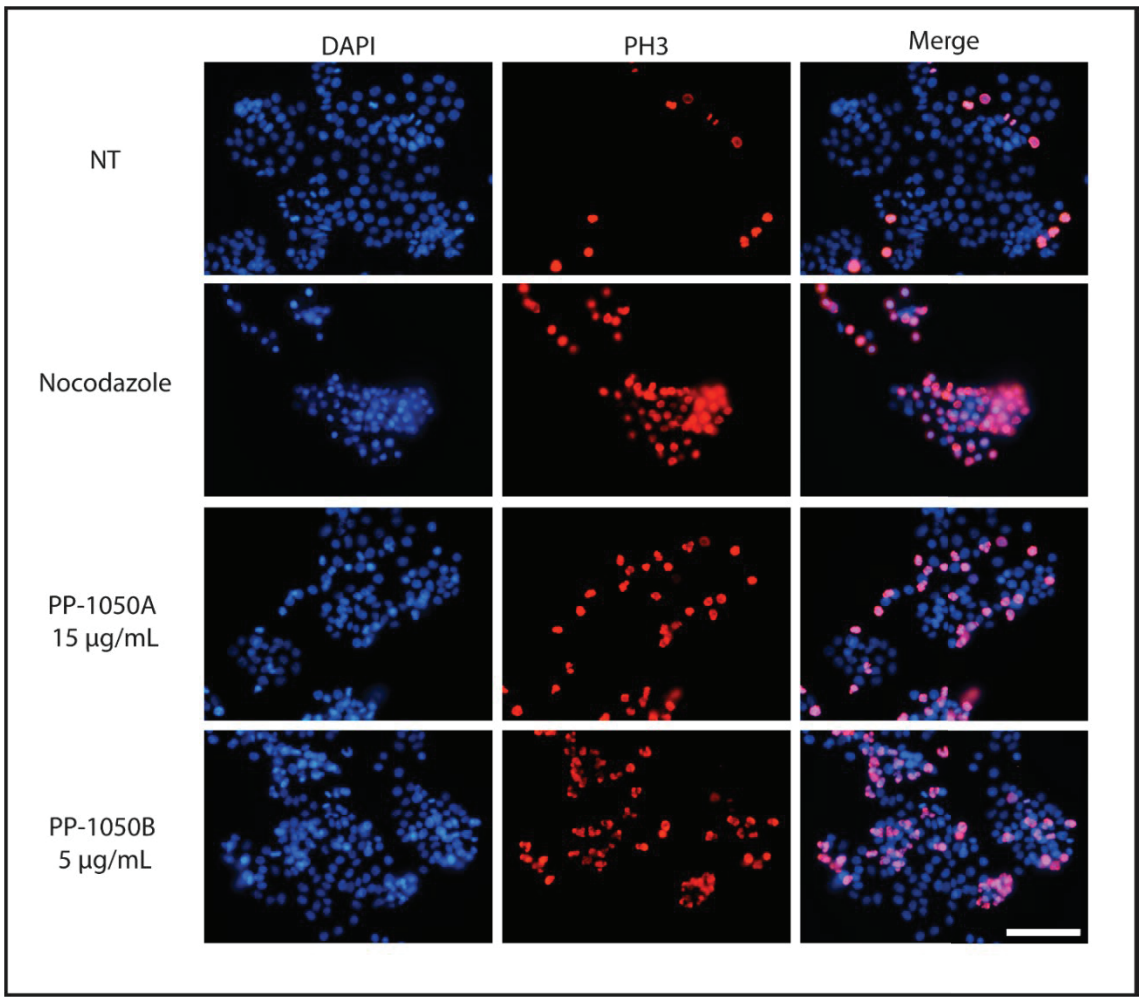

Figure 10. Mitotic cells accumulated after treatment with *A. fulgens* extracts PP-1050A at 15 and PP-1050B (A: EtOH, B: DCM) at 5 µg/mL for 16 h. Negative control: NT. Positive control: nocodazole 200 ng/mL. Analysis by immunofluorescence microscopy. Red: 62hosphor-histone H3 (mitotic cells). Blue: DAPI (DNA). Scale bar: 100 µm.

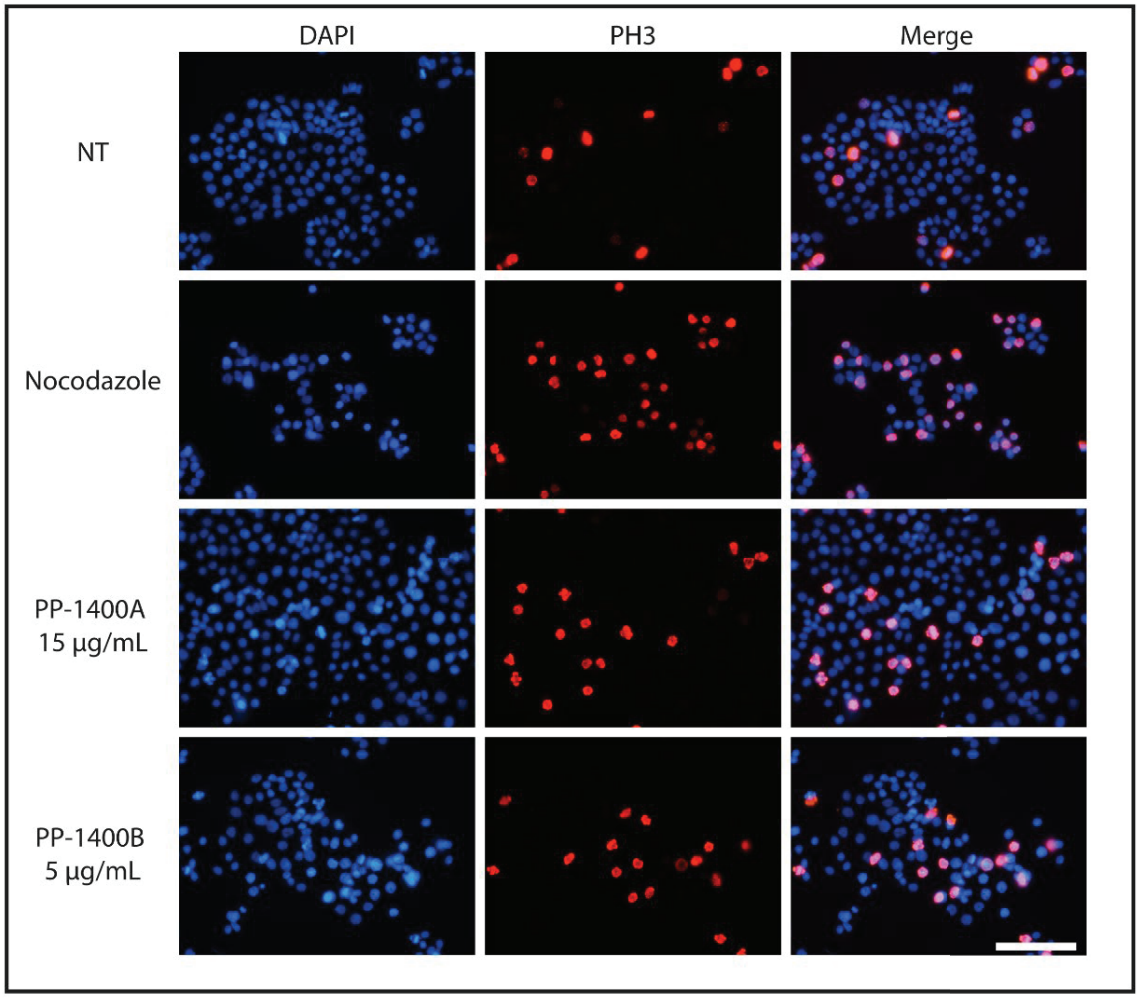

Figure 11. Mitotic cells accumulated after treatment with *H. filifolius* extracts PP-1400A at 15 and PP-1400B (A: EtOH, B: DCM) at 5 µg/mL for 16 h. Negative control: NT. Positive control: nocodazole 200 ng/mL. Analysis by immunofluorescence microscopy. Red: phospho-histone H3 (mitotic cells). Blue: DAPI (DNA). Scale bar: 100 µm.

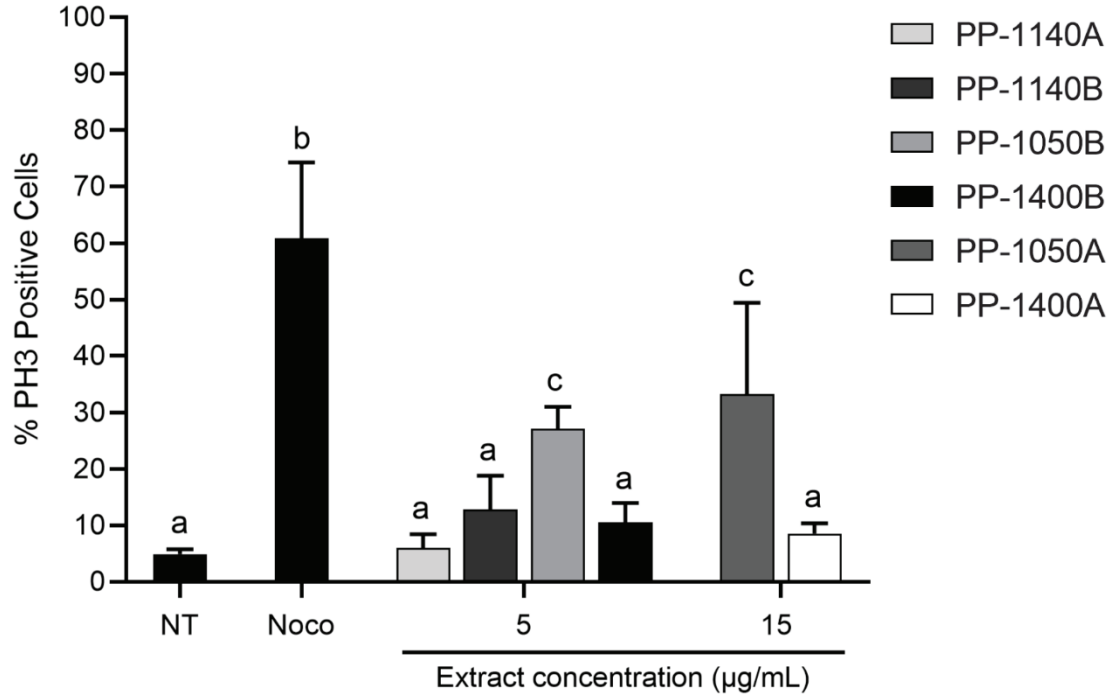

Figure 12. Mitotic indices based on mean percentages of PH3-positive HT-29 cells after treatment with six Asteraceae plant extracts at 5 and 15 µg/mL. NT and nocodazole treated cells used as negative and positive controls. Error bars represent the SEM of at least three independent experiments. Treatments that are significantly different from other treatments are represented with a different letter (a, b, c). Statistical significance was determined using one-way ANOVA followed by Tukey's post hoc test ($p < 0.05$).

4.1.3 Extracts from Asteraceae species change mitotic spindle morphology

During the course of my experiments, I was able to find a number of Asteraceae species that could arrest cells in mitosis, and I had handled other extracts with anti-mitotic activity that were in the laboratory. It was puzzling, however, that an identical activity would be distributed throughout a number of species. Furthermore, I was beginning to notice that in treated cells there were subtle differences in the organization of chromosomes by DAPI staining. In the laboratory we were beginning to suspect that although different extracts could arrest cells mitosis, the mitotic arrests were in fact different from each other.

Mitosis is a process that carefully orchestrates the duplication and separation of chromosomes. Microtubules are one structure that form during mitosis from α and β-tubulin subunits. Several chemicals induce mitotic arrest by interrupting the function of microtubules, such as paclitaxel and nocodazole. Therefore, we sought to examine the anti-mitotic activity of these Asteraceae extracts by observing mitotic spindle morphology in cells. To do this, we performed experiments in which we used immunofluorescence microscopy and anti-α-tubulin antibody to label microtubules in cells, and DAPI. Not treated cells would have a range of bi-polar spindle structures (prophase to telophase) whereas cells treated with nocodazole would not have spindles. Cells were treated with Asteraceae extracts at the same concentrations used to give PH3 immunofluorescence signals. Representative photographs are included in each figure to demonstrate the observed effects.

In NT cells we observed a range of spindle structures including a normal bipolar mitotic spindle with α-tubulin arrangements extending towards the center of the cell. The spindle poles are observed as two points of intensity at opposite ends of the cell (**Figure 13**). Nocodazole treated cells did not form microtubules (**Figure 13**), as expected because nocodazole binds 1:1 with α-tubulin preventing microtubule polymerization (Jordan et al., 1992).

After observing an increase in rounded and PH3 positive cells after treatment with *R. columnifera* extracts, we examined the α-tubulin arrangements in HT-29 cells treated with these extracts. Cells were treated with PP-1140A and PP-1140B at 5 µg/mL for 16 h. The PP-1140A extract treated cells displayed both normal bipolar α-tubulin arrangements and distorted spindle morphology (**Figure 13**), with 40.4 ± 12.7% cells containing distorted

spindles (**Figure 16**). We observed similar results in PP-1140B treated cells, which had 69.5 ± 7.6% distorted spindles (**Figure 16**).

A. fulgens extracts were shown to arrest cells in mitosis by increasing the percentage of PH3 positive cells, therefore, PP-1050A and PP-1050B were applied to cells at 15 µg/mL and 5 µg/mL respectively, to observe any effects on tubulin arrangements. As seen in **Figure 14**, HT-29 cells treated with PP-1050A at 15 µg/mL formed spindles, however 67.6 ± 5.3% cells contained distorted spindles, including spindles that did not have two clear spindle poles. Cells treated with PP-1050B formed a mitotic spindle, however 88.7 ± 5.3% were distorted spindles and cells contained three or more poles (**Figure 16**). This multipolar morphology is a new extract-induced, mitotic spindle distortion observed in our laboratory. Because of the distinct multipolar spindle distortion, PP-1050B was selected over PP-1050A for further experimentation.

Finally, we tested both *H. filifolius* extracts for their ability to impact tubulin arrangements. Cells were either not treated or treated with nocodazole, or PP-1400A at 15 µg/mL, PP-1400B and 5 µg/mL, for 16 h. We observed that cells treated with 15 µg/mL of PP-1400A contained 61.0 ± 13.2% cells with distorted α-tubulin arrangements, although some cells maintained two microtubule poles (**Figure 15**). The microtubules in cells treated with 5 µg/mL of PP-1400B also contained distorted α-tubulin arrangements and were not bipolar. Distorted spindles were observed on 64.4 ± 7.1% of cells treated with PP-1400B (**Figure 16**). This result was important because although the number of mitotic cells induced by treatment was not significantly higher than that of NT (**Figure 12**), the treated cells had distorted spindles, indicating a mitotic arrest. When considered with the cell rounding results of PP-1140, (**Figure 6**) this extract as likely contains chemicals that induce mitotic

arrest as well as those which produce another phenotype that may interfere with the mitotic arrest.

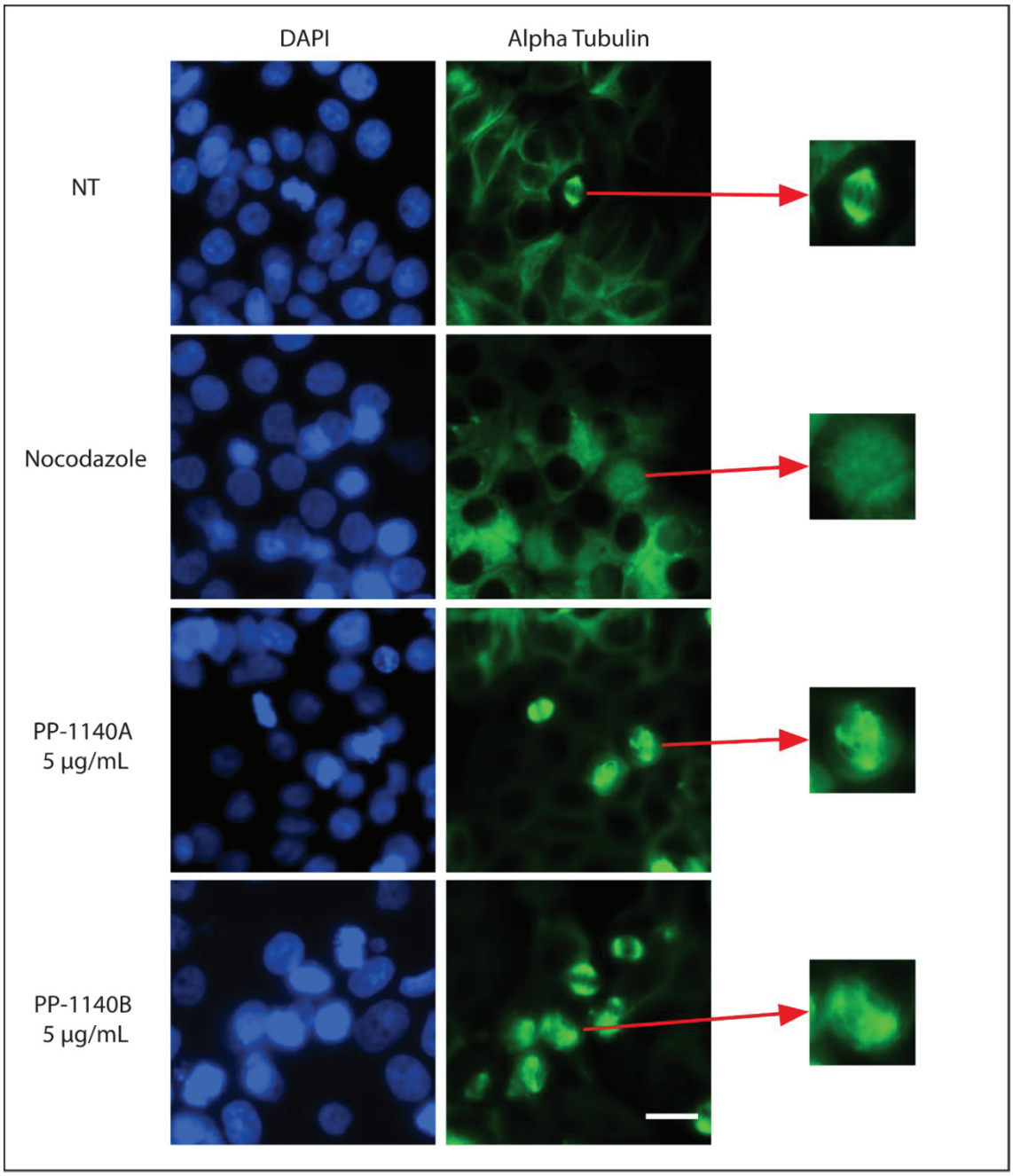

Figure 13. Mitotic spindles in HT-29 cells treated with *R. columnifera* extracts PP-1140A and PP-1140B at 5 µg/mL. (A: EtOH, B: DCM). Negative control: NT. Positive control: nocodazole 200 ng/mL. Analysis by immunofluorescence microscopy. Green: α-tubulin (mitotic spindle) Blue: DAPI (DNA). Scale bar: 20 µm.

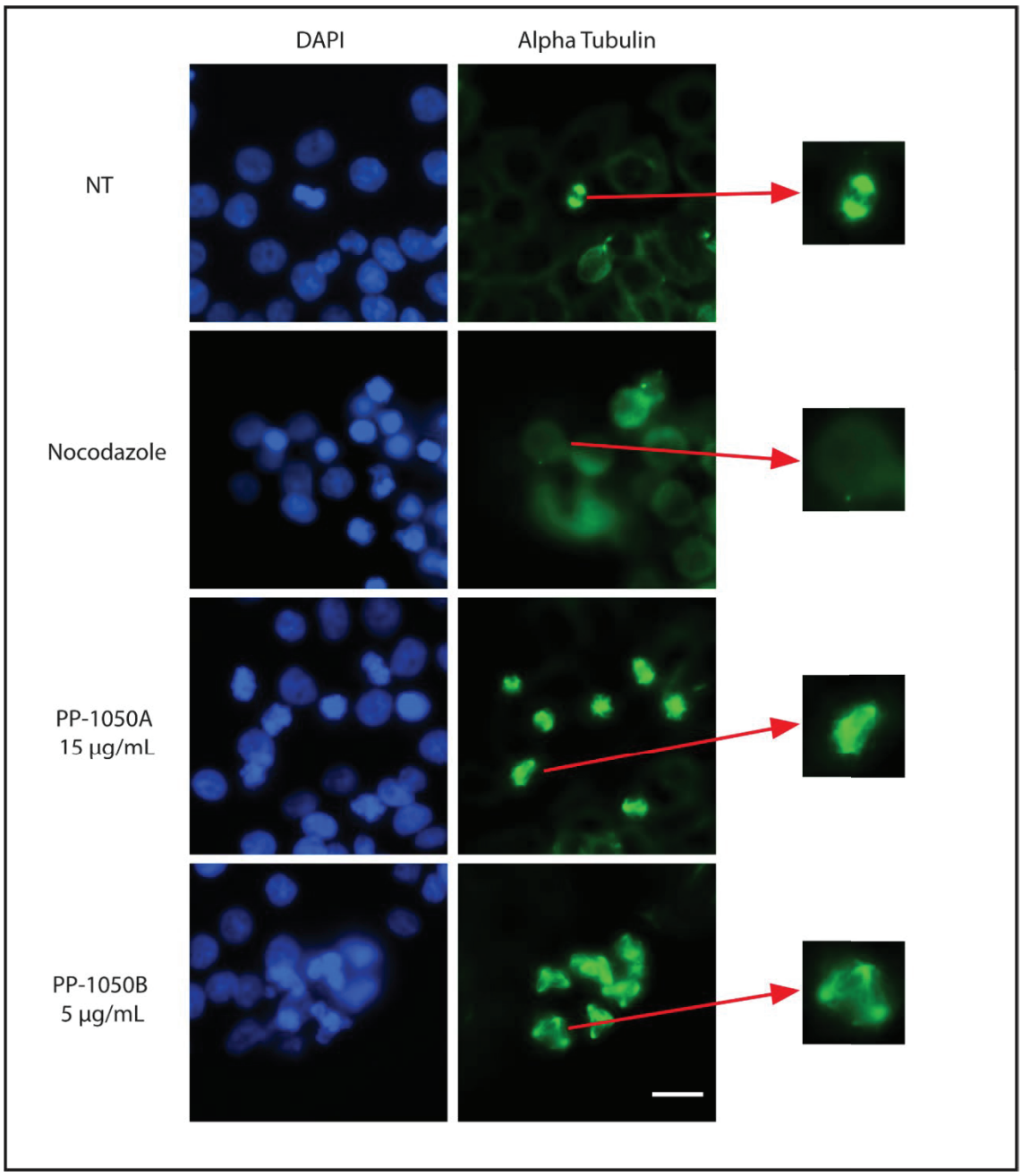

Figure 14. Mitotic spindles in HT-29 cells treated with *A. fulgens* extracts PP-1050A 15 µg/mL and PP-1050B at 5 µg/mL (A: EtOH, B: DCM). Negative control: NT. Positive control: nocodazole 200 ng/mL. Analysis by immunofluorescence microscopy. Green: α-tubulin (mitotic spindle) Blue: DAPI (DNA). Scale bar: 20 µm.

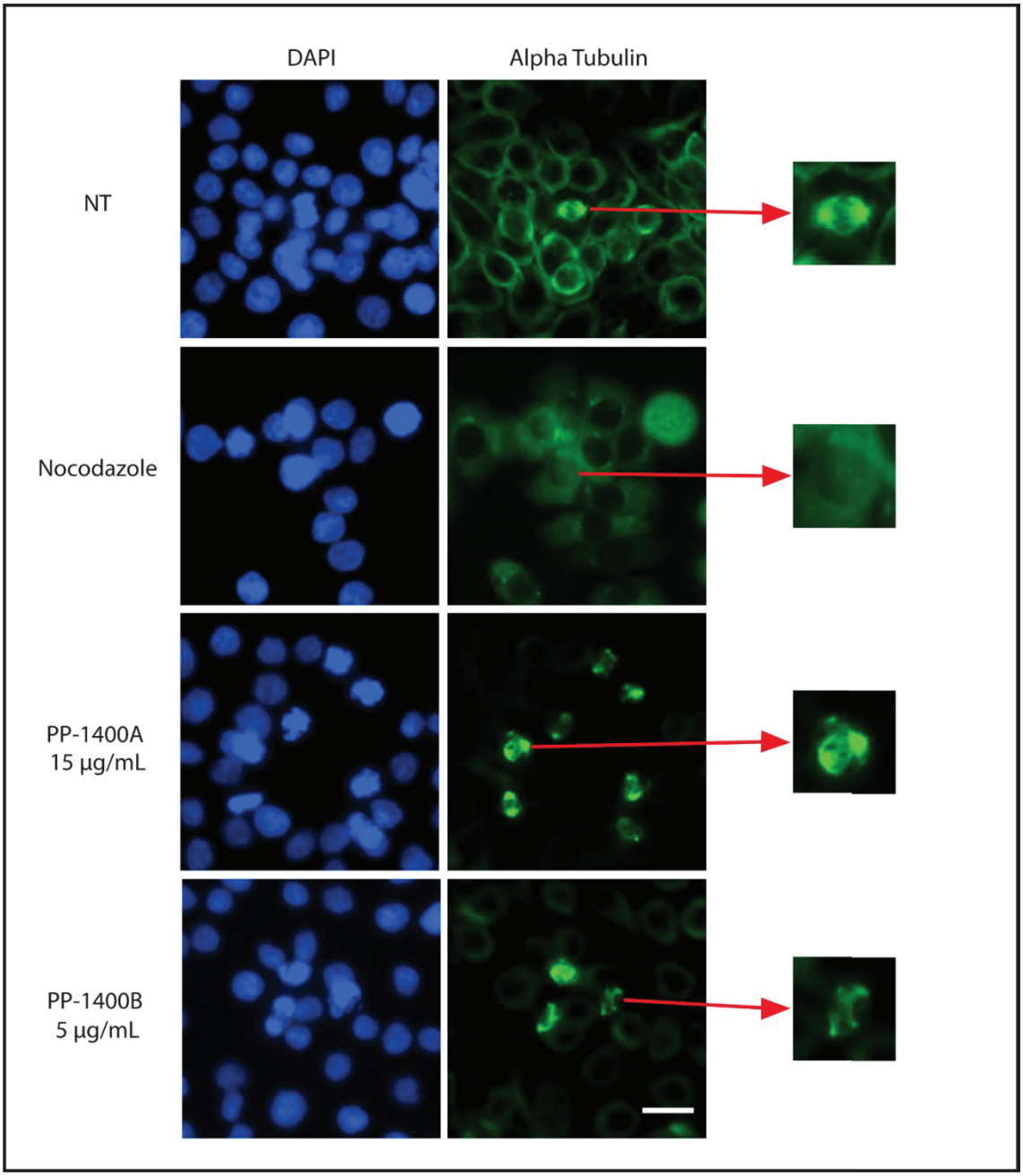

Figure 15. Mitotic spindles in HT-29 cells treated with *H. filifolius* extracts PP-1400A at 15 µg/mL and PP-1400B at 5 µg/mL (A: EtOH, B: DCM). Negative control: NT. Positive control: nocodazole 200 ng/mL. Analysis by immunofluorescence microscopy. Green: α-tubulin (mitotic spindle) Blue: DAPI (DNA). Scale bar: 20 µm.

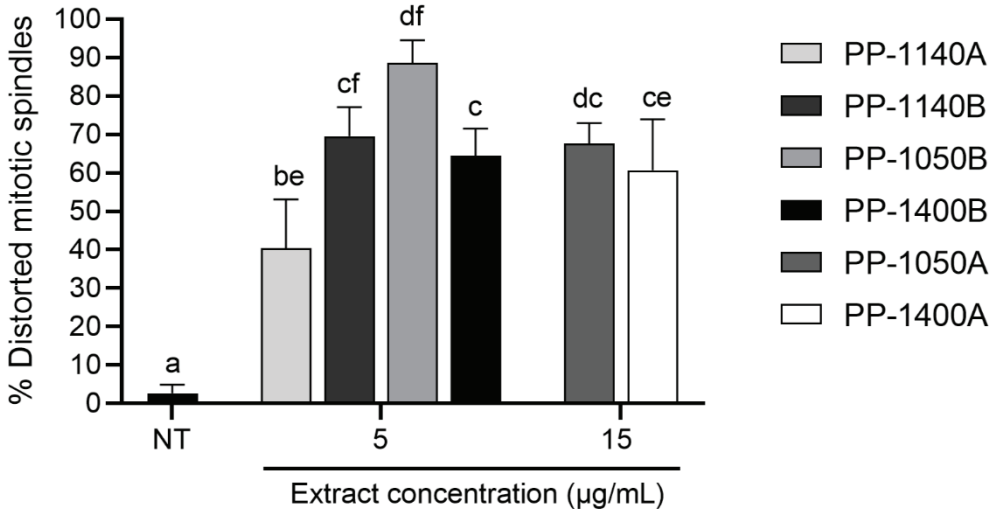

Figure 16. Percentages of cells with distorted mitotic spindle morphology after treatment with Asteraceae extracts (A: EtOH, B: DCM). Treatments that are significantly different from other treatments are represented with a different letter (a, b, c, d, e, f). Statistical significance determined via one-way ANOVA followed by Tukey's post hoc tests ($p < 0.05$). Data values represent means ± SEM.

4.2 Comparison of anti-mitotic activities of four Asteraceae species

The analysis of mitotic spindle organization in cells treated with extracts from three different Asteraceae species confirmed that the cells were arresting in mitosis, with a mitotic spindle. This type of anti-mitotic activity was distinct from that of the nocodazole class of inhibitors, which do not form a spindle. These observations also reinforced our notion that the mitotic arrests induced by different extracts might be different from each other, for example, compare PP-1140A to PP-1400A. It remained a challenge, however, to measure these differences in a meaningful way.

To compare mitotic spindle organization we performed experiments in which we treated HT-29 cells with extracts prepared from *A. cordifolia, A. fulgens,* and *R. columnifera* and compared them to anti-mitotic extracts that we have previously studied: PP-006, a *G. aristata* extract which contains a sesquiterpene called pulchelloid A; PP-420B, the dicholoromethane extract of *A. cordifolia* that arrests cells in mitosis intriguingly with bi-

polar spindles (Molina, 2018). We first performed the phenotypic assay for cell rounding, and then used immunofluorescence microscopy assays to confirm mitotic arrest and investigate mitotic spindle components. In these immunofluorescence experiments we used anti-PH3, anti-α-tubulin antibodies in addition to staining cells with DAPI. We used NT cells as our negative control, and nocodazole as controls. We also added two additional experimental parameters. We treated cells with paclitaxel (Taxol®), a microtubule toxin which, in contrast to nocodazole, induces spindle formation. Paclitaxel is the most widely used natural product cancer drug and acts as an anti-mitotic agent by stabilizing microtubules through β-tubulin binding (Yang & Horwitz, 2017). We also choose to observe a centrosome component, γ-tubulin, because centrosomes are the microtubule organizing center, and may be linked to the abnormal microtubule arrangements that we were observing (Schatten, 2008).

4.2.1 Four Asteraceae extracts induce increased cell rounding percentages

HT-29 cells were either not-treated, or treated with nocodazole, PP-006 at 50 μg/mL, PP-420B at 15 μg/mL, PP-1050B at 5 μg/mL, or PP-1140B at 5 μg/mL. We observed increased cell rounding in extract treated cells (**Figure 17A**). The cell rounding percentages for NT and nocodazole were 4.8 ± 1% and 69.4 ± 3%. The extract that induced the highest percentage of rounded cells was PP-006 with 38.2 ± 9% rounded cells. Extract PP-1050B had the second highest percentage at 31.5 ± 9%, followed by PP-420B at 28.2 ± 6%. Extract PP-1140B had the lowest cell rounding percentage at 21.4 ± 5%. We found that each extract treatment was significantly different from that of NT cells (**Figure 17B**).

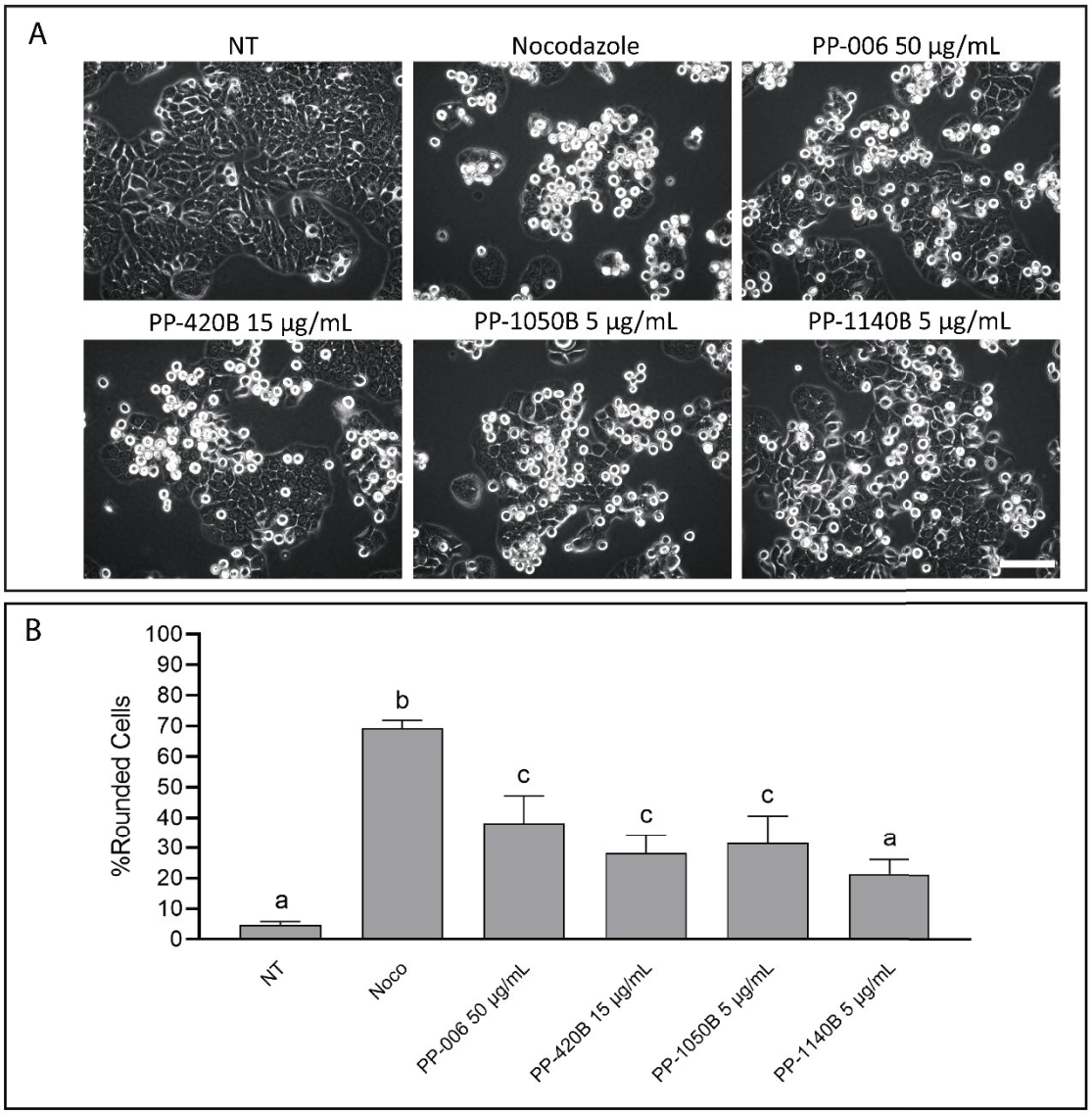

Figure 17. Percentage of rounded HT-29 cells after treatment with four Asteraceae extracts (A: EtOH, B: DCM). NT cells and nocodazole at 200 ng/mL were used as negative and positive controls for cell rounding. Scale bar: 100 µm (**A**). Rounded cells were counted from light microscopy photos taken 16 h post treatment. Treatments that are significantly different from other treatments are represented with a different letter (a, b, c). Statistical significance determined via one-way ANOVA followed by Tukey's post hoc tests ($p < 0.05$). Data values represent means ± SEM, n = 3 (**B**).

4.2.2 Four Asteraceae extracts induce mitotic arrest demonstrated by PH3 immunofluorescence assay:

We then measured mitotic arrest with phospho-histone H3 antibodies and immunofluorescence microscopy. After treatment for 16 h, we observed an increase in red PH3 positive cells for the extract treatments (**Figure 18**). Cells treated with PP-006 had 25.3 ± 2% mitotic cells. PP-1050B had a similar percentage of mitotic cells at 24.0 ± 2%. After treatment with PP-1140B the percentage of mitotic cells was 19.2 ± 2%, and after treatment with PP-420B there was 11.2 ± 3% mitotic cells. All extract treatments were significantly different from that of NT cells apart from PP-420B (**Figure 19**).

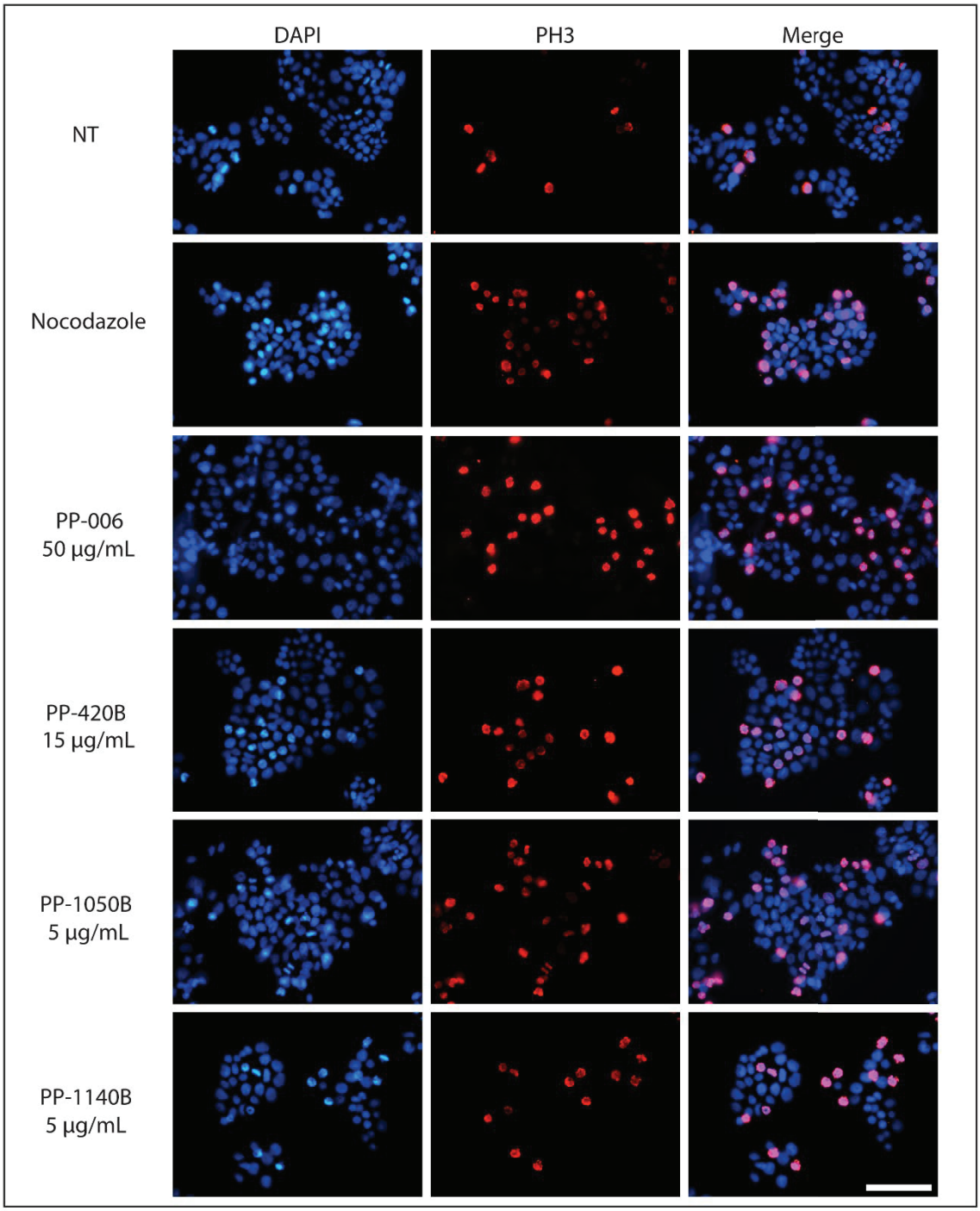

Figure 18. Mitotic cells accumulated after treatment with four Asteraceae extracts (A: EtOH, B: DCM). Negative control: NT. Positive control: nocodazole 200 ng/mL. Analysis by immunofluorescence microscopy. Red: phospho-histone H3 (mitotic cells). Blue: DAPI (DNA). Scale bar: 100 µm.

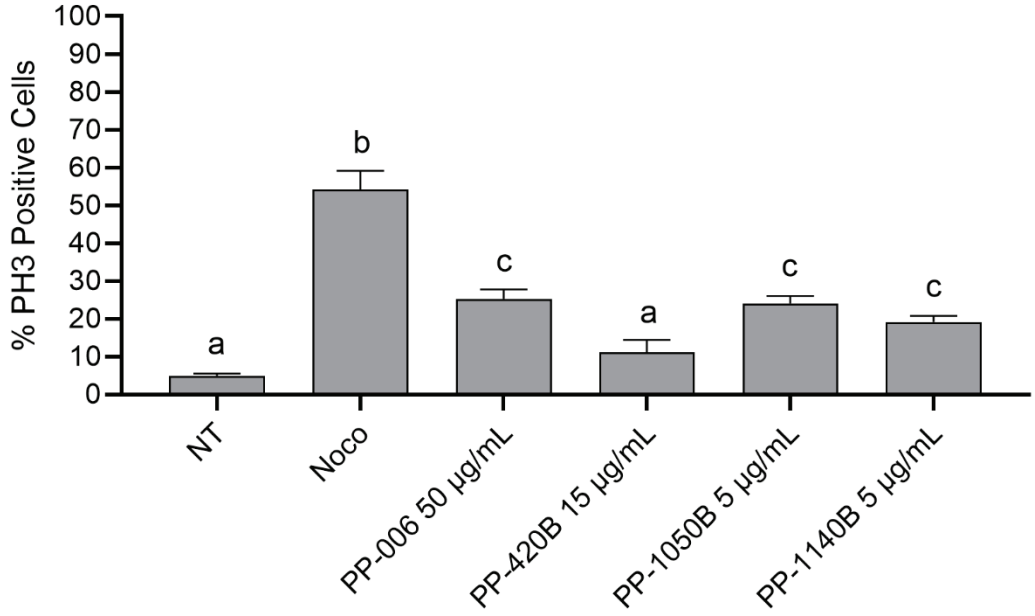

Figure 19. Mitotic indices based on mean percentages of PH3-positive HT-29 cells after treatment with four Asteraceae plant extracts (A: EtOH, B: DCM). Negative control: NT. Positive control: nocodazole 200 ng/mL. Error bars represent the SEM of at least three independent experiments. Treatments that are significantly different from other treatments are represented with a different letter (a, b, c). Statistical significance determined via one-way ANOVA followed by Tukey's post hoc tests ($p < 0.05$).

4.2.3 Asteraceae extracts induce different α-tubulin arrangements in HT-29 cells

To explore whether the mitotic arrests induced by prairie Asteraceae extracts were similar to each other, or different, we visualized the mitotic spindles in treated cells. We used NT cells and nocodazole as negative and positive controls and treated cells with extracts for 16 h at the same concentrations as the PH3 immunofluorescence experiment. NT mitotic cells displayed normal spindles with two poles and microtubules extending to the center of the cell (**Figure 20**). As expected nocodazole-treated cells failed to form mitotic spindles after 16 h.

When treated with 50 µg/mL of PP-006, 89.6 ± 1.1% of cells displayed distorted spindles (**Figure 21**) that lacked two poles, and were rounded shape (**Figure 20**). In contrast, at 15

μg/mL, PP-420B induced mitotic arrest and many of the cells had bi-polar mitotic spindles, with only 43.6 ± 18.4% distorted spindles. We observed 64.3 ± 5.8% distorted mitotic spindles without two poles in cells treated with PP-1140B (**Figures 21 and 20**). The distortion caused by PP-1140B treatment was distinct from that of the extracts, PP-006, PP-420B and PP-1050B. Finally, we observed that cells treated with PP-1050B at 5 μg/mL contained 83.7 ± 7.2% distorted mitotic spindles (**Figure 20**), many of which contained three poles (**Figure 21**). These results are important because the percentage of distorted spindles in each treatment was higher than NT, and the differences we observed in spindle morphologies supported the notion that extracts prepared from different species are likely to contain different chemicals, with different cellular interactions.

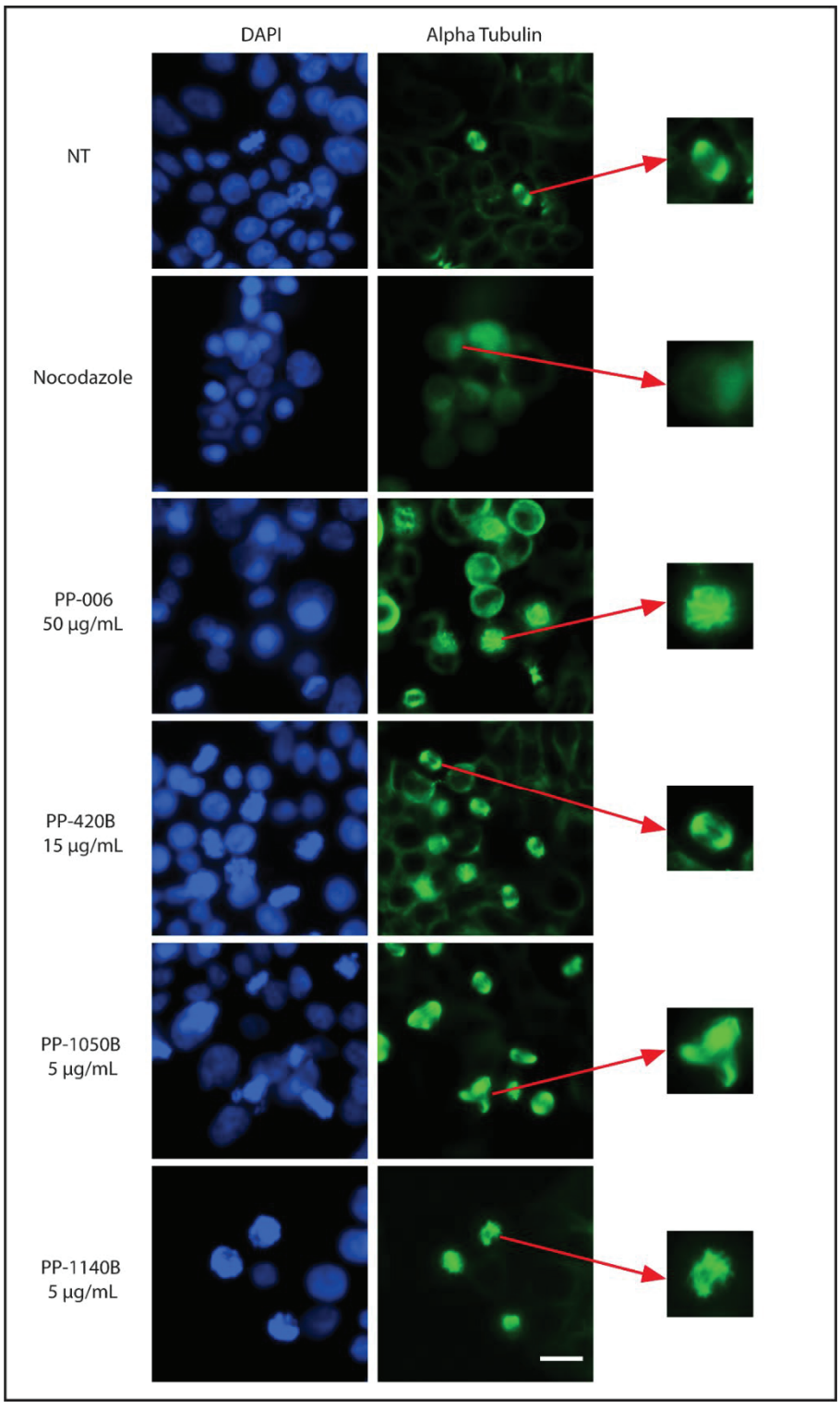

Figure 20. Mitotic spindles in HT-29 cells treated with four Asteraceae extracts. Negative control: NT. Positive control: nocodazole 200 ng/mL. Analysis by immunofluorescence microscopy. Green: α-tubulin (mitotic spindle) Blue: DAPI (DNA). Scale bar: 20 µm.

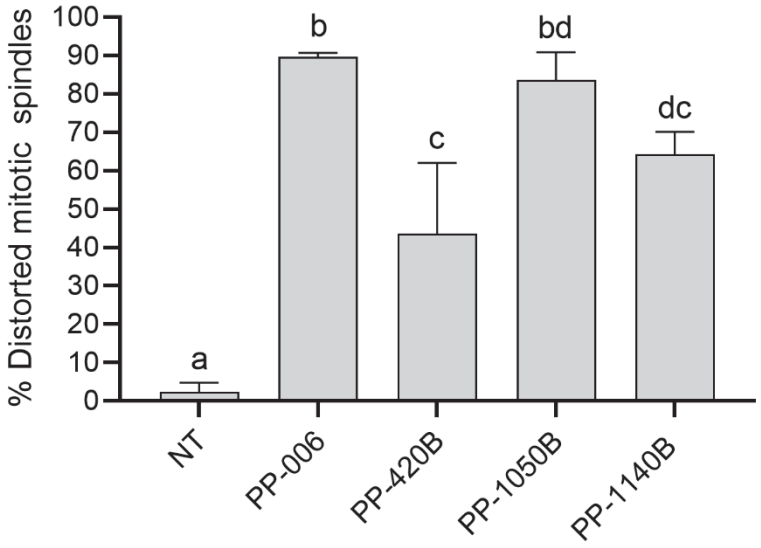

Figure 21. Percentages of HT-29 cells with distorted mitotic spindles after treatment with four Asteraceae plant extracts (A: EtOH, B: DCM). Treatments that are significantly different from other treatments are represented with a different letter (a, b, c, d). Statistical significance determined via one-way ANOVA followed by Tukey's post hoc tests ($p < 0.05$). Data values represent means ± SEM.

4.2.4 Asteraceae extracts modulate centrosome formation

Because the differences in microtubule distortion between extracts were challenging to describe and sometimes subtle, we investigated the effects of the extracts on centrosomes, another mitotic spindle component. Centrosomes were labeled with an anti-γ-tubulin antibody, DAPI was used to stain the DNA and cells were observed by immunofluorescence microscopy. We used NT cells as our negative control. After reviewing the α-tubulin results it became apparent that the extracts were not preventing tubulin association like nocodazole. Because it was difficult to visualize centrosomes in nocodazole treated cells, we changed the positive control to paclitaxel. HT-29 cells were either not-treated, treated with paclitaxel (100 nM) or with PP-006, PP-420B, PP-1140B, or PP-1050B for 16 h. Extracts were used at the same concentrations as described in

previous immunofluorescence experiments. Photographs of cells were taken and used in a plot profile analysis technique to illustrate graphically the centrosomes we observed.

NT and paclitaxel-treated cells contained centrosomes (**Figure 22A**) tightly organized into two points, illustrated by two peaks of pixel intensity observed in panel B of **Figure 22.** When cells were treated with PP-006 at 50 µg/mL two centrosomes were observed, however the γ-tubulin signal was not tightly organized into two points (**Figure 22**), graphically illustrated by pixels with higher intensity between the two points (**Figure 20B**)**.** Two centrosomes and two peaks were also observed in cells treated with extracts PP-420B at 15 µg/mL, and PP-1140B at 5 µg/mL (**Figure 22**). After treatment with 5 µg/mL of PP-1050B we observed three centrosomes in cells (**Figure 22**) which are reflected in the three peaks of the pixel intensity plot.

These observations reveal differences in mitotic arrests at the γ-tubulin level. They are important because they demonstrate, for the first time, a method to measure and compare the differences in mitotic arrests induced by each treatment. The morphological differences are likely due to different molecular targets within the cell, targeted by different chemicals. Additionally, these results support the notion that the chemicals within Asteraceae tribes are reflective of the diverse relationships within this plant family.

To summarize, we met our objective by successfully using phylogenetic information to direct investigation toward Asteraceae species for anti-mitotic activity. We found that extracts prepared from species from the selected tribes had anti-mitotic activity against HT-29 cells. Furthermore, the different mitotic spindle morphologies observed in the Asteraceae plant extracts met our second objective by providing new mitotic arrest phenotypes for our laboratory. These results suggest that the extracts have different

molecular targets in the same cell line. These results lead to challenging questions about which protein the extracts are interacting with to induce the mitotic arrests. We can use information from the mitotic spindle morphologies to estimate the stage of mitotic arrest and possible protein targets.

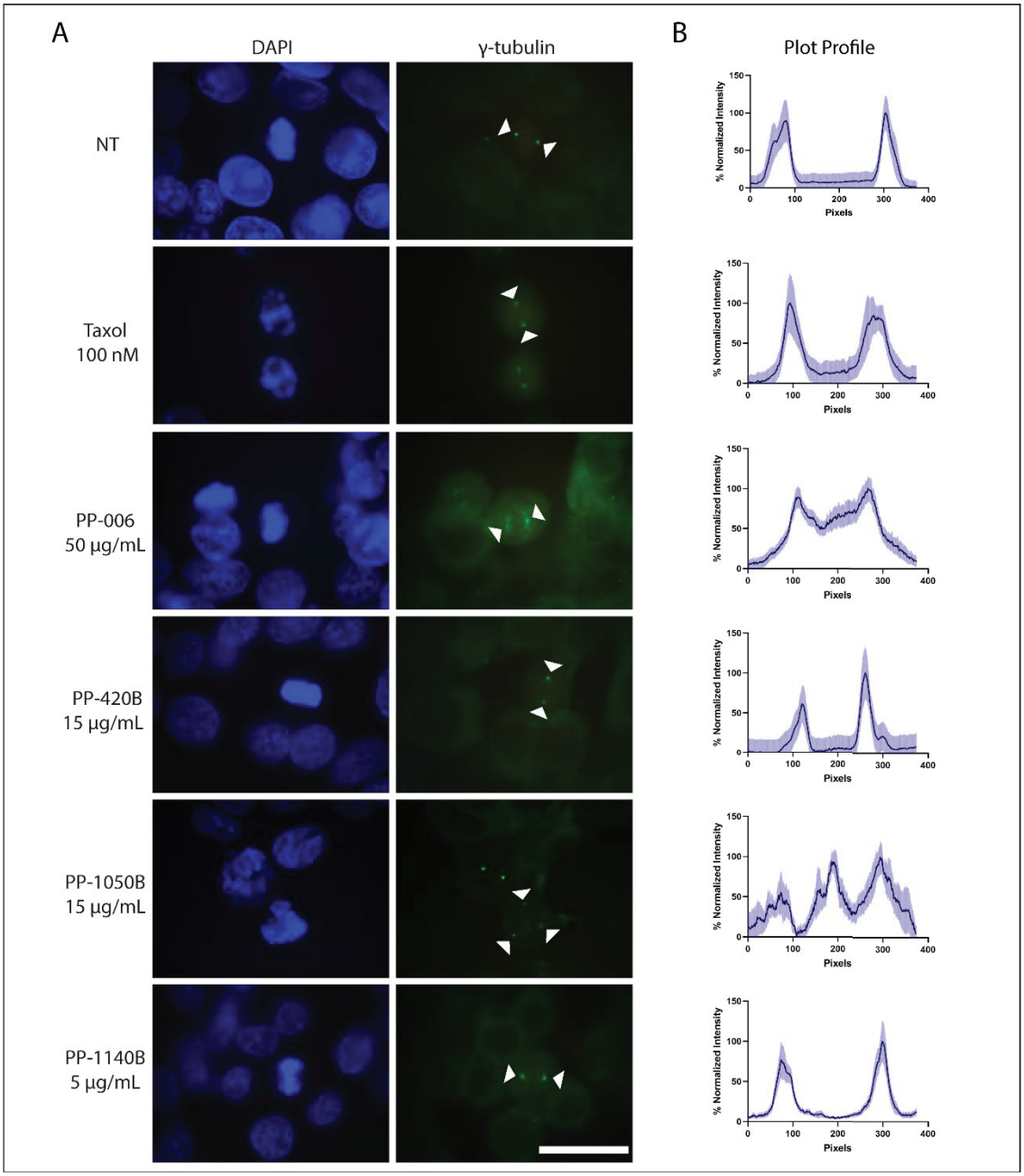

Figure 22. Centrosomes in HT-29 cells treated with four Asteraceae plant extracts. Blue: DAPI (DNA). Green: γ-tubulin (centrosomes). Arrows indicate intense γ-tubulin signal. Scale bar: 20 µm (**A**). Fluorescence intensity of γ-tubulin measured over the area of one cell. Each treatment was done in triplicate and shown are the mean and standard error of the mean of 15 cells each. Measurements were normalized to cytoplasmic intensity and highest intensity across all treatments (**B**).

4.3 Testing transcriptomic analysis of treated cells as a method to characterize plant extracts.

One of the limitations in evaluating prairie plants for chemicals with biological activity is our capacity to observe changes in treated cells. Although the phenotypic approach was successful in identifying anti-mitotic compounds, the majority of plant extracts that we tested produced phenotypes that we were unable to measure or describe adequately. We observed differences in the mitotic arrests induced by some prairie Asteraceae plant extracts, revealed by differences in mitotic spindles in treated cells. We wondered which technical approaches could be used to investigate extracts to give insight into potential targets, including anti-mitotic activity. RNA sequencing technology has been used to analyze the transcriptome in cells treated anti-mitotic microtubule interfering agents (Gasic et al., 2019), and sesquiterpene-lactones, but has not been used to differentiate mitotic arrests. This led us to design an experiment to test the technique of transcriptomics as a method to detect differences in mitotic arrests. If successful, we would then consider using the technique to characterize the analysis of all extracts.

We chose to investigate the effects of anti-mitotic chemicals upon cancer cell gene expression, for the first time in our laboratory, by transcriptome sequencing. In designing the experiments, we selected paclitaxel as a positive control because it is a well characterized cancer drug that acts as a microtubule stabilizing agent and there were publications describing transcript expression in treated cells. In addition, we were competent in using it pharmacologically. We then selected parthenolide as a test chemical because it is the best described sesquiterpene lactone, but with weak anti-mitotic activity (Bosco & Golsteyn, 2017) isolated from the Asteraceae species *Tanacetum parthenium*. Its anticancer potential has been investigated on several chemical and biological levels

(Ghantous et al., 2013) but not yet by transcriptome wide analysis. Finally, we tested pulchelloid A because it is an anti-mitotic sesquiterpene lactone from the Canadian prairie Asteraceae species, *G. aristata* (Bosco et al., 2021). Potentially, this approach may be used to investigate mitotic arrests induced by plant extracts and chemicals, providing comprehensive information for potential gene and protein targets within the cell.

4.3.1 Mitotic arrest assessed using cell rounding assay prior to RNA extraction

Prior to RNA extraction we confirmed that cells treated with pulchelloid A (pulA) and parthenolide (parth) were in mitotic arrest by calculating the percentage of rounded cells. HT-29 cells that were treated with the vehicle, DMSO, served as our not treated (NT) control group. Paclitaxel was applied at 100 nM for our positive control treatment group. HT-29 cells were treated with parth at 20 μM, and pulA at 10 uM. After 16 hours of treatment, we calculated the mean percentage of rounded cells for each treatment to confirm whether the cells had entered mitosis or not. After 16 h NT cells had 4.1 ± 0.4% rounded cells (**Figure 23**), and cells treated with paclitaxel had 43.3 ± 10.6% rounded cells. Parth-treated cells had 10.1 ± 1.6% rounded cells. Finally, pulA-treated cells had 38.6 ± 17.9% rounded cells. This result demonstrates differences in anti-mitotic activity between parthenolide and pulchelloid A, although each are members of the sesquiterpene lactone chemical class.

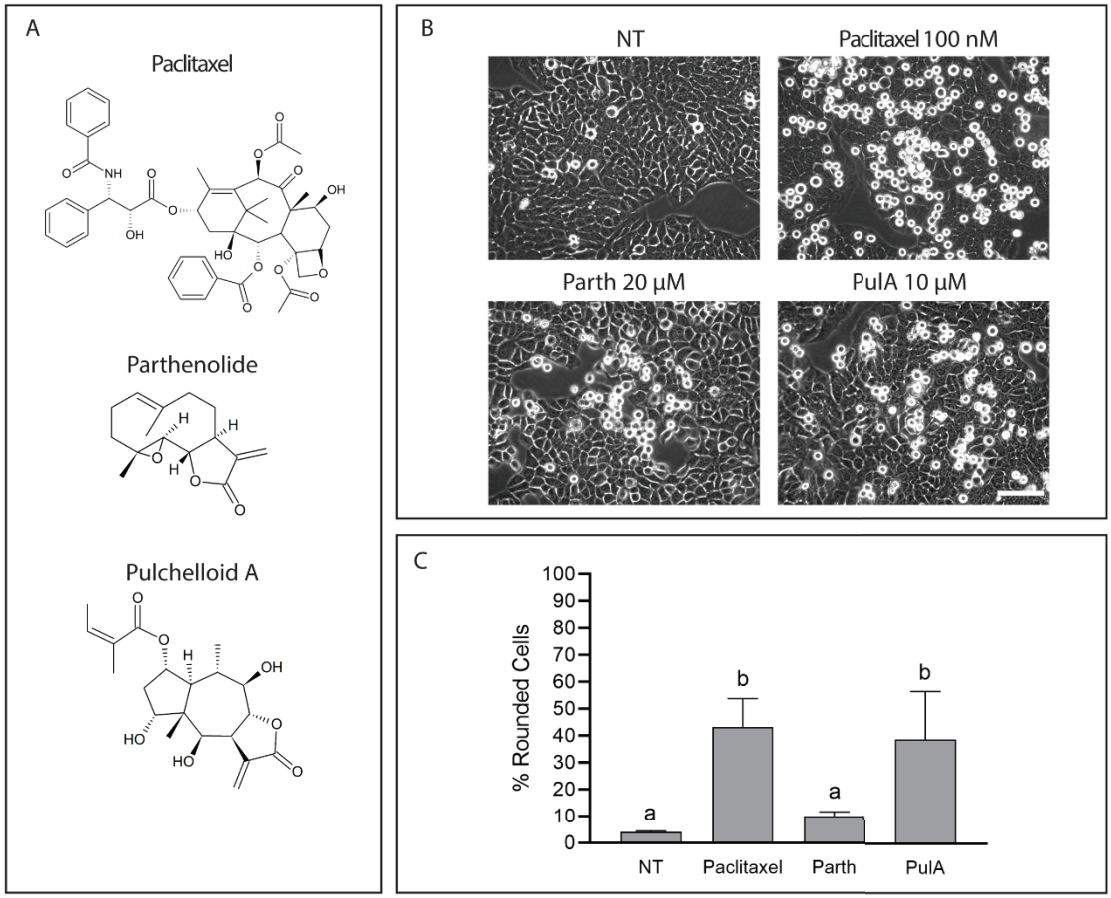

Figure 23. Percentage of HT-29 cells that acquire rounded morphology when treated with sesquiterpene lactones parthenolide and pulchelloid A. NT and paclitaxel 100 nM used as negative and positive controls for cell rounding. Rounded cells were counted from light microscopy photos taken 16 h post treatment. Scale bar: 100 µm. Treatments that are significantly different from other treatments are represented with a different letter (a and b). Statistical significance determined via one-way ANOVA followed by Tukey's post hoc tests ($p < 0.05$). Data values represent means ± SEM, n = 3.

4.3.2 Measuring quality of RNA from not-treated and treated cells

We collected total RNA from the cells after 16 h of treatment and analyzed the samples to ensure that the quality sufficient for library construction. One sample for each treatment was collected from two independent experiments for a total of two biological replicates. We extracted 52 ng/uL and 211 ng/uL of high purity total RNA from the not-treated cells (**Table 5**). All RNA samples had A260:A280 ratios higher than 1.8, indicating high purity

of RNA to other nucleic acids. The samples listed in **Table 5** were then used to generate cDNA libraries.

Table 5. Concentration and purity of cleaned extracted RNA from HT-29 cells treated with different chemicals. Minimum concentration and A260/A280 purity score required for library construction are 15 ng/ul and ≥ 1.8, respectively.

Sample	Total RNA concentration (ng/μL)	Purity Score (A260:A280)
031120-NT	52	1.8
111120-NT	211	1.9
111120-Paclitaxel	190	1.8
141120-Paclitaxel	137	1.9
111120-Parth	31	1.8
14.11.20-Parth	24	2.0
020321-PulA	100	2.0
141120-PulA	49	1.9

4.3.3 Validation of cDNA library construction prior to sequencing

After constructing the cDNA libraries, we obtained the average size distribution of the libraries to ensure that they were suitable for qPCR analysis and sequencing. We confirmed that long (>200 nucleotides) RNA libraries were constructed by analyzing each library with an Agilent Bioanalyzer, which provides the average size of the library fragments in base pairs, and produces a digital gel constructed from the absorbance readings of the samples. The standard base-pair ladder and samples were loaded with cDNA markers that appear at 10380 bp and at 35 bp (**Figure 24**). Band sizes were compared to the bp sizes of the DNA ladder, observed in lane 1 of **Figure 24**. For the cDNA libraries created from not–treated cells, we observed dark, broad bands on the gel (lanes 2 and 3, **Figure 24**) and recorded average sizes of 323 and 344 bp for the two replicates. The two paclitaxel cDNA libraries produced broad signals at 200-300 bp on the gel in lanes 4 and 5 (**Figure 24**) and were of 267 and 175 bp average size. The cDNA libraries from the parthenolide group were lower in concentration as shown by the faint bands around 250-300 bp, and the average size for these libraries were 346 and 340 bp. When we analyzed the pulA cDNA libraries, we

observed different intensity bands between the two lanes (**Figure 24**) but similar average size distributions at 334 and 335 bp. The average size in bp was used with qPCR analysis to determine the concentration of each library. The values are listed in **Table 6**.

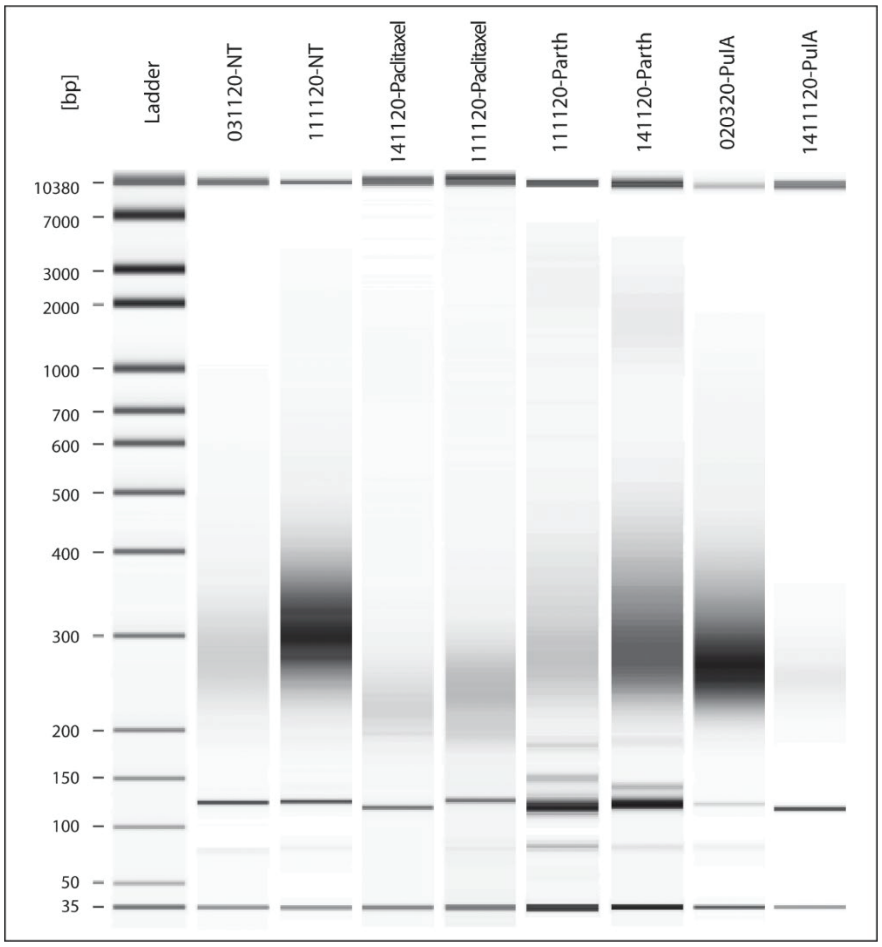

Figure 24. Digital gel image of cDNA libraries generated by Agilent Bioanalyzer.

Table 6. Average size and concentration of cDNA libraries used for RNA sequencing.

cDNA Library	Average size (bp)	Concentration (nM)
031120-NT	323	14
111120-NT	344	120
111120-Paclitaxel	267	8
141120-Paclitaxel	175	17
111120-Parth	346	29
141120-Parth	340	62
020321-PulA	334	171
141120-PulA	335	4

4.3.4 Gene expression profiles differ between HT-29 cells treated with Paclitaxel and sesquiterpene lactones

Following sequencing the cDNA libraries, each library was checked using sequencing manufacturer quality controls, producing over 6000 Mbases of data and achieving sufficient quality scores. We performed differential gene expression (DGE) analysis in which the expression levels of transcripts in the treatment groups were compared to the not-treated control group. We performed quality control checks to ensure that transcript counts were sufficiently normalized, and to assess variability between treatment replicates and treatment groups. After quality control metrics were checked, we analyzed the DGE data to identify trends and specific genes of interest. To visualize these large datasets we created volcano plots, which enable visualization of statistically significant changes in gene expression. The transcript fold change values are transformed by $\log_2$ to linearize relationships and make the data symmetrical for presentation purposes. We plotted the following values obtained from the DGE analysis: transcripts with adjusted p (padj) values < 0.05 versus their magnitude of change ($\log_2$(fold change)).

There were fewer differentially expressed transcripts (DET) in HT-29 cells treated with 100 nM paclitaxel compared to cells treated with sesquiterpene lactones (**Figure 25**). After sorting for padj values < 0.05, we found a total of 895 DET in paclitaxel-treated cells, of which 409 were upregulated and 486 transcripts were downregulated. There were 717 and 1,040 transcripts upregulated and downregulated in parthenolide treated cells for a total of 1,757 DET. In HT-29 cells treated with pulA we found 2,212 total DET of which 1425 were upregulated and 787 were downregulated. In each treatment group we observed clusters of under -20 $\log_2$(fold change) and over 20 $\log_2$(fold change) upregulated and downregulated genes as represented by the red and green points in **Figure 25**. HT-29 cells

treated with paclitaxel had 267 highly upregulated transcripts, and 258 that were highly downregulated. We found 300 and 336 transcripts were highly upregulated and downregulated, respectively in cells treated with parthenolide. Finally, we found 297 highly upregulated transcripts and 225 highly downregulated transcripts in pulA-treated cells.

Using the red and green clustering of transcripts in **Figure 25**, we then found the gene descriptions for the first ten transcripts with the greatest positive or negative fold changes. These are listed as upregulated genes in **Table 8** and downregulated genes in **Table 9**. The most downregulated transcript in paclitaxel-treated cells was ribosomal protein L13A (RPL13A). There were two centrosomal or microtubule related transcripts in the top ten downregulated paclitaxel-treated cells. These were transcripts for CEP170B (centrosomal protein 170B), and FLNB (filamin B). The most upregulated transcript in paclitaxel-treated cells was ACTB (actin beta). For parthenolide-treated cells the most downregulated transcript was for EIF2AK2 (eukaryotic translation initiation factor 2 alpha kinase 2). The gene ALMS1 (Centrosome gene ALMS1) was also one of the top ten downregulated transcripts in parthenolide-treated cells. Gene OAS3 (2'-5'-oligoadenylate synthetase 3) was the transcript with the highest fold change in parthenolide-treated cells. Additionally, we also found MACF1 (microtubule actin crosslinking factor 1) in the top ten upregulated transcripts in Parth-treated cells. In contrast, OAS3 (2'-5'-oligoadenylate synthetase 3 number 1) was the most downregulated transcript in pulA-treated cells. It was also noted that AURKA (aurora kinase A) and MAP4 (microtubule associated protein 4) were in the top ten upregulated genes for pulA-treated cells.

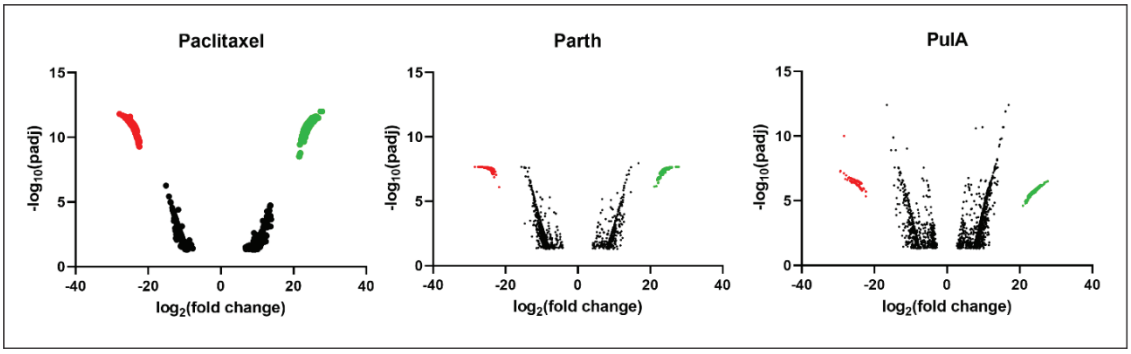

Figure 25. Gene expression profiles in HT-29 cells treated with paclitaxel, parthenolide, and pulchelloid A. DESeq2 analysis revealed 895, 1,757, and 2,212 differentially expressed genes in paclitaxel, parth, and pulA-treated cells, respectively (*padj <0.05,* n = 2) (**A**). Red points: highly downregulated transcripts. Green points: highly upregulated transcripts.

Table 7. The ten most downregulated transcripts (smallest log2(fold change)) in HT-29 cells treated with paclitaxel, parthenolide, and pulchelloid A. Genes with a mitotic connection are shown in bold text.

Treatment	Transcript ID	Gene name	Description	Log2(Fold Change)
Paclitaxel	ENST00000621674	RPL13A	ribosomal protein L13a	-28
	ENST00000676710	EEF1A1	eukaryotic translation elongation factor 1 alpha 1	-27
	ENST00000368802	REV3L	REV3 like, DNA directed polymerase zeta catalytic subunit	-27
	ENST00000355666	TTC3	tetratricopeptide repeat domain 3	-27
	ENST00000361059	MATR3	matrin 3	-26
	ENST00000375630	ATP11A	ATPase phospholipid transporting 11A	-26
	ENST00000556508	**CEP170B**	**centrosomal protein 170B**	**-26**
	ENST00000447540	CHD9	chromodomain helicase DNA binding protein 9	-26
	ENST00000358537	FLNB	filamin B	-26
	ENST00000545215	LDHA	lactate dehydrogenase A	-26
Parth	ENST00000681507	EIF2AK2	eukaryotic translation initiation factor 2 alpha kinase 2	-29
	ENST00000677236	EEF1A1	eukaryotic translation elongation factor 1 alpha 1	-28
	ENST00000555002	SYNE2	spectrin repeat containing nuclear envelope protein 2	-27
	ENST00000620157	DDX6	DEADBox helicase 6	-27
	ENST00000484298	**ALMS1**	**ALMS1 centrosome and basal body associated protein**	**-27**
	ENST00000617571	INF2	inverted formin 2	-27
	ENST00000261833	CIT	citron rho-interacting serine/threonine kinase	-27
	ENST00000537274	YAP1	Yes1 associated transcriptional regulator	-27
	ENST00000274203	**MYO10**	**myosin X**	**-27**
	ENST00000508682	RACK1	receptor for activated C kinase 1	-27
PulA	ENST00000679354	OAS3	2'-5'-oligoadenylate synthetase 3	-29
	ENST00000681507	EIF2AK2	eukaryotic translation initiation factor 2 alpha kinase 2	-29
	ENST00000676710	EEF1A1	eukaryotic translation elongation factor 1 alpha 1	-28
	ENST00000541182	ARF1	ADP ribosylation factor 1	-28
	ENST00000396432	ARHGAP21	Rho GTPase activating protein 21	-28
	ENST00000274203	**MYO10**	**myosin X**	**-28**
	ENST00000545215	LDHA	lactate dehydrogenase A	-27
	ENST00000530726	CD151	CD151 molecule (Raph blood group)	-27
	ENST00000677335	FKBP1A	FKBP prolyl isomerase 1A	-27
	ENST00000620295	KIF1B	kinesin family member 1B	-27

Table 8. The ten most highly upregulated transcripts (highest log2(fold change)) in HT-29 cells treated with paclitaxel, parthenolide, and pulchelloid A. Genes with a mitotic connection are shown in bold text.

Treatment	Transcript stable ID	Gene name	Gene description	Log2(Fold Change)
Paclitaxel	ENST00000645576	ACTB	actin beta	28
	ENST00000679562	OAS3	2'-5'-oligoadenylate synthetase 3	28
	ENST00000378215	HNRNPUL1	heterogeneous nuclear ribonucleoprotein U like 1	27
	ENST00000678991	CTSEM	cathepsin D	27
	ENST00000272203	PLEKHA6	pleckstrin homology domain containing A6	27
	ENST00000262189	KMT2C	lysine methyltransferase 2C	27
	ENST00000233057	EIF2AK2	eukaryotic translation initiation factor 2 alpha kinase 2	26
	ENST00000679595	NOTCH1	notch receptor 1	26
	ENST00000504325	RACK1	receptor for activated C kinase 1	26
	ENST00000645149	DYNC1H1	dynein cytoplasmic 1 heavy chain 1	26
Parth	ENST00000679505	OAS3	2'-5'-oligoadenylate synthetase 3	28
	ENST00000262189	KMT2C	lysine methyltransferase 2C	28
	ENST00000681516	EIF2AK2	eukaryotic translation initiation factor 2 alpha kinase 2	28
	ENST00000531253	MYO18A	myosin XVIIIA	27
	ENST00000645878	CD151	CD151 molecule (Raph blood group)	27
	ENST00000681030	P4HB	prolyl 4-hydroxylase subunit beta	27
	ENST00000372925	**MACF1**	**microtubule actin crosslinking factor 1**	**27**
	ENST00000438362	CDSE1	cold shock domain containing E1	26
	ENST00000682944	SACS	sacsin molecular chaperone	26
	ENST00000599846	ARHGEF1	Rho guanine nucleotide exchange factor 1	26
PulA	ENST00000369530	CDSE1	cold shock domain containing E1	28
	ENST00000371356	**AURKA**	**aurora kinase A**	**27**
	ENST00000341547	**LMO7**	**LIM domain 7**	**27**
	ENST00000677720	**KIF11**	**kinesin family member 11**	**27**
	ENST00000531253	MYO18A	myosin XVIIIA	27
	ENST00000395734	**MAP4**	**microtubule associated protein 4**	**27**
	ENST00000678450	ANXA2	annexin A2	27
	ENST00000233057	EIF2AK2	eukaryotic translation initiation factor 2 alpha kinase 2	26
	ENST00000679562	OAS3	2'-5'-oligoadenylate synthetase 3	26
	ENST00000262189	KMT2C	lysine methyltransferase 2C	26

4.3.5 Microtubule genes are downregulated in HT-29 cells treated with sesquiterpene lactones

To understand better the biological implications of the entire transcriptomic changes, we uploaded all the significantly (padj <0.05) DET to the Database for Annotation, Visualization, and Integrated Discovery (DAVID). We used the functional annotation cluster tool to find the biological processes most represented by transcripts in the datasets. This tool provides a report for the dataset containing a list of genes involved in each term, and their statistical values (**Figure 27**). The top two term clusters found in each gene ID analysis are shown in **Table 9**. HT-29 cells treated with paclitaxel had downregulated transcripts corresponding to cell-cell adhesion and microtubule/cytoskeleton biological processes (**Table 10**), whereas cell-cell adhesion and RNA Binding were upregulated. The top two downregulated processes for HT-29 cells treated with parthenolide were DNA damage response/DNA repair and cell-cell adhesion, while nucleotide/ATP binding and cell-cell adhesion were upregulated. We noted that microtubule related genes did appear as a cluster in the downregulated genes of parthenolide-treated cells although microtubule related genes were not in the top two clusters. PulA-treated cells had downregulated genes involved in cell-cell adhesion and microtubule/microtubule binding related genes. Cells treated with pulA had upregulated transcripts that corresponded to cell-cell adhesion and mitochondria (**Table 10**).

Because we observed microtubule distortion in HT-29 cells treated with prairie Asteraceae extracts, we were interested in the microtubule related genes affected by the sesquiterpene lactones. We collected the gene lists of the microtubule related term clusters from the DAVID analysis for each treatment and investigated them to find similarities and differences in expression. These differences are observed in the Venn Diagram and

heatmap of **Figure 27**. In total, paclitaxel-treated cells had 43 downregulated microtubule related genes, parth-treated cells had 19, and pulA-treated cells had 26 (**Figure 27A**). Six transcripts were found in all three treatment groups. There were two transcripts found in both paclitaxel and Parth-treated groups, and one transcript shared between paclitaxel and pulA-treated cells. Between parth and pulA treatment groups we found 3 downregulated transcripts related to microtubule function. There were 34 microtubule transcripts only found in paclitaxel-treated cells. We observed 8 microtubule related transcripts that were unique to parth treated cells. We found 16 transcripts that were only found in pulA-treated cells.

We then compared the expression profiles for each treatment using the list of compiled microtubule related genes (**Table 10**) and found their magnitude of change. We found highly downregulated ($\log_2$(fold change) < -20) microtubule related genes unique to each treatment. These genes appear in the red clusters of **Figure 25**. In paclitaxel-treated cells the microtubule genes highly downregulated are listed in **Table 10** as genes with a $\log_2$(fold change) < -20. Within Parth-treated cells we found the genes MACF1and CCSAP were highly downregulated. Finally, the genes KIF2C, MAPRE2, MX1, and BCL2L11 were highly downregulated in pulA-treated cells.

In summary, our objective to detect differences in mitotic arrest with transcriptomic analysis was met. We did observe variability between replicates as well as treatments, although the DGE analysis was successful and sufficient to draw conclusions. The inclusion of additional biological replicates would add additional support and further emphasize the patterns of gene expression we observed. We observed differences in the overall number of transcripts expressed, the most upregulated and downregulated genes, and specific

microtubule gene expression. We observed differences in the microtubule genes expressed in HT-29 cells treated with parth and pulA. These results suggest that the sesquiterpene constituent structure of these chemicals contributes to their effect in the cell.

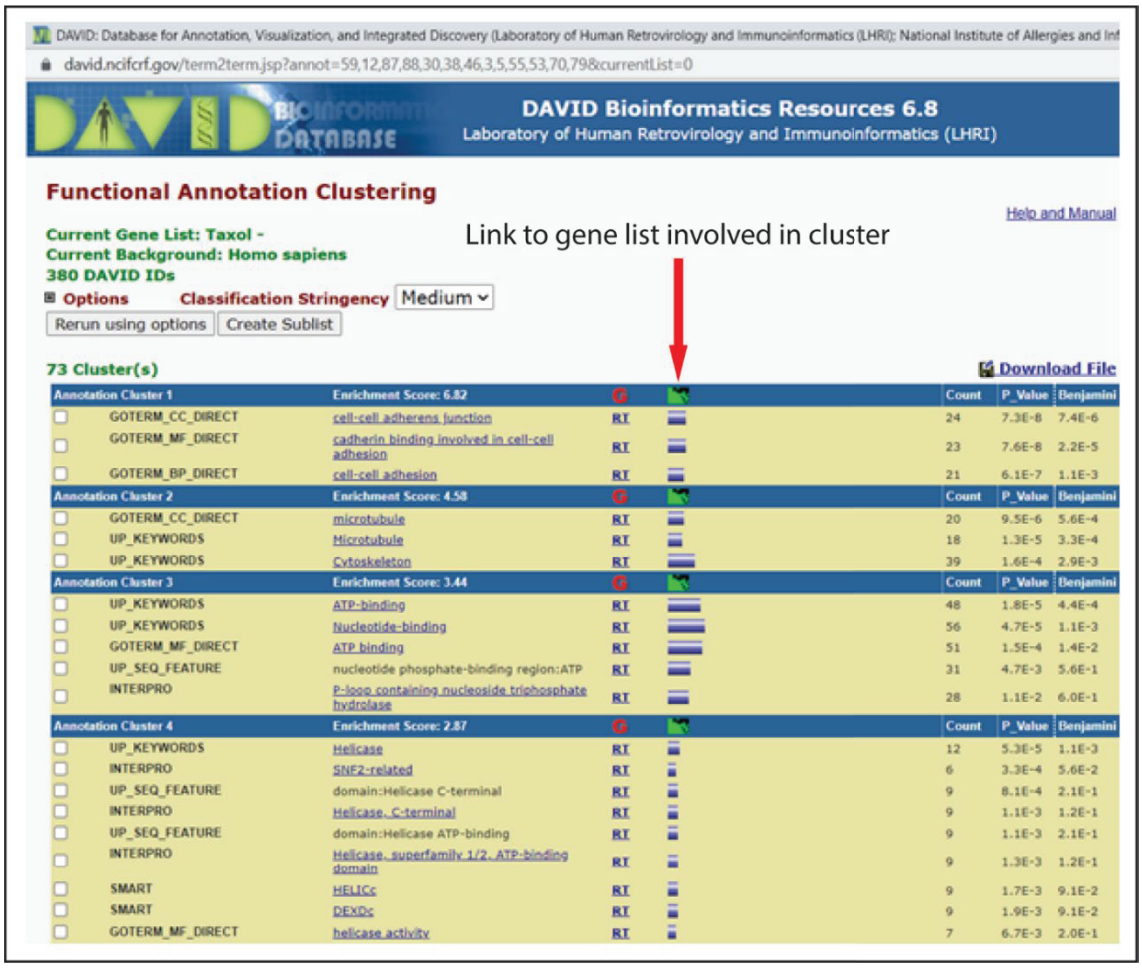

Figure 26. Representative DAVID functional annotation clustering report.

Table 9. Biological processes associated with differentially expressed genes in HT-29 cells treated with sesquiterpene lactones and paclitaxel. Gene expression in treated cells was compared to the negative DMSO control. Processes included are the top two enrich term clusters with adjusted p values <0.05 obtained from DAVID Functional Annotation Clustering.

Treatment	Downregulated Processes	Upregulated Processes
Paclitaxel	cell-cell adhesion	cell-cell adhesion
	microtubule/cytoskeleton	RNA Binding
Parth	DNA damage response/DNA repair	nucleotide and ATP binding
	cell-cell adhesion	cell-cell adhesion
PulA	cell-cell adhesion	cell-cell adhesion
	microtubule/microtubule binding	mitochondrion

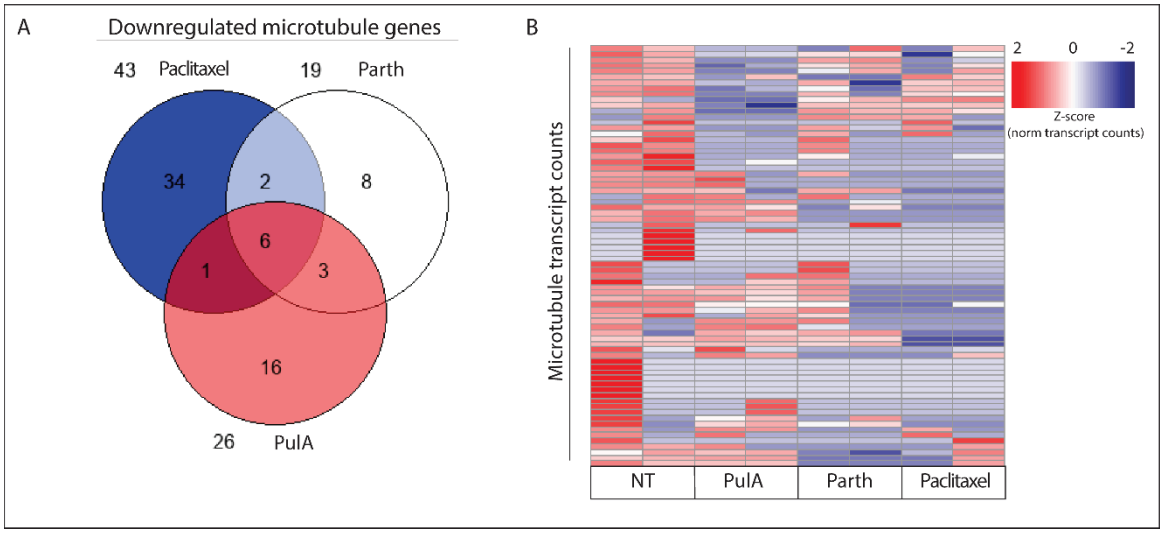

Figure 27. Venn diagram comparison of down-regulated microtubule genes differentially expressed in HT-29 cells treated with paclitaxel, parthenolide (parth), and pulchelloid A (pulA) **(A)**. Heatmap comparison showing the microtubule gene transcripts that are differentially expressed between treated and untreated HT-29 cells. NT cells used as negative control. Rows represent transcript counts. Columns represent replicates. Red corresponds to higher counts of transcripts **(B)**.

Table 10. List of unique down-regulated microtubule genes in HT-29 cells treated for 16 h with paclitaxel, parthenolide (parth), and pulchelloid A (pulA).

Treatment	Transcript ID	Gene Name	Description	Log2(Fold Change)
Paclitaxel	ENST00000325486	CEP57	centrosomal protein 57	-9
	ENST00000674306	Hsp40 member C7DNAJC7	DnaJ heat shock protein family member C7	-9
	ENST00000683227	ERCC6L2	ERCC excision repair 6 like 2	-10
	ENST00000367295	NAV1	neuron navigator 1	-10
	ENST00000468248	SPAG4	sperm associated antigen 4	-10
	ENST00000503366	ANK3	ankyrin 3	-10
	ENST00000202028	EPB41L1	erythrocyte membrane protein band 4.1 like 1	-10
	ENST00000350537	PARD3	par-3 family cell polarity regulator	-10
	ENST00000260382	LRRC49	leucine rich repeat containing 49	-10
	ENST00000505236	RELB	RELB proto-oncogene, NF-κB subunit	-11
	ENST00000473257	ACTB	actin beta	-11
	ENST00000428228	EMD	emerin	-11
	ENST00000552521	TWF1	twinfilin actin binding protein 1	-11
	ENST00000253811	DIAPH1	diaphanous related formin 1	-11
	ENST00000265348	CUL7	cullin 7	-12
	ENST00000397274	MYO9B	myosin IXB	-13
	ENST00000354558	CKAP5	cytoskeleton associated protein 5	-23
	ENST00000543033	TAOK2	TAO kinase 2	-24
	ENST00000564258	ZFYVE19	zinc finger FYVE-type containing 19	-24
	ENST00000449803	SEPT9	septin 9	-24
	ENST00000347230	ZFYVE26	zinc finger FYVE-type containing 26	-24
	ENST00000243344	TTC21B	tetratricopeptide repeat domain 21B	-24
	ENST00000356413	CD79A binding protein 1IGBP1	immunoglobulin binding protein 1	-24
	ENST00000676512	ZFYVE26	zinc finger FYVE-type containing 26	-24
	ENST00000441708	CTNNB1	catenin beta 1	-24
	ENST00000366543	CEP170	centrosomal protein 170	-24
	ENST00000683184	TBCD	tubulin folding cofactor D	-24
	ENST00000243706	HAUS3	HAUS augmin like complex subunit 3	-24
	ENST00000401393	INO80	INO80 complex subunit	-25
	ENST00000572105	ACTG1	actin gamma 1	-25
	ENST00000427191	PTPN13	protein tyrosine phosphatase, non-receptor type 13	-25
	ENST00000681435	TUBB	tubulin beta class I	-26

	ENST00000407971	SEPT2	septin 2	-26
	ENST00000358537	FLNB	filamin B	-26
	ENST00000556508	CEP170B	centrosomal protein 170B	-26
Parth	ENST00000268699	GAS8	growth arrest specific 8	-5
	ENST00000551264	KIF21A	kinesin family member 21A	-10
	ENST00000682079	MAP2	microtubule associated protein 2	-10
	ENST00000455394	KIF3C	kinesin family member 3C	-10
	ENST00000681114	TUBG1	tubulin gamma 1	-10
	ENST00000585746	TBCB	tubulin folding cofactor B	-10
	ENST00000361689	MACF1	Microtubule Actin crosslinking factor 1	-25
	ENST00000284617	CCSAP	centriole, cilia and spindle associated protein	-25
PulA	ENST00000581888	RASSF5	Ras association domain family member 5	-3
	ENST00000012443	PPP5C	protein phosphatase 5 catalytic subunit	-4
	ENST00000539410	GAS2L3	growth arrest specific 2 like 3	-4
	ENST00000313695	ARHGEF2	Rho/Rac guanine nucleotide exchange factor 2	-4
	ENST00000372814	ODF2	outer dense fiber of sperm tails 2	-5
	ENST00000263710	CLASP1	cytoplasmic linker associated protein 1	-5
	ENST00000684063	KIF9	kinesin family member 9	-6
	ENST00000547905	RACGAP1	Rac GTPase activating protein 1	-8
	ENST00000449570	OGG1	8-oxoguanine DNA glycosylase	-10
	ENST00000435611	MX2	MX dynamin like GTPase 2	-10
	ENST00000620862	BCL2L11	BCL2 like 11	-10
	ENST00000336838	CCDC88A	coiled-coil domain containing 88A	-10
	ENST00000403245	CEP162	centrosomal protein 162	-11
	ENST00000372217	KIF2C	kinesin family member 2C	-24
	ENST00000413393	MAPRE2	microtubule associated protein RP/EB family member 2	-24
	ENST00000680942	MX1	MX dynamin like GTPase 1	-24
	ENST00000622612	BCL2L11	BCL2 like 11	-25

CHAPTER 5

Discussion

The continuation of life depends on the faithful replication and division of genetic material during mitosis. Mitotic errors can result in various chromosomal abnormalities that have implications for embryogenesis, immune response, and development of diseases like cancer (Storchova, 2021). The events of mitosis have been studied using cell biology, biochemistry, and genomic approaches, but the entire scope of involved proteins and their interactions is not well understood. The technique of chemical biology using small molecules to manipulate and study biological systems, can also be used to study mitosis. With the discovery of chemicals that arrest cells in mitosis the role of various proteins may be revealed during this crucial phase of the cell cycle. We approach the protein interaction knowledge gap by isolating chemicals from plants and testing whether they act as anti-mitotic agents. These chemicals may be used in future chemical biology studies to develop a more complete understanding of protein interactions during mitosis. They may also become valuable medicines (Newman & Cragg, 2020). We hypothesize that treating cancer cells with different anti-mitotic chemicals results in different mitotic arrests. In this project we used two approaches to explore different mitotic arrests: cell biology and transcriptomics.

This project was the first in our laboratory to use taxonomic and phylogenetic information to target a species and test it for anti-mitotic activity. It was also the first project in the laboratory to test whether mitotic arrests could be distinguished by transcriptomic analysis. At the beginning of my project, research by my laboratory and others had reported anti-

mitotic activity in extracts isolated from species of the Asteraceae family. Two sesquiterpene lactones with anti-mitotic activity have been isolated from Canadian members of the Asteraceae plant family: pulchelloid A from *Gaillardia aristata* and hymenoratin from *Hymenoxys richardsonii* (Bosco et al., 2021; Molina et al., 2021b). These observations led us to ask what is the range of inhibitors that are harboured within Canadian Prairie species, and do they have the same or different targets? Are the morphological observations of mitotic arrests within treated cells indicative of chemicals interacting through striking precision with a number of distinct yet related targets? We can begin to answer these questions by investigating the connection between phylogeny and chemical diversity within the Asteraceae plant family. Our project addresses phylogeny by incorporating Asteraceae members from several tribes and species from the Canadian prairie ecological zone. Our hypothesis is that the phylogenetic diversity within the Asteraceae family is reflected in the biological activity of the chemicals within. Here we use phylogenetic information to direct investigation towards sources of such chemical diversity and use cell biology techniques to evaluate this hypothesis. The goal of our investigation of anti-mitotic activity within Asteraceae plant extracts may provide new sources of anti-mitotic chemicals.

There are many methods available to explore the effects of anti-mitotic chemicals. We know morphological analysis can provide an indication of mitotic arrest; however, there may be more than one protein target that was inhibited and causing this outcome. A different approach such as using transcriptomic analysis may allow one to detect cellular responses that are not visible by other methods. Recently this approach been used to

determine pathways and protein interactions affected by treatment with an anti-mitotic sesquiterpene lactone (Hegazy et al., 2021). In this project we tested whether transcriptomic analysis could be used as a technique to detect differences in mitotic arrests, in support of our hypothesis that there may be different proteins that are inhibited by anti-mitotic chemicals. By combining cell biology and transcriptomic approaches we are more likely to evaluate the range of mitotic arrests induced by Asteraceae extracts and anti-mitotic chemicals.

5.1 Comparison of four Asteraceae extracts anti-mitotic activity

To understand better the range of anti-mitotic chemicals within the Asteraceae family, we tested and compared extracts prepared from the Canadian species *Ratibida columnifera* (tribe Heliantheae), *Arnica fulgens* (tribe Madieae), *Hymenopappus filifollius* (tribe Bahieae (**Figure 2**)). These species were located within the prairie ecological zone of southern Alberta. We predicted to observe different anti-mitotic arrests in these selected species because the distantly related species *G. aristata* and *A. cordifolia* demonstrated different anti-mitotic activities (Molina, 2018). Chemical similarity can be found between closely related species, as demonstrated by Scotti et al. (2012) who analyzed 1,111 sesquiterpene lactones from 658 Asteraceae species. They found similarities in the degree of oxidation (number of oxidations divided by the number of carbons), and the atom types within the sesquiterpene lactones from Heliantheae and Helenieae tribes.

Consideration of phylogeny has proven to be a valuable approach for finding species with specific biological activities (Saslis-Lagoudakis et al., 2012). The isolation of paclitaxel from *Taxus brevifolia* motivated investigation of the related species *Taxus baccata* and led

to the discovery of docetaxel (Goodman, 2001; Molina et al., 2021a). The presence of cell rounding in morphology assays showed that *A. fulgens* and *R. columnifera* extracts were anti-mitotic and this was further supported by PH3 percentages. In contrast, *H. filifolius* did not show clear cell rounding activity, although a trend was detected. Despite being arrested in a common cell cycle phase, mitosis, we observed differences in the mitotic spindle distortions in cells treated with specific extracts. Our data provide evidence that these species may be sources of different chemicals that lend to cytotoxic and anti-mitotic activity against human cancer cells.

A weakness of phenotypic assays is that there may be many chemicals within the extract competing for molecular targets, and only the strongest of possibly many activities are visible. While an increase in the percentage of rounded cells was observed with increasing concentrations of *H. filifolius* extracts, this phenomenon was overwhelmed by another activity producing a cytotoxic effect. We did observe distorted spindles in cells arrested in mitosis by *H. filfolius*, indicating the presence of chemicals that interact with microtubule proteins. It is possible that the chemical or chemicals responsible for cell rounding and microtubule distortion in the *H. filifloius* extracts are not as prominent in either quantity or reactivity as those affecting cell death pathways. Plant extracts contain a plethora of chemicals that may affect cells synergistically or individually. At least 66 chemicals have been isolated from *Tanacetum parthenium L.* the plant source of parthenolide (Pareek et al., 2011). Using biology-guided fractionation to isolate the anti-mitotic fraction of the *H. filifolius* extract may lead to the identification of the responsible chemical(s) within.

We hypothesized that the mitotic arrests induced by different Asteraceae plant extracts would be different from each other. Indeed, by comparing the anti-mitotic activities of extracts to *G. aristata* and *A. cordifolia* extracts we obtained data that support our hypothesis. Different Asteraceae extracts produced different positive PH3 indices, as well as different types of spindle distortions. There are multiple ways to interpret different types of mitotic arrests. One interpretation for differences in the number of PH3 positive cells is that the arrest may be due to the concentration of one chemical. For example, the mitotic index decreases when lower concentrations of nocodazole are applied to cells (Matsui et al., 2012), because there is less chemical available to bind to α-tubulin. Differences in mitotic spindle morphologies present a challenge to interpret because the distortions may be due to the type of chemical(s) present in addition to their concentration. We observed multi-polar spindles, bipolar distorted spindles, and distorted spindles with no observable spindle poles in HT-29 cells treated with Asteraceae plant extracts. The differences in mitotic spindle morphologies likely indicate different protein targets. We can interpret these observations as the interaction between different chemicals and mitotic spindle proteins.

Distortions to the mitotic spindle are challenging to measure because there is no common scientific vocabulary to describe all distortions, the distorted shapes might be a continuum rather than discrete steps, and there are few prior examples of such observations. To address this, we investigated a critical and simple component of the spindle: centrosomes. They are microtubule organizing centers composed of γ-tubulin that can be labeled with immunofluorescent anti-bodies (Schatten, 2008). This approach provided a different view

of the mitotic spindle and a measure of differences in mitotic arrest. We observed three centrosomes in cells treated with *A. fulgens* extract PP-1050B and observed centrosomes with disorganized γ-tubulin in PP-006 (*G. aristata*) treated cells. These results suggest that these extracts contain different chemicals with different protein targets. Chemicals within *A. fulgens* extract PP-1050B may inhibit the function of proteins that modulate centriole duplication, whereas extract PP-006 may inhibit those that function in γ-tubulin localization. In each case however, the mitotic spindle is distorted. The γ-tubulin intensity plots demonstrated that the Asteraceae species we selected may be used as new sources of different anti-mitotic chemicals; some which distort microtubules and centrosomes.

Four natural products have been identified that overamplify the centriole number in human cells (Graciotti et al., 2016). Although no sesquiterpenes have yet been found to impact centriole number, sesquiterpene lactones calein-C and dehydrocostus lactone have been found to downregulate the expression of PLK-1, a polo-like kinase that regulates the separation of centriole pairs from the procentriole during mitosis (Caldas et al., 2018; Yang et al., 2021). In PP-006 treated cells we observed a different centrosome morphology shown by γ-tubulin filaments extending towards the center of the cell. Filamentous fibers called γ-tubules, composed of pericentrin and γ-tubulin complex proteins, have been observed in human and mouse cell lines during the G1 phase of the cell cycle (Lindström & Alvarado-Kristensson, 2018). Based on the filaments and three gamma tubulin peaks we observed, Asteraceae extracts from *A. fulgens* and *G. aristata* disrupt the normal γ-tubulin framework. The analysis γ-tubulin of is not widely used to study the action of anti-mitotic natural products. In addition to Graciotti et al. (2016), we found four previous studies that used γ-

tubulin staining to investigate mitotic arrest induced by a natural product (Bennett et al., 2012; Lee & Shyur, 2012; Rebacz et al., 2007; Yuan et al., 2011). One study investigating the effects of the sesquiterpene lactone deoxyelephantopin, with two normal centrosomes observed (Lee & Shyur, 2012). This and our data demonstrate that activity against centrosomes is specific to only certain sesquiterpene lactones. We believe this technique should be applied to all investigations about natural products that induce mitotic arrest because it appears to help distinguish how cells might be arrested.

Members of the Asteraceae family are a rich source of sesquiterpene lactones produced as special metabolites that function as defence or signaling compounds (Wink, 2003). Different anti-mitotic sesquiterpene lactones from the Asteraceae plant family induce mitotic arrest but have differences in their biological activity. For example, parthenolide isolated from *Tanacetum parthenium*, stimulates tubulin assembly and promotes the formation of microtubule filaments in breast cancer cells (Miglietta et al., 2004). A recent study by Hotta et al. (2021) found that parthenolide forms adducts on cysteine and histidine residues on α-tubulin to block detyrosination, resulting in distorted microtubules and mitotic spindles in HeLa cells. There are also sesquiterpene lactones that arrest cells in mitosis but not through tubulin interactions. A sesquiterpene lactone isolated from *R. columnifera* (9alpha-hydroxy-seco-ratiferolide-5alpha-O-(2-methylbutyrate) induced G2/M arrest in p53 mutant cells but did not influence tubulin polymerization/depolymerization (Cui et al., 1999). Our data support the likelihood that different Asteraceae species contain different sesquiterpene lactones that are responsible for the various biological activities in these extracts.

One explanation for the various anti-mitotic activities we observed is that sesquiterpene lactones from Asteraceae plant extracts may inhibit members of the ubiquitin-proteasome system. E3 ubiquitin ligases are protein complexes that polyubiquitinate proteins to mark them for proteasomal degradation (Cardozo & Pagano, 2004). The activity of E3 ligases is required for cell cycle progression. The transition from mitosis to G1 is regulated by the APC/C, an E3 ubiquitin-proteasome complex that promotes anaphase progression and polyubiquitinates mitosis specific proteins leading to their degradation (Cardozo & Pagano, 2004). In addition to the progression out of mitosis, protein degradation by E3 ubiquitin-ligases has been connected to centriole duplication (Badarudeen et al., 2021). Activity based profiling experiments have shown that there are 211 E3 ligases with 562 cysteines that could be modified by small molecules like sesquiterpene lactones (Kiely-Collins et al., 2021). Sesquiterpene lactones react with cysteines by Michael-type addition by their α-methylene-γ-butyrolactone moiety, and it has been shown that this moiety is required for their reactivity (Jackson et al., 2017). Within one molecule different moieties can act as recognition groups while others mediate reactions that promote ligand binding. A study by Wang et al. (2021) investigated competitive peptide bonding between the chemicals parthenolide, which contains a Michael acceptor moiety, and orlistat, which contains a β-lactone, and a probe labeled α-methylene-β-lactone which contains both moieties (**Figure 28**). It was found that using different recognizing groups affected the overall number of peptides and specific selection of proteins targets for chemical probes (Wang et al., 2021). These data lead us to think that while the lactone moiety forms covalent bonds, the non-

lactone component of sesquiterpene lactones contributes to which specific E3 ligases these chemicals form complexes with.

Interaction between sesquiterpene lactones and E3 ligases could occur by one of two mechanisms. One is that sesquiterpene lactones bind to E3 ligase itself to inhibit enzyme specificity. There is evidence that sesquiterpene lactones and other natural products inhibit the activity of ubiquitin-ligases. 6-O-Angeloylplenolin an Asteraceae sesquiterpene lactone inhibits a component of an E3 ligase, Skp1-Cullin-F-box containing (SCF) complex (Liu et al., 2015). Small molecules, including the natural product nimbolide, interact with cysteine residues to bind to E3 ligases and inhibit ubiquitination and degradation of target proteins (Kiely-Collins et al., 2021). Given the high sesquiterpene lactone content of Asteraceae species and the variety of biological affects we observed, extracts may be interacting with a protein regulator like ubiquitin-ligases rather than one specific protein. Not all sesquiterpene-lactones are anti-mitotic, suggesting that the non-lactone component may be the determinant for this biological activity. The Michael addition reaction is likely required for anti-mitotic activity, as shown by the activity of *ent*-15-oxokaurenoic acid which contains a Michael acceptor, is not a sesquiterpene lactone, and has anti-mitotic activity (Rundle et al., 2006). The different mitotic arrests we observed could be due to aberrant protein degradation by E3 ligase instead of a direct protein interaction. This could be tested by performing biology guided fractionation to isolate the responsible sesquiterpene lactones, and then performing an experiment like with biotinylated-ubiquitin probe to identify proteins that are not targeted for degradation (Min et al., 2014). To test if sesquiterpene lactones interact directly with E3 ligases, one could perform western blotting

with antibodies specific to the ligase subunits, such as the Cdc20 subunit of the APC/C E3 ligase (Sackton et al., 2014).

Mitotic cycle progressions are driven by degradation of E3 ligase substrates. Therefore, different mitotic arrests may be induced by inhibiting the function of different E3 ligases, or different forms of E3 ligases. The ubiquitin ligases form complexes with different substrate specific adaptors (Cdc20 and Cdh1) that control what substrates it degrades at different points in mitosis (Cardozo & Pagano, 2004). APC/C-Cdc20 targets securin for degradation to promote anaphase (Dang et al., 2021) while and APC/C-Cdh1 targets Aurora A and B for degradation after anaphase to promote telophase progression (Toda et al., 2012). In addition to the APC/C, there are other E3 ligases that contribute to mitotic progression as well. For example, inhibiting the function of SCF ubiquitin ligase would result in Emi1 not being degraded and cells would arrest in prophase. However if inhibited Cul3 was inhibited, one could have an anaphase arrest due to failed Aurora B degradation (Sumara et al., 2008). To date there are very few inhibitors described that demonstrate specific E3 ligase inhibition.

It became apparent from our results that there could be many possible proteins to react with in the cell for the anti-mitotic chemicals within the extracts. Mitotic spindle assembly and centrosome dynamics are regulated by hundreds of proteins (Petry, 2016). For this reason, we chose to test a new technique in our laboratory to differentiate mitotic arrests in human cancer cells. Transcriptomic analysis can provide valuable information for specific genes that are affected by treatment with anti-mitotic chemicals (Gasic et al., 2019). We therefore

tested the ability to find differences in mitotic arrests using two sesquiterpene lactones, and paclitaxel to understand mitotic arrest.

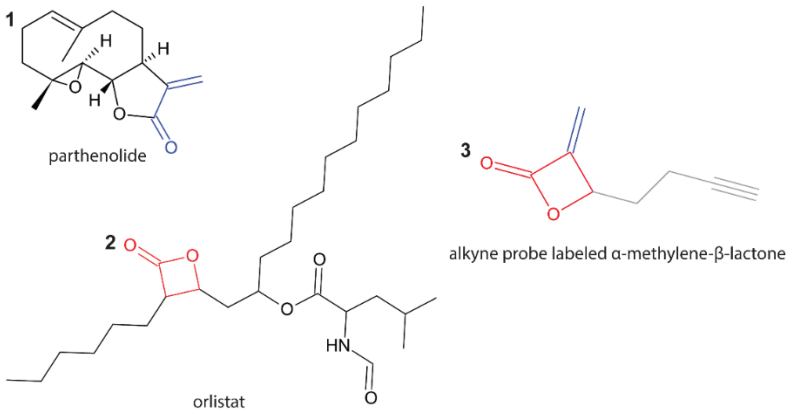

Figure 28. Comparison of chemicals with different reactive moieties investigated by Wang et al. (2021). 1) Michael acceptor moiety highlighted in blue on parthenolide, 2) β-lactone moiety highlighted red on orlistat, 3) α-methylene-β-lactone moiety containing a combination of both groups on an alkyne labeled probe. Black moieties are recognition groups which facilitate complex formation between protein and chemical.

5.2 Transcriptomic analysis reveals differences in mitotic arrests in HT-29 cells treated with anti-mitotic chemicals

The challenge to interpret how cells are affected by treatments with plant extracts prompted us to investigate transcriptomic analysis as a method of detecting differences in mitotic arrest in human cancer cells. This was the first time in the laboratory that mitotic arrest was evaluated by analyzing the entire transcriptome of treated human cancer cells, and there were few examples of this approach described in the literature (Gangapuram et al., 2021; Hegazy et al., 2021; Long et al., 2020; Wu et al., 2018). We chose the chemicals paclitaxel, parthenolide (parth), and pulchelloid A (pulA). Paclitaxel is a widely used and well characterized cancer drug, whereas parth and pulA are anti-mitotic sesquiterpene lactones that differ in mitotic activity, structure, and species source (Bosco et al., 2021; Miglietta et al., 2004). Since several anti-mitotic chemicals interfere with the mitotic spindle,

expression of genes associated with its function may provide insight into different mitotic arrests.

The strength of transcriptomic analysis is that it can reveal chemical interactions that are not visible by morphological assays. While we found microtubule related processes downregulated in each treatment, we also found other process were affected after treatment with anti-mitotic chemicals, such as expression of genes involved in cell-cell adhesion. These proteins promote adhesion between cells and between cells to extracellular matrix, and mediate cell signaling, organization of the cytoskeleton, and gene expression (Janiszewska et al., 2020). Three studies have investigated sesquiterpene lactones and the mechanisms by which they affect cell adhesion. Deoxyelephantopin disrupts focal adhesions by inhibiting the catalytic activity of m-calpain activity, a cysteine protease that cleaves cell adhesion proteins to regulate cell migration and invasion (Lee & Shyur, 2012). Sesquiterpenes parthenolide, costunolide, dehydrocostus lactone, and antrocin inhibitFAK1 (focal adhesion kinase 1) (Berdan et al., 2019; Chiu et al., 2016). We found expression of two cell-cell adhesion genes that have not been associated with sesquiterpene lactones within the transcriptomes of parth and pulA-treated cells. Our results showed that LIM domain 7 expression was upregulated by 4.7-fold in pulA-treated cells. This transcriptional regulator binds to cell-cell adhesion proteins and has been shown to interact with SAC (spindle assembly checkpoint) protein MAD1 to contribute to mitotic progression (Tzeng et al., 2018). The MYO10 gene produces the protein myosin-X which binds with one domain to F-actin to contribute to cell-cell adhesion, and binds to microtubules through a separate domain, to regulate spindle assembly and function during

mitosis (Chan et al., 2014). Direct binding of MYO10 to microtubules promotes proper spindle positioning (Tokuo, 2020). Our results connect anti-mitotic sesquiterpene lactones to proteins involved in both cell-cell adhesion processes and mitotic spindle function.

Transcriptomic analysis has been used to investigate microtubule dynamics in cells, with a focus on tubulin, a main microtubule constituent. Recently, this technique has been used to investigate tubulin gene expression changes in response to treatment with microtubule interfering agents. Gasic et al. (2019) found that tubulin genes are upregulated during interphase in response to microtubule stabilizers and are downregulated as a response to destabilizing agents. Our data showed differences in the tubulin genes expressed between paclitaxel and sesquiterpene lactone treated cells. We found unique tubulin genes downregulated in paclitaxel (TBCB; -4.6 fold change, TUBB; -4.7 fold change) and parth treated cells (TUBG1; -10 fold change), but not in pulA-treated cells. This trend of downregulated tubulin genes is different from the findings of (Gasic et al., 2019) where paclitaxel treatment induced upregulation of tubulin genes in RPE1 hTert cells. A main difference between our study and Gasic et al. (2019) is that they were investigating microtubule dynamics during interphase, and specifically avoided mitotic arrest. The tubulin polymers composing microtubules are dynamic structures that grow and shorten differently throughout the cell cycle to perform their functions (Singh et al., 2008). Our results together with Gasic et al. (2019) suggest that anti-mitotic chemicals may have different effects on tubulin gene expression during different cell cycle phases.

Our data validate the findings of other transcriptomic analysis studies that show that microtubule processes are deregulated by anti-mitotic chemicals. By analyzing the

transcriptome of esophageal cancer cells Wu et al. (2018) found the processes of cell adhesion was upregulated in paclitaxel resistant cells. We found that the process of cell adhesion was both upregulated and downregulated in paclitaxel treated cells. In addition to cell adhesion, transcription factor genes have been linked to paclitaxel response. Analysis of DEGs in paclitaxel resistant A2780 ovarian cancer cells showed upregulated (fold change > 4) genes involved in processes of cell adhesion, TNF signaling, NFKB1 signaling (Szenajch et al., 2020). In contrast, we found expression of transcription factor RELB, an oncogenic NFκβ family member was downregulated by 3.5-fold in paclitaxel treated cells. This may be due to differences in resistant and sensitive cells, which can display opposite expression patterns. TUBB and MAPs genes are upregulated by 1.4-fold and 0.6 to 4-fold, respectively, in paclitaxel resistant esophageal cancer cell lines and downregulated in sensitive cells (Wu et al., 2018). Other genes in our results validate the findings of groups such as (Long et al., 2020) who found that paclitaxel treatment decreased the amount of LDHA mRNA in glioma cells. Other studies also found that microtubule genes involved in sister chromatid segregation, kinetochore attachment, and transport pathways were differentially expressed as well (Galletti et al., 2020; Gangapuram et al., 2021).

One transcriptomic study with a sesquiterpene lactone has been conducted. 2α-hydroxyalantolactone induces mitotic arrest and causes differential expression of mitotic microtubule genes DYNLL1 (dynein light chain LC8-type 1) by 2.2-fold, and INCENP (inner centromere protein) by -2.0-fold in leukemia cancer cells (Hegazy et al., 2021). We did not find those genes downregulated within our microtubule related gene set, rather we found mitotic microtubule genes were both upregulated and downregulated after treatment

with anti-mitotic chemicals (**Table 11**). Our results highlight that although reports of the effect of anti-mitotic chemicals on microtubule processes are present in the literature, more comprehensive studies reporting specific genes need to be conducted to make comparisons more effective. Our findings suggest that transcriptomics analyses should be used more specifically as a technique to differentiate mitotic arrests by expression of specific microtubule genes.

Table 11. Mitotic microtubule related genes that were affected by treatment with anti-mitotic chemicals in HT-29 cancer cells.

Gene	Fold Change	Function in mitosis	Treatment and response
RACK1	4.7	Centrosome	Paclitaxel; upregulated
DYNC1H1	4.7	Spindle positioning	
CEP170B	4.7	Microtubule assembly	Paclitaxel; downregulated
TAOK1	4.6	Spindle positioning	
SEPT9	4.6	Cytokinesis	
TBCD	4.6	Tubulin folding	
HAUS3	4.6	Cytokinesis	
TUBB	4.7	Microtubule formation	
PTPN13	4.6	Cytokinesis	
KIF3C	3.3	Microtubule motor protein	Parth; downregulated
MAP2	3.3	Microtubule stabilization	
CCSAP	4.6	Microtubule stability, associates at centrosomes	
TBCB	3.3	Tubulin folding	
TUBG1	3.3	Microtubule nucleation	
AURKA	4.8	Centrosome	PulA; upregulated
MAP4	4.7	Spindle forces	
KIF11	4.7	Bi-polar spindle formation	
GAS2L3	2.0	Cytokinesis	PulA; downregulated
ODF2	2.3	Centriole	
CLASP1	2.3	Centrosomes	
RACGAP1	3.0	Cytokinesis	
CEP162	3.5	Centrosome separation	
KIF2C	4.6	Depolymerization of MT at plus end	
MAPRE21	4.6	Mitosis entry and progression	

5.3 Possible explanations for different mitotic arrests induced by anti-mitotic chemicals

Our results indicate that transcriptomic analysis provides a method for finding differences in mitotic arrests. There are still questions that remain to be answered such as: how do anti-mitotic chemicals regulate the expression of microtubule genes? One possibility is that they interact with transcription factor proteins to alter the expression of their target genes. Such as the FOXM1 transcription factor that controls KIF20A expression and mediates paclitaxel resistance in cancer (Khongkow et al., 2016). Sesquiterpene lactones are known to inhibit transcription factor NF-κβ by alkylating cysteine residues in the DNA binding loop and the E' region to inhibit interaction with DNA (Rungeler et al., 1999). It is possible that the downregulation we observed in our study may be due to an upstream inhibition at the protein level of another transcription factor. Our study is limited in that we examined only the top ten upregulated and downregulated transcripts and microtubule function genes, when downregulated transcription factors may be present in the data elsewhere. This could be explored with bioinformatics programs like NetworkAnalyst (Zhou et al., 2019) which may reveal connections between transcripts.

Within the differentially expressed microtubule genes, we observed some E3 ligase protein targets were differentially expressed after cells were treated with pulA. PulA may be interacting with proteins in such a way that polyubiquitination is inhibited rather than the entire function of the APC/C. Our transcriptomic data provides support for this level of interaction, as we saw downregulation of some genes that correspond to proteins that Min et al. (2014) found are targeted by the APC/C at mitotic exit (MAP4, KIF2C, BCL2L11 and RACGAP1), and increased expression of others (KIF11 and AURKA). Interaction with

different targets of the APC/C by different sesquiterpene lactones may account for differences in mitotic microtubule gene expression. This supports our above-mentioned hypothesis that sesquiterpene lactones interact with components of the ubiquitin-proteasome system.

Transcriptomic analysis is useful as tool to discover genes that influence drug resistance (Dienstmann et al., 2017) but a gap can remain between how the drugs interact with proteins to have this outcome. Although our findings agree with the findings of other groups in terms of the overall biological processes and several specific genes, we observed an assortment of disconnected mitotic microtubule genes in each treatment, rather than one pathway or genes relating to one spindle protein family. On their own, genes in the transcriptomic data may seem disconnected, but using it in combination with other protein analysis techniques can be a powerful tool for discovery. An analysis performed by Stockwell et al. (2012) used a Connectivity Map approach to compare the transcript expression profiles of small molecule CCT020312 and pharmacological agents. They observed similarity between the expression profiles of CCT020312 and thioridazine and 15-delta prostaglandin J2. These similarities led them to investigate the small molecules effect on HSP90, PI3 kinase, and EIF2AK3 using western blotting. They discovered that CCT020312 activates EIF2AK3/PERK signaling pathways to arrest cells in G1/S. The results of our transcriptomic analysis may be compared with future proteomic analyses to elucidate the mechanism of action for pulA.

5.4 Future Directions

Future research with the Asteraceae extracts we examined could involve biology-guided fractionation to isolate the anti-mitotic chemicals, to determine if the anti-mitotic chemicals are indeed, as we suspect, sesquiterpene lactones. Furthermore, extracts from *H. filfolius* could be fractionated to separate cell rounding activity from cytotoxicity by separating the active chemicals. It will also be vital to study the affects of these extracts in non-cancerous human cell lines to test their selectivity against cancer cells. Subsequent studies with pulA should work towards functionally validating the downregulated genes we observed with qPCR and western blotting. These approaches would evaluate if the downregulations we observed are restricted to transcription or if the activity of corresponding proteins is affected. An approach that would provide insight to the E3 ligase hypothesis would be an experiment with biotinylated ubiquitin to find which proteins are being targeted for degradation and those that are not, an approach Min et al. (2014) used. Another approach to investigate interaction between proteins and anti-mitotic sesquiterpene lactones would be activity-based-profiling with click chemistry. In this technique an alkyne probe is attached to the small molecule of interest, and after reacting with proteins a fluorophore or affinity label is attached to the probe by a CuAAC (copper (I)-catalyzed azide-alkyne cycloaddition) reaction allowing visualization and identification of proteins.

Increasing the number of available anti-mitotic chemicals may prove valuable in future cancer treatments and cell division research. For this reason, Canadian Asteraceae species should continue to be investigated for their potential as sources of anti-mitotic chemicals.

References

Adams, Carlson, Milner, Hood, Cairns, & Herzog. (2004). Beneficial grazing management practices for Sage-Grouse (*Centrocercus urophasianus*) and ecology of silver sagebrush (*Artemisia cana*) in southeastern Alberta. In *Technical Report, Public Lands and Forests Division* (Vol. T/049).

Adeleke, & Babalola. (2020). Oilseed crop sunflower (*Helianthus annuus*) as a source of food: Nutritional and health benefits. *Food Sci. Nutr., 8*, 4666-4684.

Alberta-Agriculture. (1995). Poisonous Outdoor Plants. In. Edmonton, Alberta, Canada: Alberta Agriculture and Rural Development.

Anderson. (1982). *Herbs of Long Ago: Kayas Muskekeya*. Edmonton, AB.

Badarudeen, Anand, Mukhopadhyay, & Manna. (2021). Ubiquitin signaling in the control of centriole duplication. *The FEBS Journal*, 10.1111/febs.16069.

Bakker, Ritchie, Olff, Milchunas, & Knops. (2006). Herbivore impact on grassland plant diversity depends on habitat productivity and herbivore size. *Ecol. Lett., 9*, 780-788.

Baldwin, Wessa, & Panero. (2002). Nuclear rDNA evidence for major lineages of helenioid Heliantheae (Compositae). *Syst. Bot., 27*, 161-198.

Balick. (1990). Ethnobotany and the identification of therapeutic agents in the rainforest. In D. J. Chadwick & J. Marsh (Eds.), *Bioactive Compounds From Plants* (pp. 22-30). Chichester, UK: John Wiley and Sons.

Barrett. (2003). Medicinal properties of Echinacea: a critical review. *Phytomedicine, 10*, 66-86.

Benedek, & Kopp. (2007). *Achillea millefolium* L. s.l. revisited: recent findings confirm the traditional use. *Wien Med Wochenschr, 157*, 312-314.

Bennett, Chan, Rattner, & Schriemer. (2012). Low-dose laulimalide represents a novel molecular probe for investigating microtubule organization. *Cell Cycle, 11*, 3045-3054.

Berdan, Ho, Lehtola, To, Hu, Huffman, . . . Nomura. (2019). Parthenolide covalently targets and inhibits focal adhesion kinase in breast cancer cells. *Cell Chem. Biol., 26*, 1027-1035.

Bijak. (2017). Silybin, a major bioactive component of milk thistle (*Silybum marianum* L. Gaernt.)- chemistry, bioavailability, and metabolism. *Molecules, 22*, 1942.

Bohlmann. (1984). Guaianolides and heliangolides from *Hymenopappus newberryi*. *Phytochemistry, 23*, 1055-1058.

Bosco. (2017). *A novel anti-mitotic activity on human cells by pulchelloid A, a compound isolated from the Prairie plant Gaillardia aristata.* (master's thesis). University of Lethbridge, Canada.

Bosco, & Golsteyn. (2017). Emerging anti-mitotic activities and other bioactivities of sesquiterpene compounds upon human cells. *Molecules, 22*, 459-480.

Bosco, Molina, Kernéis, Hatzopoulos, Favez, Gönczy, . . . Golsteyn. (2021). Pulchelloid A, a sesquiterpene lactone from the Canadian prairie plant *Gaillardia aristata* inhibits mitosis in human cells. *Mol. Biol. Rep.*, 5459–5471.

Breecker, McFadden, Sharp, Martinez, & Litvak. (2012). Deep autotrophic soil respiration in shrubland and woodland ecosystems in Central New Mexico. *Ecosystems (New York), 15*, 83-96.

Briske. (1996). Strategies of plant survival in grazed systems: a functional interpretation. In J. Hodgson & A. W. Illius (Eds.), *The Ecology and Management of Grazing Systems* (pp. 37-67). Wallingford, U.K.: CAB International.

Briskin. (2000). Medicinal plants and phytomedicines. Linking plant biochemistry and physiology to human health. *Plant Physiol., 124*, 507-514.

Brouillet, Coursol, Meades, Favreau, Anions, Bélisle, & Desmet. (2010). VASCAN, the Database of Vascular Plants of Canada. Retrieved from http://data.canadensys.net/vascan/. Accessed October 28, 2021.

Cadart, Zlotek-Zlotkiewicz, Le Berre, Piel, & Matthews. (2014). Exploring the function of cell shape and size during mitosis. *Dev. Cell, 29*, 159-169.

Caldas, Horvath, Ferreira-Silva, Ferreira, Ionta, & Sartorelli. (2018). Calein C, a sesquiterpene lactone isolated from *Calea Pinnatifida* (Asteraceae), inhibits mitotic progression and induces apoptosis in MCF-7 cells. *Front. Pharmacol., 9*, 1191-1201.

Calera, Soto, Sanchez, Bye, Hernandez-Bautista, Anaya, . . . Mata. (1995). Biochemically active sesquiterpene lactones from *Ratibida mexicana*. *Phytochemistry, 40*, 419-425.

Cardozo, & Pagano. (2004). The SCF ubiquitin ligase: insights into a molecular machine. *Nature Reviews Molecular Cell Biology, 5*, 739-751.

Chadwick, Trewin, Gawthrop, & Wagstaff. (2013). Sesquiterpenoids lactones: benefits to plants and people. *Int. J. Mol. Sci., 14*, 12780-12805.

Chan, Hsu, Liu, Lai, & Chen. (2014). Adducin-1 is essential for mitotic spindle assembly through its interaction with myosin-X. *J. Cell Biol., 204*, 19-28.

Chen, Frezza, Schmitt, Kanwar, & Dou. (2011). Bortezomib as the first proteasome inhibitor anticancer drug: current status and future perspectives. *Curr. Cancer Drug Targets, 11*, 239-253.

Cheng, Saville, Gollen, Veronesi, Mohajerani, Joseph, & Zovoilis. (2021). Increased Alu RNA processing in Alzheimer brains is linked to gene expression changes. *EMBO reports*, e52255-e52255.

Chiu, Wu, Chia, Hsu, & Tzeng. (2016). Inhibition of growth, migration and invasion of human bladder cancer cells by antrocin, a sesquiterpene lactone isolated from *Antrodia cinnamomea*, and its molecular mechanisms. *Cancer Lett., 373*, 174-184.

Clegg, Scott, Hewitson, Sidhu, & Waugh. (2002). Clinical and cost effectiveness of paclitaxel, docetaxel, gemcitabine, and vinorelbine in non-small cell lung cancer: a systematic review. *Thorax, 57*, 20-28.

Committee. (1993). *Flora of North America. North of Mexico*. New York, NY: Oxford University Press.

Cragg. (1998). Paclitaxel (Taxol): a success story with valuable lessons for natural product drug discovery and development. *Med. Res. Rev., 18*, 315-331.

Cui, Lee, Chai, Tucker, Fairchild, Raventos-Suarez, . . . Kinghorn. (1999). Cytotoxic Sesquiterpenoids from *Ratibida columnifera*. *J. Nat. Prod., 62*, 1545-1550.

Dang, Nie, & Wei. (2021). Ubiquitin signaling in cell cycle control and tumorigenesis. *Cell Death Differ., 28*, 427-438.

Daniels, Van Slambrouck, Lee, Arguello, Browning, Pullin, . . . Steelant. (2006). Effects of extracts from two Native American plants on proliferation of human breast and colon cancer cell lines in vitro. *Oncol. Rep., 15*, 1327-1331.

de Almeida, Luiz-Ferreira, Cola, Di Pietro Magri, Batista, de Paiva, . . . Souza-Brito. (2012). Anti-ulcerogenic mechanisms of the sesquiterpene lactone onopordopicrin-enriched fraction from *Arctium lappa* L. (Asteraceae): role of somatostatin, gastrin, and endogenous sulfhydryls and nitric oxide. *J. Med. Food, 15*, 378-383.

Deeg, Eichhorn, Alexie, Kretschmer, Andersch, Bauer, & Efferth. (2012). Growth inhibition of human acute lymphoblastic CCRF-CEM leukemia cells by medicinal plants of the West-Canadian Gwich'in Native Americans. *Nat. Prod. Bioprospect., 2*, 35-40.

Dienstmann, Vermeulen, Guinney, Kopetz, Tejpar, & Tabernero. (2017). Consensus molecular subtypes and the evolution of precision medicine in colorectal cancer. *Nature Reviews Cancer, 17*, 79-92.

Dinkova-Kostova, Kostov, & Canning. (2017). Keap1, the cysteine-based mammalian intracellular sensor for electrophiles and oxidants. *Arch. Biochem. Biophys., 617*, 84-93.

Downing, Eid, Tang, Ahmed, Harris, Haddad, . . . Cuerrier. (2019). Growth environment and organ specific variation in in-vitro cytoprotective activities of *Picea mariana* in PC12 cells exposed to glucose toxicity: a plant used for treatment of diabetes symptoms by the Cree of Eeyou Istchee (Quebec, Canada). *BMC Complement Altern Med, 19*, 137.

Drogosz, & Janecka. (2019). Helenalin - a sesquiterpene lactone with multidirectional activity. *Curr. Drug Targets, 20*, 444-452.

Eid, J., Bohlmann, Watson, & Estes. (1988). Further guaianolides from *Hymenopappus* species. *Phytochemistry, 27*, 193-195.

Ekenaes, Zebrowska, Schuler, Vrede, Andreasen, Backlund, . . . Bohlin. (2008). Screening for anti-inflammatory activity of 12 *Arnica* (Asteraceae) species assessed by inhibition of NF-κB and release of human neutrophil elastase. *Planta Med., 74*, 1789-1794.

Erb, & Kliebenstein. (2020). Plant secondary metabolites as defenses, regulators, and primary metabolites: The blurred functional trichotomy. *Plant Physiol., 184*, 39-52.

Evans. (1978). Stocking the Canadian Range. *Alta Hist., 26*, 1-8.

Galileo-Educational-Network. (2016). Nitsitapiisinni Stories and Spaces. Retrieved from https://galileo.org/kainai/. Accessed 18 January 2021.

Galletti, Zhang, Gjyrezi, Cleveland, Zhang, Powell, . . . Giannakakou. (2020). Microtubule engagement with taxane is altered in taxane-resistant gastric cancer. *Clin. Cancer Res., 26*, 3771-3783.

Gandolfi, Laubach, Hideshima, Chauhan, Anderson, & Richardson. (2017). The proteasome and proteasome inhibitors in multiple myeloma. *Cancer Metastasis Rev., 36*, 561-584.

Gangapuram, Mazzio, Redda, & Soliman. (2021). Transcriptome profile analysis of triple-negative breast cancer cells in response to a novel cytostatic tetrahydroisoquinoline compared to paclitaxel. *Int. J. Mol, 22*, 7694.

Gasic, Boswell, & Mitchison. (2019). Tubulin mRNA stability is sensitive to change in microtubule dynamics caused by multiple physiological and toxic cues. *PLoS Biol., 17*, e3000225.

Ghantous, Gali-Muhtasib, Vuorela, Saliba, & Darwiche. (2010). What made sesquiterpene lactones reach cancer clinical trials? *Drug Discov. Today, 15*, 668-678.

Ghantous, Sinjab, Herceg, & Darwiche. (2013). Parthenolide: from plant shoots to cancer roots. *Drug Discov. Today, 18*, 894-905.

Goodman. (2001). *The story of taxol: nature and politics in the pursuit of an anti-cancer drug*: Cambridge University Press.

Government of Alberta. (1995). Poisonous Outdoor Plants. Retrieved from https://open.alberta.ca/publications/4869444. Accessed January 18 2021.

Government of Canada. (2021a). Canadian Climate Normals 1981-2010 Station Data. Retrieved from https://climate.weather.gc.ca/climate_normals/results_1981_2010_e.html?searchType=stnProv&lstProvince=AB&txtCentralLatMin=0&txtCentralLatSec=0&txtCentralLongMin=0&txtCentralLongSec=0&stnID=2263&dispBack=0. Accessed January 20 2021.

Government of Canada. (2021b). Photovoltaic Potential and Solar Resource Maps of Canada. Retrieved from https://fgp-pgf.maps.arcgis.com/apps/webappviewer/index.html?id=c91106a7d8c446a19dd1909fd93645d3. Accessed January 20 2021.

Graciotti, Fang, Johnsson, & Gönczy. (2016). Chemical genetic screen identifies natural products that modulate centriole number. *ChemBioChem, 17*, 2063-2074.

Groesser, Cooper, & Rydberg. (2008). Lack of bystander effects from high-LET radiation for early cytogenetic end points. *Radiat. Res., 170*, 794-802.

Haghi, Hatami, Safaei, & Mehran. (2014). Analysis of phenolic compounds in *Matricaria chamomilla* and its extracts by UPLC-UV. *Res. Pharm. Sci., 9*, 31-37.

Hartmann. (1996). Diversity and variability of plant secondary metabolism: A mechanistic view. *Entomol. Exp. Appl., 80*, 177-188.

Hegazy, Dawood, Mahmoud, Elbadawi, Sugimoto, Klauck, . . . Efferth. (2021). 2α-hydroxyalantolactone from *Pulicaria undulata*: activity against multidrug-resistant tumor cells and modes of action. *Phytomedicine, 81*, 153409.

Hellson. (1974). *Ethnobotany of the Blackfoot Indians*. Ottawa: National Museums of Canada

Herz, Kulanthaivel, & Goedken. (1985). Structures of the ratibidanolides, sesquiterpene lactones with a new carbon skeleton, and unusual xanthanolides from *Ratibida columnifera*. *J. Org. Chem., 50*, 610-617.

Hind. (2006). 566. *Ratibida columnifera* var. pulcherrima. *Curtis's Bot. Mag., 23*, 267-277.

Ho, Peh, Chan, & Wong. (2014). Artemisinins: pharmacological actions beyond anti-malarial. *Pharmacol. Ther., 142*, 126-139.

Hotta, Haynes, Blasius, Gebbie, Eberhardt, Sept, . . . Ohi. (2021). Parthenolide destabilizes microtubules by covalently modifying tubulin. *Curr. Biol., 31*, 900-907.

Hyam, Lee, Gu, Kim, Jeong, Jang, . . . Kim. (2013). Arctigenin ameliorates inflammation in vitro and in vivo by inhibiting the PI3K/AKT pathway and polarizing M1 macrophages to M2-like macrophages. *Eur. J. Pharmacol., 708*, 21-29.

Ingham, & Detling. (1984). Plant-herbivore interactions in a North American mixed-grass prairie : III. Soil nematode populations and root biomass on *Cynomys ludovicianus* colonies and adjacent uncolonized areas. *Oecologia, 63*, 307-313.

Iszkuło, Pers-Kamczyc, Nalepka, Rabska, Walas, & Dering. (2016). Postglacial migration dynamics helps to explain current scattered distribution of Taxus baccata. *Dendrobiol., 76*, 81-89.

Jaakola, & Hohtola. (2010). Effect of latitude on flavonoid biosynthesis in plants. *Plant, Cell Environ., 33*, 1239-1247.

Jackson, Widen, Harki, & Brummond. (2017). Covalent modifiers: a chemical perspective on the reactivity of α,β-unsaturated carbonyls with thiols via hetero-Michael addition reactions. *J. Med. Chem., 60*, 839-885.

Janiszewska, Primi, & Izard. (2020). Cell adhesion in cancer: beyond the migration of single cells. *J. Biol. Chem., 295*, 2495-2505.

Jia, & Sun. (2011). SCF E3 ubiquitin ligases as anticancer targets. *Curr. Cancer Drug Targets, 11*, 347-356.

Johnston. (1987). *Plants and The Blackfoot*. Lethbridge: Graphcom Printers, Limited.

Jones, Clements, Wasi, & Daoud. (2000). Enhancement of camptothecin-induced cytotoxicity with UCN-01 in breast cancer cells: abrogation of S/G2 arrest. *Cancer Chemother. Pharmacol., 45*, 252-258.

Jordan, Thrower, & Wilson. (1992). Effects of vinblastine, podophyllotoxin and nocodazole on mitotic spindles. Implications for the role of microtubule dynamics in mitosis. *J. Cell Sci., 102*, 401-416.

Kearns. (1997). Pharmacokinetics of the taxanes. *Pharmacotherapy, 17*, 105-109.

Keeler, & Baker. (1990). Myopathy in cattle induced by alkaloid extracts from *Thermopsis montana*, *Laburnum anagyroides* and a *Lupinus sp*. *J Comp Pathol, 103*, 169-182.

Keeler, Johnson, & Chase. (1986). Toxicity of *Thermopsis montana* in cattle. *Cornell Vet., 76*, 115-127.

Kershaw, & Allen. (2020). *Vascular Flora of Alberta: An illustrated guide*. Bolton, ON, Canada: Amazon Canada.

Khadem, & Marles. (2011). Chromone and flavonoid alkaloids: occurrence and bioactivity. *Molecules, 17*, 191-206.

Khongkow, Gomes, Gong, Man, Tsang, Zhao, . . . Lam. (2016). Paclitaxel targets FOXM1 to regulate KIF20A in mitotic catastrophe and breast cancer paclitaxel resistance. *Oncogene, 35*, 990-1002.

Kiely-Collins, Winter, & Bernardes. (2021). The role of reversible and irreversible covalent chemistry in targeted protein degradation. *Cell Chem. Biol., 28*, 952-968.

Kim, & Kim. (2020). Transcriptome analysis of the inhibitory effect of astaxanthin on *Helicobacter pylori*-induced gastric carcinoma cell motility. *Mar. Drugs, 18*, 365.

Kindscher. (1992). *Medicinal Wild Plants of the Prairie*. Lawrence, Kansas: University Press of Kansas.

Kuijt. (1982). *A Flora of Waterton Lakes National Park*. Edmonton: University of Alberta.

Kupchan, Fessler, Eakin, & Giacobbe. (1970). Reactions of alpha methylene lactone tumor inhibitors with model biological nucleophiles. *Science, 168*, 376-378.

Lara-Gonzalez, Westhorpe, & Taylor. (2012). The spindle assembly checkpoint. *Curr. Biol., 22*, 966-980.

Laws. (2015). *Fifty plants that changed the course of history*. Richmond Hill, ON: Firefly Books Ltd.

Laycock. (1978). Coevolution of poisonous plants and large herbivores on rangelands. *J. Range Manag., 31*, 335-342.

Lee, & Shyur. (2012). Deoxyelephantopin impedes mammary adenocarcinoma cell motility by inhibiting calpain-mediated adhesion dynamics and inducing reactive oxygen species and aggresome formation. *Free Radic. Biol. Med., 52*, 1423-1436.

Leighton. (1985). *Wild plant use by the woods Cree (Nihithawak) of East-Central Saskatchewan*. Ottawa: National Museums of Canada

Lewis, & Elvin-Lewis. (1995). Medicinal plants as sources of new therapeutics. *Annal Missouri Botan. Garden, 82*, 16-24.

Lewis, Taylor, Kubara, Marshall, Meijer, & Golsteyn. (2013). A western blot assay to measure cyclin dependent kinase activity in cells or in vitro without the use of radioisotopes. *FEBS Lett., 587*, 3089-3095.

Linde, Barrett, Wölkart, Bauer, & Melchart. (2006). Echinacea for preventing and treating the common cold. *Cochrane Database Syst Rev*, Cd000530.

Lindström, & Alvarado-Kristensson. (2018). Characterization of gamma-tubulin filaments in mammalian cells. *Biochimica et Biophysica Acta. Molecular Cell Research, 1865*, 158-171.

Liu, Chen, Wang, Soares, Fischer, Meng, . . . He. (2017). Transcriptional landscape of the human cell cycle. *Proc. Natl. Acad. Sci. U.S.A., 114*, 3473-3478.

Liu, Lin, Zhang, Ma, Han, Jia, . . . Li. (2019). The novel nature microtubule inhibitor ivalin induces G2/M arrest and apoptosis in human hepatocellular carcinoma SMMC-7721 cells in vitro. *Medicina (Kaunas, Lithuania), 55*, 470.

Liu, Wang, Cheng, Lu, Wang, Li, . . . Zhou. (2015). Skp1 in lung cancer: clinical significance and therapeutic efficacy of its small molecule inhibitors. *Oncotarget, 6*, 34953-34967.

Long, Peng, Chu, Jia, Dong, & Liu. (2020). Paclitaxel inhibits the migration of CD133+ U251 malignant glioma cells by reducing the expression of glycolytic enzymes. *Exp. Ther. Med., 20*, 72.

Love, Huber, & Anders. (2014). Moderated estimation of fold change and dispersion for RNA-seq data with DESeq2. *Genome Biology, 15*, 550.

Lughadha, Goverts, Belyaeva, Black, Lindon, Allkin, . . . Nicolson. (2016). Counting counts: revised estimates of numbers of accepted species of flowering plants, seed

plants, vascular plants and land plants with a review of other recent estimates. *Phytotaxa 272*, 82-88.

Majak, Brooke, & Ogilvie. (2008). *Stock-poisoning plants of Western Canada*. Ottawa, Canada: Research Branc Agriculture Canada.

Manzoni, Kia, Vandrovcova, Hardy, Wood, Lewis, & Ferrari. (2018). Genome, transcriptome and proteome: the rise of omics data and their integration in biomedical sciences. *Brief. Bioinformatics, 19*, 286-302.

Marles, Clavelle, Monteleone, Tays, & Burns. (2012). *Aboriginal Plant Use in Canada's Northwest Boreal Forest*. Edmonton, AB: Canada Forest Service.

Marshall, Schut, & Ballard. (1999). *A national ecological framework for Canada: Attribute data*. Ottawa/Hull: Agriculture and Agri-Food Canada, Research Branch, Centre for Land and Biological Resources Research, and Environment Canada, State of the Environment Directorate, Ecozone Analysis Branch.

Martin. (2011). Cutadapt removes adapter sequences from high-throughput sequencing reads. *EMBnet.Journal, 17*, 10-12.

Matsui, Nakayama, Okamoto, Fukumoto, & Yamaguchi. (2012). Enrichment of cell populations in metaphase, anaphase, and telophase by synchronization using nocodazole and blebbistatin: a novel method suitable for examining dynamic changes in proteins during mitotic progression. *Eur. J. Cell Biol., 91*, 413-419.

McCutcheon, Ellis, Hancock, & Towers. (1992). Antibiotic screening of medicinal plants of the British Columbian native peoples. *J. Ethnopharmacol., 37*, 213-223.

McCutcheon, Roberts, Gibbons, Ellis, Babiuk, Hancock, & Towers. (1995). Antiviral screening of British Columbian medicinal plants. *J. Ethnopharmacol., 49*, 101-110.

McLean, Chaix, Ohi, & Gould. (2011). State of the APC/C: organization, function, and structure. *Crit. Rev. Biochem. Mol., 46*, 118-136.

Merfort, & Wendisch. (1993). Sesquiterpene lactones of *Arnica cordifolia*, subgenus *Austromontana*. *Phytochemistry, 34*, 1436-1437.

Miglietta, Bozzo, Gabriel, & Bocca. (2004). Microtubule-interfering activity of parthenolide. *Chem. Biol. Interact., 149*, 165-173.

Mijaljica, Prescott, & Devenish. (2012). A late form of nucleophagy in *Saccharomyces cerevisiae*. *PLoS One, 7*, e40013.

Miller. (2011). The discovery of medicines from plants: A current biological perspective. *Econ. Bot., 65*, 396-407.

Min, Mayor, Dittmar, & Lindon. (2014). Using in vivo biotinylated ubiquitin to describe a mitotic exit ubiquitome from human cells. *Mol. Cell Proteomics, 13*, 2411-2425.

Moerman. (2009). *Native American Medicinal Plants: An Ethnobotanical Dictionary*. Oregon: Timber Press, Inc.

Molina. (2018). *Anti-mitotic activity of six Asteraceae plant extracts and identificaiton of the sesquiterpene lactone hymenoratin from the Canadian plant Hymenoxys richarsonii.* (master's thesis). University of Lethbridge, Canada.

Molina, Allard, Kernéis, & Golsteyn. (2021a). Connecting plant species and natural products from the Canadian prairie ecological zone to biomedical knowledge. *Botany*, doi.org/10.1139/cjb-2021-0067.

Molina, Williams, Andersen, & Golsteyn. (2021b). Isolation of a natural product with anti-mitotic activity from a toxic Canadian prairie plant. *Heliyon, 7*, e07131.

Moss, & Packer. (1983). *Flora of Alberta: a manual of flowering plants, conifers, ferns and fern allies found growing without cultivation in the province of Alberta, Canada* (2nd ed.). Toronto: University of Toronto Press.

Moujir, Callies, Sousa, Sharopov, & Seca. (2020). Applications of sesquiterpene lactones: a review of some potential success cases. *Appl. Sci., 10*, 3001.

Muhammad, Guerrero-Analco, Martineau, Musallam, Madiraju, Nachar, . . . Arnason. (2012). Antidiabetic compounds from Sarracenia purpurea used traditionally by the Eeyou Istchee Cree First Nation. *J. Nat. Prod., 75*, 1284−1288.

Myster. (2011). Above-ground vs. below-ground interactive effects of mammalian herbivory on tallgrass prairie plant and soil characteristics. *J. Plant Interact., 6*, 283-290.

Nersesian, Banks, & McArthur. (2011). Titrating the cost of plant toxins against predators: determining the tipping point for foraging herbivores. *J. Anim. Ecol., 80*, 753-760.

Newman, & Cragg. (2020). Natural products as sources of new drugs over the nearly four decades from 01/1981 to 09/2019. *J. Nat. Prod., 83*, 770-803.

Newman, Cragg, & Snader. (2000). The influence of natural products upon drug discovery. *Nat Prod Rep, 17*, 215-234.

Nisi, Hernandez, English, & Rogers. (2015). Patterns of selective herbivory on five prairie legume species. *The American Midland Naturalist, 173*, 110-121.

Nistor Baldea, Martineau, Benhaddou-Andaloussi, Arnason, Lévy, & Haddad. (2011). Inhibition of intestinal glucose absorption by anti-diabetic medicinal plants derived from the James Bay Cree traditional pharmacopeia. *J. Ethnopharmacol., 132*, 473–482.

Omar, Dibwe, Tawila, Sun, Kim, & Awale. (2019). Chemical constituents from *Artemisia vulgaris* and their antiausterity activities against the PANC-1 human pancreatic cancer cell line. *Nat. Prod. Res.*, 1-7.

Padilla-Gonzalez, dos Santos, & Da Costa. (2016). Sesquiterpene lactones: More than protective plant compounds with high toxicity. *Crit. Rev. Plant Sci., 35*, 18-37.

Panero, & Funk. (2002). Toward a phylogenetic subfamilial classification for the Compositae (Asteraceae). *Proc. Biol. Soc. Wash., 115*, 909-922.

Pareek, Suthar, Rathore, & Bansal. (2011). Feverfew (*Tanacetum parthenium* L.): A systematic review. *Pharmacognosy reviews, 5*, 103-110.

Pavarini, Pavarini, Niehues, & Lopes. (2012). Exogenous influences on plant secondary metabolite levels. *Animal Feed Science and Technology, 176*, 5-16.

Petry. (2016). Mechanisms of mitotic spindle assembly. *Annu. Rev. Biochem., 85*, 659-683.

Pfister, Manners, Gardner, Price, & Ralphs. (1996). Influence of alkaloid concentration on acceptability of tall larkspur (*Delphinium spp*.) to cattle and sheep. *J. Chem. Ecol., 22*, 1147-1168.

Picman. (1986). Biological activities of sesquiterpene lactones. *Biochem. Syst. Ecol., 14*, 255-281.

Potier, Guéritte-Voegelein, & Guénard. (1994). Taxoids, a new class of antitumour agents of plant origin: recent results. *Nouv Rev Fr Hematol, 36*, S21-23.

Poutaraud, Michelot-Antalik, & Plantureux. (2017). Grasslands: A source of secondary metabolites for livestock health. *J. Agric. Food Chem., 65*, 6535-6553.

Ramirez-Erosa, Huang, Hickie, Sutherland, & Barl. (2007). Xanthatin and xanthinosin from the burs of *Xanthium strumarium* L. as potential anticancer agents. *Can. J. Physiol. Pharmacol., 85*, 1160-1172.

Rebacz, Larsen, Clausen, Rønnest, Löffler, Ho, & Krämer. (2007). Identification of griseofulvin as an inhibitor of centrosomal clustering in a phenotype-based screen. *Cancer Res., 67*, 6342-6350.

Ringel, & Horwitz. (1991). Studies with RP 56976 (taxotere): a semisynthetic analogue of taxol. *J. Natl. Cancer Inst., 83*, 288-291.

Rodziewicz, Swarcewicz, Chmielewska, Wojakowska, & Stobiecki. (2014). Influence of abiotic stresses on plant proteome and metabolome changes. *Acta Physiol. Plant, 36*, 1-19.

Rojas, Villena, Jimenez, & Mata. (1991). Chemical studies on Mexican plants used in tradtional medicine, xxi. Ratibinolide-II, a new sesquiterpene lactone from *Ratibida latipalearis*. *J. Nat. Prod., 54*, 1279-1282.

Royal Botanic Gardens Kew and Missouri Botanic Garden. (2013). The Plant List. Retrieved from http://www.theplantlist.org. Accessed March 27.

Rundle, Nelson, Flory, Joseph, Th'ng, Aebersold, . . . Roberge. (2006). An ent-kaurene that inhibits mitotic chromosome movement and binds the kinetochore protein ran-binding protein 2. *ACS Chem. Biol., 1*, 443-450.

Rungeler, Castro, Mora, Goren, Vichnewski, Pahl, . . . Schmidt. (1999). Inhibition of transcription factor NF-kappaB by sesquiterpene lactones: a proposed molecular mechanism of action. *Bioorg. Med. Chem., 7*, 2343-2352.

Sackton, Dimova, Zeng, Tian, Zhang, Sackton, . . . King. (2014). Synergistic blockade of mitotic exit by two chemical inhibitors of the APC/C. *Nature, 514*, 646-649.

Saslis-Lagoudakis, Savolainen, Williamson, Forest, Wagstaff, Baral, . . . Hawkins. (2012). Phylogenies reveal predictive power of traditional medicine in bioprospecting. *Proc. Natl. Acad. Sci. U.S.A., 109*, 15835-15840.

Schatten. (2008). The mammalian centrosome and its functional significance. *Histochem. Cell Biol., 129*, 667-686.

Schiff, Fant, & Horwitz. (1979). Promotion of microtubule assembly in vitro by taxol. *Nature 277*, 665-667.

Schmidt, & Willuhn. (2000). Sesquiterpene lactone and flavonoid variability of the *Arnica angustifolia* aggregate (Asteraceae). *Biochem. Syst. Ecol., 28*, 133-142.

Sciortino, Gurtner, Manni, Fontemaggi, Dey, Sacchi, . . . Piaggio. (2001). The cyclin B1 gene is actively transcribed during mitosis in HeLa cells. *EMBO Reports, 2*, 1018-1023.

Scotti, Emerenciano, Ferreira, Scotti, Stefani, da Silva, & Mendonça Junior. (2012). Self-organizing maps of molecular descriptors for sesquiterpene lactones and their

application to the chemotaxonomy of the Asteraceae family. *Molecules, 17*, 4684-4702.

Seaman. (1982). Sesquiterpene lactones as taxonomic characters in the Asteraceae. *Bot. Rev., 48*, 121-595.

Septembre-Malaterre, Lalarizo Rakoto, Marodon, Bedoui, Nakab, Simon, . . . Gasque. (2020). *Artemisia annua*, a traditional plant brought to light. *Int. J. Mol., 21*, 4986.

Shang, Saleem, Musallam, Walshe-Roussel, Badawi, Cuerrier, . . . Haddad. (2015). Novel approach to identify potential bioactive plant metabolites: Pharmacological and metabolomics analyses of ethanol and hot water extracts of several canadian medicinal plants of the Cree of Eeyou Istchee. *PLoS One, 10*, e0135721.

Shemluck. (1982). Medicinal and other uses of the Compositae by Indians in the United States and Canada. *J. Ethnopharmacol., 5*, 303-358.

Singh, Rathinasamy, Mohan, & Panda. (2008). Microtubule assembly dynamics: an attractive target for anticancer drugs. *IUBMB Life, 60*, 368-375.

Sithara, Dhanya, Arun, Sini, Dan, Kokkuvayil Vasu, & Nisha. (2018). Zerumbone, a cyclic sesquiterpene from *Zingiber zerumbet* induces apoptosis, cell cycle arrest, and antimigratory effects in SW480 colorectal cancer cells. *J. Agric. Food Chem., 66*, 602-612.

Smilanich, & Nuss. (2019). Unlocking the genetic basis of monarch butterflies' use of medicinal plants. *Mol. Ecol., 28*, 4839-4841.

Soejarto, Addo, & Kinghorn. (2019). Highly sweet compounds of plant origin: From ethnobotanical observations to wide utilization. *J. Ethnopharmacol., 243*, 112056.

Sorokina, & Steinbeck. (2020). Review on natural products databases: where to find data in 2020. *J Cheminform, 12*, 20.

Spotswood, Bradley, & Knops. (2002). Effects of herbivory on the reproductive effort of 4 prairie perennials. *BMC Ecol., 2*, 2.

Spring, Priester, & Hager. (1986). Light-induced accumulation of sesquiterpene lactones in sunflower seedlings. *J. Plant Physiol., 123*, 79-89.

Spring, Schmauder, Lackus, Schreiner, Meier, Wellhausen, . . . Frey. (2020). Spatial and developmental synthesis of endogenous sesquiterpene lactones supports function in growth regulation of sunflower. *Planta, 252*, 2.

Srinameb, Nuchadomrong, Jogloy, Patanothai, & Srijaranai. (2015). Preparation of inulin powder from Jerusalem artichoke (*Helianthus tuberosus* L.) tuber. *Plant Foods Hum Nutr, 70*, 221-226.

Stebbins. (1981). Coevolution of grasses and herbivores. *Annal. Miss. Botanic. Garden, 68*, 75-86.

Stockwell, Platt, Barrie, Zoumpoulidou, Te Poele, Aherne, . . . Mittnacht. (2012). Mechanism-based screen for G1/S checkpoint activators identifies a selective activator of EIF2AK3/PERK signalling. *PLoS One, 7*, e28568.

Storchova. (2021). Consequences of mitotic failure - The penalties and the rewards. *Semin. Cell Dev. Biol., 117*, 149-158.

Street, Sidana, & Prinsloo. (2013). Cichorium intybus: Traditional Uses, Phytochemistry, Pharmacology, and Toxicology. *Evid. Based Complement. Alternat. Med., 2013*, 579319.

Sumara, Maerki, & Peter. (2008). E3 ubiquitin ligases and mitosis: embracing the complexity. *Trends Cell Biol., 18*, 84-94.

Szenajch, Szabelska-Beręsewicz, Świercz, Zyprych-Walczak, Siatkowski, Góralski, . . . Handschuh. (2020). Transcriptome remodeling in gradual development of inverse resistance between paclitaxel and cisplatin in ovarian cancer cells. *Int. J. Mol., 21*, 9218.

Toda, Naito, Mase, Ueno, Uritani, Yamamoto, & Ushimaru. (2012). APC/C-Cdh1-dependent anaphase and telophase progression during mitotic slippage. *Cell Div., 7*, 4.

Tokuo. (2020). Myosin X. *Adv. Exp. Med. Biol., 1239*, 391-403.

Turner, Thompson, Thompson, & York. (1990). *Thompson Ethnobotany: Knowledge and usage of plants by the Thompson Indians of British Columbia*. Victoria, BC: Royal British Columbia Museum.

Tzeng, Li, Chen, Yang, Chang, & Juang. (2018). LMO7 exerts an effect on mitosis progression and the spindle assembly checkpoint. *Int. J. Biochem. Cell Biol., 94*, 22-30.

Ulappa, Kelsey, Frye, Rachlow, Shipley, Bond, . . . Forbey. (2014). Plant protein and secondary metabolites influence diet selection in a mammalian specialist herbivore. *J. Mammal., 95*, 834-842.

Ulloa Ulloa, Acevedo-Rodriguez, Beck, Belgrano, Bernal, Berry, . . . Jorgensen. (2017). An integrated assessment of the vascular plant species of the Americas. *Science, 358*, 1614-1617.

Uprety, Asselin, Dhakal, & Julien. (2012). Traditional use of medicinal plants in the boreal forest of Canada: review and perspectives. *J. Ethnobiol. Ethnomed., 8*, 7-21.

Verweij, Clavel, & Chevalier. (1994). Paclitaxel (Taxol) and docetaxel (Taxotere): not simply two of a kind. *Ann. Oncol., 5*, 495-505.

Wall, & Wani. (1996). Camptothecin and taxol: from discovery to clinic. *J. Ethnopharmacol., 51*, 239-253; discussion 253-234.

Wang, Riel, Bajrami, Deng, Howell, & Yao. (2021). α-methylene-β-lactone scaffold for developing chemical probes at the two ends of the selectivity spectrum. *ChemBioChem, 22*, 505-515.

Wen, Liu, Wen, Yu, & Wei. (2018). Artesunate promotes G2/M cell cycle arrest in MCF7 breast cancer cells through ATM activation. *Breast Cancer, 25*, 681-686.

Wink. (2003). Evolution of secondary metabolites from an ecological and molecular phylogenetic perspective. *Phytochemistry, 64*, 3-19.

Wolf. (2006). *Flora of North America North of Mexico* (Vol. 21). New York, NY: Oxford University Press.

Wöll, Kim, Greten, & Efferth. (2013). Animal plant warfare and secondary metabolite evolution. *Nat Prod Bioprospect, 3*, 1-7.

Wood. (1996). *Scenes of togetherness: A Cree Elder's philosophy of health and healing.* (M.Ed. master's thesis). University of Alberta, Edmonton, AB.

Wooton, & Standley. (1915). Flora of New Mexico. *Contr. U.S. Natl. Herb., 19*, 3-794.

Wu, Chen, Yu, Li, Zhang, Yang, . . . Wu. (2018). Single-cell transcriptome analyses reveal molecular signals to intrinsic and acquired paclitaxel resistance in esophageal squamous cancer cells. *Cancer Lett., 420*, 156-167.

Wu, Zhu, Yuan, Chen, Xiong, Zhang, . . . Zhang. (2017). Britanin ameliorates cerebral ischemia-reperfusion injury by inducing the Nrf2 protective pathway. *Antioxid. Redox Signal., 27*, 754-768.

Yang, & Horwitz. (2017). Taxol: the first microtubule stabilizing agent. *Int. J. Mol., 18*, 1733.

Yang, Sheng, Li, Xu, Zhang, & Lu. (2021). Dehydrocostus lactone induces apoptosis and cell cycle arrest through regulation of JAK2/STAT3/PLK1 signaling pathway in human esophageal squamous cell carcinoma cells. *Anti-Cancer Agents in Medicinal Chemistry, Advance online publication*, 10.2174/1871520621666210805142200.

Youyou. (2016). Artemisinin—a gift from traditional Chinese medicine to the world (Nobel Lecture). *Angewandte Chem Internatl Ed, 55*, 10210-10226.

Yuan, Sanhaji, Krämer, Reindl, Hofmann, Kreis, . . . Strebhardt. (2011). Polo-box domain inhibitor poloxin activates the spindle assembly checkpoint and inhibits tumor growth in vivo. *Am. J. Clin. Pathol., 179*, 2091-2099.

Zdero, & Bohlmann. (1990). Systematics and evolution within the Compositae, seen with the eyes of a chemist. *Plant Systematics and Evolution, 171*, 1-14.

Zhang, Won, Ong, & Shen. (2005). Anti-cancer potential of sesquiterpene lactones: bioactivity and molecular mechanisms. *Curr. Med. Chem. Anticancer Agents, 5*, 239-249.

Zhou, Soufan, Ewald, Hancock, Basu, & Xia. (2019). NetworkAnalyst 3.0: a visual analytics platform for comprehensive gene expression profiling and meta-analysis. *Nucleic Acids Res., 47*, 234-241.

Züst, Heichinger, Grossniklaus, Harrington, Kliebenstein, & Turnbull. (2012). Natural enemies drive geographic variation in plant defenses. *Science, 338*, 116-119.